5-11-2018

Toxicological Assessments of Released Engineered Nanoparticles from Aerosolized Products on Human Small Airway and Bronchial Epithelial Cells

Kaitlin Pearce

Toxicological Assessments of Released Engineered Nanoparticles from Aerosolized Products on Human Small Airway and Bronchial Epithelial Cells

By

Kaitlin Marie Pearce

April 19, 2018

ABSTRACT

Nanotechnology has led to the development of novel applications and materials incorporated into consumer products known as nano-enabled products (NEPs). Consequently, the wide-spread use of NEPs has led to a concern of human exposure to constituent engineered nanomaterials (ENMs) utilized in the consumer products. This growing public health issue is largely due to limited safety regulations imposed on manufacturers and a lack of hazard characterization of NEP exposures to understand the human health implications. This *in vitro* study focused on NEPs such as aerosolized cosmetics, which are becoming more mainstream within the general population. A large majority of constituent ENMs such as metal nanoparticles (NPs) that are heavily used in the cosmetic industry have been associated with asthma, inflammation, and other pulmonary conditions upon exposure. Within this study, we utilized a novel aerosol exposure system to monitor and sample released nanoparticle (rNP) aerosols from two separate cosmetic lines to determine potential differences in manufacture or production. The exposure system consisted of a stainless-steel glove box containing a mannequin head with fitted outlet sample portals that allowed monitoring of aerosols using scanning mobility particle sizer (SMPS). To generate cosmetic aerosols, an automated nebulizer controlled by proprietary software that controlled spray durations, length of exposures, and aerosol concentrations was fitted in the glove box. The enclosed glove box system was pressurized using a vacuum while HEPA filtered air was used to regulate air flow (11 L/min) and aerosol release from the nebulizer. The generated aerosols or rNPs were sampled or collected on to mixed cellulose ester (MCE) filters for subsequent aqueous extraction and off-line physico-chemical characterization of collected rNPs to determine particle morphology and elemental composition using scanning electron microscopy coupled with energy dispersive x-ray spectroscopy (SEM-EDS). Colloidal characterization was performed on extracted rNPs and pristine nanoparticles (pNPs) iron-oxide (Fe_2O_3) and titanium dioxide (TiO_2), which are found in great quantities in each of the raw or whole cosmetics determined by inductively coupled plasma mass spectrometry (ICP-MS). The toxicological profiles of acute 24-hour exposure to extracted rNPs and pNPs were then compared using human bronchial (16HBE) and primary small airway epithelial cells (SAEC) to model airway responses to NEP exposures. The results indicate that SAEC were most susceptible to exposure to rNPs than 16HBE. It was also determined that rNPs, specifically the darker shades of cosmetics induced higher levels of reactive oxygen species, oxidative stress, and cytotoxicity. Immunocytochemistry confirmed by western blot analysis of 3-week sub-chronic exposures to rNPs indicated epithelial mesenchymal transition (EMT), suggesting fibrotic changes in exposed SAEC. While further studies are needed to provide a more comprehensive picture of the effects of rNPs, this study has established findings that can be used towards future research regarding inhalation exposure to NEPs. Moreover, the findings indicate that susceptible populations such as darker skinned individuals or individuals with pre-existing conditions may be at higher risk to the adverse effects of NEP cosmetic exposures.

Toxicological Assessments of Released Engineered Nanoparticles from Aerosolized Products on Human Small Airway and Bronchial Epithelial Cells

By

Kaitlin Marie Pearce

Bachelor of Science, Georgia Gwinnett College

April 19, 2018

A Thesis Submitted to the Graduate Faculty
of Georgia State University in Partial Fulfillment
of the
Requirements for the Degree

MASTER OF PUBLIC HEALTH

ATLANTA, GEORGIA
30303

APPROVAL PAGE

Toxicological Assessments of Released Engineered Nanoparticles from Aerosolized Products on Human Small Airway and Bronchial Epithelial Cells

By

Kaitlin Marie Pearce

Approved:

Dr. Christa Wright
Committee Chair

Dr. Roby Greenwald
Committee Member

Dr. Imoh Okon
Committee Member

Dr. Lisa Casanova
Department Chair

April 19, 2018
Date

Acknowledgments

I want to extend my thanks and appreciation to my mentor and committee chair, Dr. Christa Wright for providing me with this opportunity, encouraging me, and giving me guidance and direction. I also want to thank my other committee members Dr. Roby Greenwald and Dr. Imoh Okon for agreeing to take this journey with me. Lastly, I want to thank my family and soon-to-be husband for being patient and respectful, always having my back, and supporting me through my journey. I am eternally grateful for everyone's part in this achievement.

Author's Statement Page

In presenting this thesis as a partial fulfillment of the requirements for an advanced degree from Georgia State University, I agree that the Library of the University shall make it available for inspection and circulation in accordance with its regulations governing materials of this type. I agree that permission to quote from, to copy from, or to publish this thesis may be granted by the author or, in his/her absence, by the professor under whose direction it was written, or in his/her absence, by the Associate Dean, School of Public Health. Such quoting, copying, or publishing must be solely for scholarly purposes and will not involve potential financial gain. It is understood that any copying from or publication of this dissertation which involves potential financial gain will not be allowed without written permission of the author.

Kaitlin Marie Pearce
Signature of Author

TABLE OF CONTENTS

List of Tables

List of Figures

1. INTRODUCTION

Nanotechnology, or the synthesis and manipulation of materials that measure <100 nanometers, is currently used in numerous industries to design or revamp products and applications to meet the continuing market demand for innovation and efficiency. Since the 1980s, nanotechnology and the resulting nanomaterials have had beneficial uses in a wide array of fields, such as electronics, healthcare, environmental remediation, and in everyday products, such as fabrics, degreasers, baseball bats, tennis rackets, luggage, eyeglasses, food packaging, and camera lenses (United States National Nanotechnology Initiative, n.d.). While there have been recorded examples of premodern uses of nanotechnology, evidence of production of consumer nano-enabled products (NEPs) has been present in the marketplace since around 1999 (United States National Nanotechnology Initiative, 2014). Since then, the need for better, cheaper, and stronger products, as well as motive for increasing production, profit, and reliability, has scaled up the use of nanomaterials.

In 2007, the National Science Foundation estimated that $70 billion of NEPs were sold annually in the United States alone (Rice University, 2007). In 2013, it was estimated that there was $1 trillion in global revenue from NEPs and it is projected that nanotechnology will have a market value of $4.4 trillion by 2018 (Lux Research, 2014; NSF, 2014). There is currently a working list of consumer products that contain nanomaterials called the Woodrow Wilson Nanotechnology Consumer Products Inventory (CPI) (Vance et al., 2015). The CPI has information on over 1,600 manufacturer-identified nanotechnology-based consumer products that have been released into the market within the last twenty years (Vance et al., 2015). While this provides some helpful insight as to characteristics and details about some of these products, new products and formulations are being continually released, along with various permeations of

nanomaterials and regulations, that makes it difficult to track the most up-to-date and accurate number of NEPs being distributed globally. What poses an additional hurdle in the quest to identify the number of NEPs in the market is that manufacturers are not required to label their products that are composed of nanomaterials (Kessler, 2011). While, as recently as 2017, the U.S. Environmental Protection Agency (EPA) has tried to regulate nanomaterials under the Toxic Substances Control Act, it does not include all the existing nanomaterials and only requires "premanufacture notifications for new nanomaterials" (US EPA, 2015a). This one-time reporting and recordkeeping of existing exposure and health and safety information on nanomaterial exposure is an attempt to understand them in commerce (US Department of Commerce, 2018; US EPA, 2015b). Over time, this regulation may allow the EPA to obtain more information from the manufacturers about these products, but as NEP production continues to skyrocket, this will pose little-to-no safety presently for consumers who may potentially be exposed to these products daily without knowing it.

While use of nanotechnology in products does provide some promising benefits, such as improved drug delivery systems and drinking water treatment, both the acute and chronic adverse effects are largely unknown, especially concerning personal consumer NEPs, such as sunscreens, toothpaste, shampoos, lotions, and cosmetics (Adeleye et al., 2016; Kessler, 2011; Valavanidis & Vlachogianni, 2016). These products contain engineered nanomaterials (ENMs) that are designed or tailored for a specific purpose by varying physicochemical properties, such as chemical composition, small particle sizes, solubility, aggregation, and structures (Nel, Xia, Mädler, & Li, 2006; Park et al., 2017). Because of these unique properties that can be manipulated, ENMs are considerably more variable and unknown than naturally-occurring ambient nanoparticles.

ENM exposure can be primary or direct contact with the cell, where the ENMs elicit responses related to toxicity, DNA damage, inflammation, or oxidative stress, or secondary, such as causing inflammation in various body systems and alterations in organ functions (Armstead & Li, 2016; Nel et al., 2009; Nurkiewicz et al., 2011; Pal et al., 2015; Schrand, Dai, Schlager, & Hussain, 2012; Song et al., 2011; C. Watson et al., 2014; Watson, DeLoid, Pal, & Demokritou, 2016). Nanoparticles are known to have the ability to cross blood-brain, blood-testis, and blood-placental barriers, delaying risk assessment and regulations could have adverse effects on future generations and epigenetics (Lim, Baeg, Srinivasan, Dheen, & Bay, 2017; Martirosyan & Schneider, 2014; Miura & Shinohara, 2009).

Nanoparticles can take five main routes of exposure: inhalation, ingestion, ocular, dermal, and intravenous, also known as nanomedicine. The route of greatest concern to the public is the inhalation route because it is the most common route occupational workers and consumers are exposed to most frequently. It is easy for dry, airborne ENMs to mimic gas particles and agglomerate in the air and be transported further to various parts of the body (Yokel & MacPhail, 2011). When airborne particles containing ENMs are inhaled, these particles can settle in various regions of the respiratory tract depending on their size. Larger, more agglomerated particles tend to settle in the upper respiratory areas, such as the nasal cavity, which smaller particles can penetrate lower into the pulmonary regions of the respiratory tract. Given each of the pathways, ENMs can ultimately migrate to the circulatory system and settle in various organs, such as liver, however, if the gastrointestinal (GI) tract or nasal cavity is exposed to ENMs, they can alternatively migrate to the lymphatic system or brain, respectively (Yokel & MacPhail, 2011). Inhaled ENMs have been observed to have similar characteristics to known disease-causing agents, such as asbestos, particulate matter (PM), and silica, which warrant the

need for further research on the biological activity of ENMs after inhalation (Bunderson-Schelvan, Holian, & Hamilton, 2017).

Inhalation exposure is the most studied and has been linked to cardiorespiratory and mortality, especially since there can be large particles mixed in cities with high pollution (Kelly & Zhu, 2016; Miller et al., 2017). With ENMs being able to be deposited so compactly deep into the lungs and cause oxidative stress, it has been thought to have been linked to inflammation and breathing problems but also more serious disease outcomes such as asthma, airway and lung fibrosis, and cancer (Donaldson et al., 2005; Miller, Shaw, & Langrish, 2012; Nikota et al., 2016; Poulsen et al., 2015; Ryman-Rasmussen et al., 2009). It has also been suggested that nanoparticles may be able to translocate and circulate throughout the body and accumulate in organs, such as the liver and heart, and be associated with cardiovascular disease (Hirn et al., 2011; Husain et al., 2015; Miller et al., 2017; Mills et al., 2009; Oberdörster et al., 2002). ENMs have also been observed to trigger macrophages due to inflammation events in the lungs, which suggest that ENMs can cause cellular damage and may trigger specific activation sites for immune response (Huang et al., 2017; Tsugita, Morimoto, & Nakayama, 2017; C. Y. Watson et al., 2015). Though not all knowledge is known for inhalation exposure to ENMs, potential adverse effects can be based on existing knowledge of toxicological outcomes of inhaled particles or substances (Nikota et al., 2016; Puzyn, Leszczynska, & Leszczynski, 2009).

ENMs may be contained in products in a fixed form, which keeps the nanoparticles in place and tends to have a low potential to be released, and a free form, which has the highest risk of exposure to the public, as these are the nanoparticles found in everyday consumer products, such as cosmetics, food, and medicines (Boxall et al., 2007). The release of ENMs may depend

on concentration, frequency, and amount administered and researchers believe that the majority of the release will happen with consumer end-use, as opposed to during manufacturing (Boxall et al., 2007). The released airborne nanoparticles (rNPs) found in NEPs can function differently than the same pristine nanoparticles (pNPs) found in bulk as their toxicological, biologically, and chemical properties can change and they can be mixed with solvents or create volatile organic compounds (VOCs) or other compounds upon release (Nazarenko et al., 2011). In particular, added stabilizers, such as surfactants, polymers, and thiols have been observed to increase the mobility of nanoparticles (Boxall et al., 2007; Tungittiplakorn, Lion, Cohen, & Kim, 2004). Both these added chemicals and the form the consumer product is created in (e.g. whether it is a applied powder, liquid, or spray) can affect agglomeration of these particles, as well as chemically modifying them (Nazarenko et al., 2011). As products are modified, this can change the magnitude of effects ENMs have on humans as opposed to when humans are exposed to pNPs. pNPs have mainly been characterized, as opposed to rNPs, partially due to the fact that there are complex methods that need to be developed for testing (which can be time consuming and costly), deficits in knowledge of how they are prepared in NEPs, and uncertainties with dose metrics (Becker, Herzberg, Schulte, & Kolossa-Gehring, 2011). However, there are a few studies that have characterized aerosolized nanoparticle releases from NEPs (Nazarenko et al., 2011; Nazarenko, Zhen, Han, Lioy, & Mainelis, 2012; Pal, Watson, et al., 2015; D. Singh et al., 2017). It has been observed that there is a decrease in cellular viability that is found with increasing doses of smaller particles, which is not observed as readily with larger particles using the same delivered dose (Pal, Watson, et al., 2015; Watson-Wright, Singh, & Demokritou, 2017). In plastics that have metal oxides (such as TiO_2) or iron additives (such as Fe_2O_3) added, the emission of polycyclic aromatic hydrocarbons (PAHs) increased significantly after combustion

compared to plastics without these components (D. Singh et al., 2017; Watson-Wright et al., 2017). In cosmetic powders, the rNPs were determined to be delivered into both head airways and alveolar regions and can be delivered to all other regions of human respiratory system in agglomerates that vary in size and, when mixed with other ingredients and aerosolized, can affect distribution and potential toxic effects (Nazarenko et al., 2011, 2012). These results show the importance and need for understanding ENM transport mechanisms, dosimetry, comprehensive toxicological profiles, and interactions with different cell lines while updating and validating various toxicological testing methodology and realistic inhalation simulations in concert.

One of the potential disease outcomes related to ENM exposure is asthma. It has been observed that oxidative stress has a key role in pathogenesis of asthma by factors, such as causing increased airway inflammation and fibrotic changes in lung tissue and decreased defenses against oxidative stress in the form of antioxidants (Cho & Moon, 2010; Sahiner, Birben, Erzurum, Sackesen, & Kalayci, 2011). There is strong evidence that shows that ENMs (particularly those containing metals) create free radicals and thus can lead to either beginning or worsening allergic responses (Ihrie & Bonner, 2018; Johnson, Mendoza, Raghavendra, Podila, & Brown, 2017; Pal, Bello, Budhlall, Rogers, & Milton, 2011). This can be especially important when pertaining to applied consumer products, such as cosmetics, as factors, such as race, gender, location, diet, and socioeconomic status (SES) can all play a part in possibly magnified effects due to oxidative stress. For example, darkly-pigmented cosmetics aimed at being used by predominately African Americans or other darker races might contain more metal ENMs, such as Fe_2O_3, to provide more color to the product. This, in turn, can more adversely affect them due to racial differences in lung functions, decreased levels of antioxidants, and higher levels of oxidative stress and thus make African Americans a more susceptible population (Harik-Khan,

Muller, & Wise, 2004; Morris et al., 2012). Cheaper NEPs might also have different chemical formulations with various levels of ENMs, which could also make people that have low SES a more susceptible population. Other factors, such as sex differences, living in a highly polluted area, and diets low in antioxidants may contribute to higher risk to adverse effects due to ENM exposure (Cabello et al., 2015; Schulz et al., 2015; Shvedova et al., 2016; Sonane, Moin, & Satish, 2017).

To address current knowledge gaps regarding the safety of NEPs and potential human inhalation exposures to released nanoparticles (rNPs), we utilized human primary small airway epithelial cells (SAEC) and human SV40-immortalized bronchial epithelial cells (16HBE). These cell types are being utilized to assess how rNPs may have differing effects depending on their size and how they settle in the upper or lower respiratory tract. SAEC are more sensitive, reside the distal portion of the lungs and regulate immune responses through chemokines while 16HBE have been used a model to study the cystic fibrosis transmembrane conductance regulator (CFTR), reside in the bronchial walls form tight junctions and play a role in ion transport (Cozens et al., 1994; Crystal, Randell, Engelhardt, Voynow, & Sunday, 2008; Jiang, Malavia, Suresh, & George, 2009). Various toxicological assays were used to determine the impact of both pNP and rNP exposures. The pNPs were obtained in bulk and the rNPs were obtained using a custom-made exposure system by IEStechno to simulate real-world exposure scenarios and provide rNPs from NEPs to perform accurate toxicological assessments. A light and a dark shade of two brands of airbrush foundation makeup were selected as the NEPs known to have various rNPs, such as iron (III) oxide (Fe_2O_3) and titanium dioxide (TiO_2), as a part of its chemical formulation. The airbrush kit was assembled and collected in the exposure system for 20 minutes for each product, thoroughly cleaned after each use according to manufacturer

instructions. The SAEC and 16HBE were exposed for 24 hours to either pristine Fe_2O_3, TiO_2, or rNPs before assays were conducted. Cellular viability was examined using the MTS cell proliferation assay while oxidative stress and produced reactive oxygen species (ROS) were measured using the CellRox® Orange and total glutathione (GSH) assays. Differing levels of proteins were visualized using the immunocytochemistry (ICC) fluorescent assay and western blots were performed to visualize upregulation and downregulation of proteins involved in the epithelial–mesenchymal transition (EMT) pathway. The proposed hypothesis for this thesis is that the rNPs have higher toxicity profiles due to the adsorption of chemical additives than pNPs. With this data collected, this could suggest that rNPs, especially those that pose inhalation exposure risks, could warrant both more of a hazard to human and environmental health than pNPs alone and an even higher risk for vulnerable populations.

2. REVIEW OF THE LITERATURE

2.1 Evolution of Nanotechnology and Nanotoxicology

The terms “nanotechnology” and “nanomaterials” are becoming increasingly more important as more nanomaterial-containing chemicals are being manufactured. Not much is known about the mechanisms, distributions, toxicity to humans and the environment, or even potential therapeutic properties of nanomaterials, however, toxicological methodologies and technologies are rapidly advancing in detecting these substances. Nanomaterials are characterized as ultrafine particles that are <0.1μm in diameter (Hodgson, 2010). The smaller the diameter of a substance, the more toxicity increases, as these particles can reach more regions in the body and deposit in clusters. Nanomaterials can either be naturally occurring (ambient) or manufactured by man (ENMs). Ambient nanoparticles have varying shapes, compositions, and sizes while ENMs are uniform compounds (Hood, 2004). Ambient nanoparticles tend to be found in urban areas and near highways and their concentrations can fluctuate based on certain factors, such as traffic patterns, amounts of smoke and exhaust released, and seasons, while ENMs are manufactured and have a more controlled and consistent concentration. Ambient nanoparticles have been found to be mainly composed of silicon, carbon, oxygen, nitrogen, and sulfur while ENMs can consist of a wider range of elements (Johnston et al., 2013). With more elements introduced, it could potentially pose a wider array of risks on human health and could complicate analysis of specific health effects on future generations.

2.2 Engineered Nanomaterial Uses

ENMs are useful in a variety of sectors such as automotive, electronics, chemical and material industries, agriculture, energy, health and pharmaceuticals, biomedical, environmental,

metals and plastics, product safety, and cosmetics (Ostiguy & IRSST (Québec), 2010). One of the more popular uses for ENMs using silver nanoparticles (AgNPs) to improve fabric sterilization, water purification, and wound dressing, as compared to bulk silver (Musee, Thwala, & Nota, 2011). It also acts as an antibacterial agent because it is effective at protecting against fungi and antibiotic resistant strains of bacteria, such as *Streptococcus* sp (Musee et al., 2011). Other ENMs with antibacterial characteristics include carbon fullerenes (C_{60}), zinc oxide (ZnO), TiO_2, and single-walled carbon nanotubes (SWCNT) (Musee et al., 2011). These bacteria inhibiting properties found in these and other ENMs can be useful in the biomedical industry, such as being used to lower the viral load of HIV in HIV+ patients and protect the cells from apoptosis (Sun et al., 2005). There continues to be more applications found for ENMs for other public health problems, which, while could have some positive outcomes, could also unintentionally introduce chronic exposure to unknown levels of these materials in the environment and in humans using various mechanisms.

2.3 Routes of Exposure

As described in the introduction, there are five routes of exposure ENMs take, with the most pertinent route being inhalation. Another route of exposure ENMs take is through ingestion. Currently, little is known about adverse effects due to oral ingestion and the bioavailability of ENMs under the tongue (sublingual site) or mouth (buccal cavity) but the gastrointestinal (GI) tract does absorb some ENMs in areas where the gastric epithelial cells are compromised or where there is a low concentration of mucin (Yokel & MacPhail, 2011). Absorption into the GI tract depends on the size of the ENMs and the smaller ENMs are more likely to be absorbed more readily. A couple of *in vivo* fish studies have observed uptake of

AuNPs and cerium dioxide (CeO_2) into the GI tract via ingestion of ENMs at a size of 25 and 35 nm, respectively (Gaiser et al., 2009, 2011). By aquatic species biologically taking up and storing these ENMs in their tissues, this could potentially be a cause of concern for humans via exposure through eating fish or other related foods.

Ocular exposure can happen with airborne ENMs and can occur intentionally or unintentionally. Intentional exposure happens when cosmetics that contain ENMs are placed near the eye and unintentional exposure happens with chemical splashes in the eyes or transfer of ENMs off hands by rubbing eyes, which has been observed to happen to approximately 37% of adults per hour (Hendley, Wenzel, & Gwaltney, 1973). Through this route of exposure, ENMs can gain access inside of the body through the cornea into the eye or it can be drained into the nasal cavity (Yokel & MacPhail, 2011). There have been only a couple of studies that have researched the effects of nanoparticles on the ocular system, particularly ambient nanoparticles present in the ozone, and these studies have observed that graphene oxide (GO) and airborne TiO_2 have observed reversible eye damage via oxidative stress and ocular surface damage, respectively (Eom et al., 2016; Wu et al., 2016). Possible therapeutic interventions using ocular injections of various drugs containing nanoparticles are being examined for safety and toxicity (Mehra, Cai, Kuo, Hein, & Palakurthi, 2016).

Dermal exposure has also been studied very little and this type of exposure is observed to provide little harm because the skin serves as an impassible primary barrier to foreign agents and, thus, can protect the body from these potentially harmful agents. However, these materials may pass through the top layer of the outermost epidermis, known as the stratum corneum, into the second or third layer, known as the stratum granulosum and stratum spinosum, respectively. If ENMs penetrate these layers of the epidermis, there is little protection offered and these

materials may be absorbed by the circulatory and lymphatic system and may produce an immune response by triggering keratinocytes to release pro-inflammatory cytokines (Gopee et al., 2007). Consumer materials that may put the public at risk for dermal exposure include quantum dots, titania, gold, silver, and zinc oxides that are found in sunscreens, cosmetics, and other topical agents applied directly to the skin (Brouwer et al., 2016; Cao, Li, Tang, Chen, & Zhao, 2016). Drug carrier and delivery has also been studied for dermal effects due to ENM exposure but little is still known about the effects of delivering nanoparticle-based drugs through intact skin (Lademann et al., 2013). More research can also be done in determining risk of harmful effects from unintentional occupational dermal exposure (Brouwer et al., 2016).

Nanomedicine, or internally introducing nanomaterials intentionally inside of the body, is an up-and-coming technique that is gaining utilization in medical research and health care settings. This can involve performing Intra-peritoneal (IP) or intravenous (IV) injections of nanoparticles to deliver a drug that will circulate throughout the system or that can deposit into an organ, such as the liver, or can even target tumors (Armstead & Li, 2016). By injecting the nanoparticles directly into the body, it can bypass normal absorption processes but may accumulate in tissues and organs (Zhao & Castranova, 2011). One study looked at how intra-articular injected cobalt chromium (CoCr) affected male rats' reproductive systems and observed increases in abnormal sperm and testicular damage and physiological changes possibly due to oxidative stress (Wang et al., 2013). Another study looked at the same nanoparticle but injected peri-articular in mice to observe if there was a genotoxic effect or immune reaction and found that there was increased DNA damage in bone marrow, a heightened sensitivity to nickel and chromium, and more mice developed a Th1 driven response (Brown et al., 2013). Nanoparticles partnered with biodegradable polymers have also been studied as well to help increase blood

circulation and reduce deposition in the liver (Gref et al., 1994). Another revolutionary functionality discovered is nanocarriers that can be used for cancer treatments with a lower solubility than current treatment options to help effectively bind and specifically target cancerous cells (Luo et al., 2012; Peer et al., 2007). Nanoparticles have also been utilized in burn wards and have aided in sealing wounds and keeping out bacteria in severe burns (Jahromi et al., 2017). Quantum dots can also be used in diagnostic imaging used for more precise medical diagnoses (De Silva, 2007). Many aspects of nanomedicine could be explored to help revamp current medicine and medical practices to help treat public health related issues, but possibly negative implications could also come from using nanoparticles without conducting more toxicological testing.

These other routes of exposure taken by ENMs are important because they can also cause morbidity. For example, dermal exposure can lead to skin sensitization, which may translate to possible changes in absorption and disposition of the ENMs through the skin and into the body (Heylings et al., 1996; S. Smulders, Golanski, Smolders, Vanoirbeek, & Hoet, 2015). Ingestion of ENMs can lead to interruption of internal microbiota in the GI tract and inflammatory diseases (Bouwmeester, van der Zande, & Jepson, 2017; van den Brule et al., 2016). Ocular exposure to ENMs runs the risk of expressing reversible irritation and inflammation in the eye and cervical lymph nodes as well after multiple acute durations of exposure (Eom et al., 2016; Wu et al., 2016). Little is known about the long-term effects of direct injections of ENMs into whole-body systems but they are known to accumulate in various organs and tissues and increased immune response (Brown et al., 2013; Stijn Smulders et al., 2016). More research should be conducted on all routes of exposure to be able to accurately characterize the continuum of risks associated with ENM exposure to human and environmental health.

2.4 Inhalation Mechanisms of Engineered Nanomaterial Exposure

Since ENMs are have such a small diameter, they can penetrate deeper into the lungs, even into the distal lung region but still can deposit throughout the whole respiratory tract. They also tend to stick together and form agglomerates, which can create more surface area and be harder to dislodge them when breathing or coughing. The more time spent in the lungs, the more chance of causing adverse effects, such as generating ROS and oxidative stress. One upper respiratory clearance mechanism the human respiratory tract is equipped with is the mucociliary escalator, which is when mucous attempts to trap particles before they reach the alveoli to prevent damage (Hodgson, 2010).This escalator traps and pushes particles up into the trachea, where they can be swallowed and moved to the GI tract (Hodgson, 2010). This is the most common clearance method and transport depends on the amount of cilia and the lung lining layer (Kreyling & Scheuch, 2000) Another mechanism is lung phagocytosis, which can direct particles to the lymph, however, they can be stored there for a long residency period and it could cause damage (Hodgson, 2010). In clinical studies, nanoparticles have been observed to accumulate in the liver and spleen because of opsonization and the mononuclear phagocytic system (MPS) (Garcia et al, 2014). In fact, this has led to the development of zwitterionic-coatings to help make nanoparticles more biocompatible and reduce the risk of non-specific absorption of proteins or lipids (Pombo García et al., 2014). With further developments such as these, it can pave the way for nanoparticles to be used in more therapeutic manners and reduce side effects in individualized therapeutic interventions for a wide variety of diseases.

If the nanoparticles manage to sneak by the various innate clearance mechanisms, they may compromise lymphatic drainage, enter the blood stream, and disseminate into secondary

organs (Geiser & Kreyling, 2010). Since particle clearance kinetics in humans is extremely slow, this could mean that 10-20% of insoluble particles will never be cleared from the lungs and can be associated with potentially increased chances of fibrotic pathogenesis (Geiser & Kreyling, 2010). Even if the particles are translocated to the larynx interstitium, they may still either be taken up by epithelial cells or relocate and end up back on the surface of the lungs (Geiser & Kreyling, 2010). In addition to these effects, nanoparticles can also cause premature cell death, increase instances of exocytosis, can generate more ROS, inflammation, etc. (Fröhlich, 2016).

2.5 Pristine Nanoparticles Versus Real Exposure Methodologies

ENM exposure has typically been measured from pNPs, as compared to actual exposure, which can overestimate the harmful effects of ENMs (Pal, Watson, et al., 2015). By developing a protocol that follows the amount that is released and what can be captured based on the route of exposure, toxicological assessments can be conducted to get one step closer to developing dose-response curves and determining perceived versus actual risk. Real-time monitoring, as well as integrated monitoring, of the rNPs are integral parts to measuring exposure because it can help develop a cause-effect association between release of these nanomaterials and exposure (Pal, Watson, et al., 2015). One framework that has been used is the sampling, extraction, dispersion, and dosimetry (SEDD) methodology (Pal, Watson, et al., 2015). In this frame work, total particle numbers, size, distribution, mass concentration, and other physical, chemical, and morphological characteristics must be determined first for the particles so that it can provide a better understanding of the sites where they deposit in the lungs when inhaled (Pal, Watson, et al., 2015).This could be done using a vast array of equipment, including a water-based condensation particle counter to measure concentrations, both a scanning mobility particle sizer and an

aerodynamic particle sizer used to measure size distribution, a Q-track to measure environmental conditions during release, and a photo ionization-based system for measuring volatile organic compounds (VOCs) (Pal, Watson, et al., 2015).

The next step is to extract the sampled particles from collection impaction substrates by using aqueous extractions for extraction efficiencies greater than 90% or ethanol extractions for extraction efficiencies less than 90% (Pal, Watson, et al., 2015). These masses are then weighed using a gravimetric analysis technique to determine the total amount collected and particle extraction efficiencies can be calculated. The third step in this framework is measuring dispersion and colloidal characterization suspended in a liquid, which is of great importance to accurately measure the size of the particles, charge, conductivity, and any possible agglomerate activity that may form, thus affecting the surface area and penetrability into the lungs (Pal, Watson, et al., 2015).

Nanoparticle characterization of size and concentration can be measured using turnable resistance particle sizing (TRPS), which looks at changing ionic currents as the particles pass through a membrane with pores that have a certain nanometer size (Anderson, Kozak, Coleman, Jämting, & Trau, 2013; Kozak, Anderson, Vogel, et al., 2012; Kozak, Anderson, Grevett, & Trau, 2012; Pal et al., 2014). Mode, mean, percent cell viability and percentages can be calculated using individual measurements (Anderson et al., 2013). After this step, the doses obtained from *in vitro* experiments should be adjusted for *in vivo* to account for varying parameters, such as rates of respiration and breathing patterns and frequency, so it can be more accurately generalizable to humans. The relative *in vitro* dose (RID) and toxic doses at 50 and 90% (t50 and t90) can be calculated (Pal, Watson, et al., 2015)

The last step is to examine cell toxicity by studying toxicological or cellular responses, such as oxidative stress, cytotoxicity, and genotoxicity, as well as measuring the strength of the association of the dose-response curve (Pal, Watson, et al., 2015). This can be done using various *in vitro* assays that are commonly used in nanotoxicology, such as metabolic activity (MTS or MTT, CellTiter 96® Aqueous One (Promega)), which determines the capacity of cell metabolism by introducing a soluble tetrazolium salt to the cells and observe if it is metabolized, and lactate dehydrogenase (LDH), which determines if damage has incurred to cellular membranes by fluorescing based on how much lactate has been released from the cytoplasm of the damaged or dead cells. MTS and LDH are inversely related to each other because MTS determines cellular viability while LDH determines irreversible cell death. Another common way to measure cellular viability is using trypan blue to stain the deceased cells and is not taken up in living, healthy cells (Hillegass et al., 2010). CellRox™ or ROS-Glo H_2O_2™ are assays used for analyzing the effects of oxidative stress on exposed cells using stains and luminescence, respectively, to identify upregulation or downregulation of proteins involved with membranous proteins (Peruzynska et al., 2017). The clonogenic assay (CFE) shows affects after exposure by measuring cell proliferation, survival, and colony behavior for several weeks (Herzog et al., 2007). Other common assays to determine cytotoxicity include calcein AM, Live/Dead, alamar blue and neutral red (Hillegass et al., 2010).

Assays can also be conducted for examination of genotoxicity and gene expression. Two popular assays conducted for genotoxicity include the Ames assay, which uses *Salmonella typhimurium* and *Escherichia coli* to determine if the nanoparticles can cause mutations in DNA and allow colonies to grow on histidine-free media, and the Comet assay, which uses a custom gel with pores between 20 and 40 microns to assess single or double stranded DNA breaks by

visualization of DNA damage using SYBR gold stain (Ames, Durston, Yamasaki, & Lee, 1973; C. Watson et al., 2014). Other genotoxic assays include chromosomal aberration introduction and micronuclei and using oxidized guanine bases to determine point mutations (Fung, Kow, Van Houten, & Mossman, 1997; Mori et al., 2006). Gene expression can be measured by Northern blots, polymerase chain reaction (PCR), and various microarrays (Hillegass et al., 2010).

2.6 Engineered Nanomaterial Hazard Characterization

Various endpoints have been reported from hazard characterization from ENMs from oxidative stress, inflammation, genotoxicity, and cytotoxicity. For example, TiO_2 has been classified as possibly carcinogenic to humans (Group 2B) after inhalation and intratracheal exposure and has observed increased inflammation, changes in signal transduction, reduced DNA methylation, and epigenetic changes (Chen, Yan, & Li, 2014; Shi, Magaye, Castranova, & Zhao, 2013; Stoccoro et al., 2017). Genotoxic, oxidative, and inflammatory effects were also observed in transformed alveolar cells when exposed and bronchial cells having an increased susceptibility to cytotoxic events (Ursini et al., 2014). Genotoxicity can also be due to direct DNA damage from particles or indirect interactions with ROS created from toxic ions released from the ENMs (Barnes et al., 2008; Kisin et al., 2007; A. Kumar & Dhawan, 2013). Other genotoxic endpoints have observed that ENMs are unlikely to induce micronuclei and were able to damage DNA (which was able to be viewed more easily with acute, short exposure times because there is less time for DNA to be repaired) and possible increased cell transformation (Stoccoro et al., 2017). Overall, it has been observed that increased inflammatory response can lead to cytotoxic effects, oxidative stress caused by ROS created by ENMs can alter cell growth,

change can occur in the immune system or macrophage recruitment system, and the large, complex surface area of the agglomerated particles can lead to DNA damage (Tolaymat, El Badawy, Sequeira, & Genaidy, 2015).

Since there are currently many gaps in the knowledge about potentially harmful effects on humans and the environment from both ambient ENMs and NEPs, they are typically not evaluated in risk assessment (Handy, Owen, & Valsami-Jones, 2008; Klaine et al., 2012; Mitrano, Motellier, Clavaguera, & Nowack, 2015; Nowack & Bucheli, 2007). With more products being released on a daily basis without proper evidence of safety and health risks, the effects of ENMs in products could get more complicated with more variables, less certainty in associations, and aged throughout the products' life cycles (Mitrano et al., 2015). As products get altered, this can change the magnitude of effects ENMs have on humans as opposed to when humans are exposed to pristine ENMs. This could also change the structure, potential toxicity and risks, and transformation of the ENMs depending on route of exposure. For example, when inhaled, more secondary particles created from aerosolized ENMs may have a different or worse toxic effect on humans. By changing the coating, size, surfaces, and more of ENMs, it can alter their behavior and cause unpredictable effects.

2.7 Nano-enabled Products and Current Regulations

In 2007, the National Science Foundation estimated that $70 billion worth of NEPs were sold each year in the United States alone and manufacturers are not required to list ENMs on any products containing them (Bergeson et al., 2010; Kessler, 2011). In 2013, it was estimated that there was $1 trillion in global revenue from NEPs (NSF, 2014). Companies keep updating and changing various aspects of ENMs (there are at least 50,000 different types of SWCNT as of

2007) that make the need for research and regulation become more apparent (Schmidt, 2007). Currently, there is limited regulation for nanomaterials in the U.S. The United States Environmental Protection Agency (EPA) is trying to establish comprehensive regulatory activities and has tried to enact several control measures, such as limiting the use of nanoscale materials, requiring the use of personal protective equipment (PPE) when working with these particles, limiting environmental release, and requiring environmental and health tests to be done to determine how harmful these particles could be (US EPA, 2015b). Effective as of 2017, the EPA is requiring that there should be a one-time reporting and recordkeeping of existing exposure and health and safety information on nanomaterial exposure in an attempt to understand them in commerce (US EPA, 2015b). After data is collected, the EPA will then determine if any further measures are needed to address the use of nanomaterials. This could help control the use of nanoparticles down the road but, with the use of NEPs skyrocketing, regulations may not be able to keep up.

Regulations are important, not only because new products are being released, but old products are being reformulated with nanoparticles. While nanoparticles have been known to be present in paints, sunscreens, toothpaste, shampoos, lotions and cosmetics, it has also been found in edible products like food and dietary supplements (Kessler, 2011). Some of the food it is found in is chewing gum, salad dressings, candy and other sweets, and milk (Binh et al., 2015; Martirosyan & Schneider, 2014; Weir, Westerhoff, Fabricius, Hristovski, & von Goetz, 2012). There are currently a few studies that have made suggestions to guide a development of risk assessment in these food but still little is known or being done about the risks (Lim et al., 2017; Noonan, Whelton, Carlander, & Duncan, 2014; G. Singh, Stephan, Westerhoff, Carlander, & Duncan, 2014; Szakal et al., 2014). Even if there is little risk in ingesting or application of NEPs,

it can still get washed off in showers or excreted into waste water and runoff, which can affect freshwater ecosystems and other organisms that come in contact with the water (Binh et al., 2015).

As of 2013, according to the research conducted by Vance *et al.*, there 1814 consumer products from 622 companies in 32 countries that contain engineered nanomaterials (2015). About 30% of the products have been identified as containing nanomaterials suspended in liquid and most are intended to be used on the skin (Vance et al., 2015). Silver is the most used nanomaterial but almost half (49%) of products do not specify what nanomaterials are used in them (Vance et al., 2015). This reinforces the notion of the importance of swiftly continuing to characterize, test, and research ENMs and their potentially hazardous effects.

SiO_2, TiO_2, and carbon nanotubules are some of the more common ENMs found in NEPs (Schmidt, 2007; Sotiriou et al., 2014). Since there are so many NEPs released, there are some studies researching toxicological testing mechanisms, as well as designing safer nanoparticles that can be used instead to keep performance high with less risk to the environment and human health (Pal, Watson, et al., 2015; Sotiriou et al., 2014). Particle size and characterization alone cannot determine toxicological risks of ENM exposure, as it is also dependent on how they are released, what secondary and tertiary byproducts are created, and the interaction of biomolecules and cells within the body (Becker et al., 2011; A. E. Nel et al., 2009). There has been a lack of identifying safety of ENM because of lack of reliable tests, interference of ENMs with reagents in tests, incorrect characterization of ENMs or unknown methods for ENM synthesis (Howard, 2010; A. Kumar & Dhawan, 2013; Stone, Johnston, & Schins, 2009). Pristine nanomaterials have mainly been characterized, as opposed to released nanomaterials, partially due to the fact

that there are complex methods that need to be developed for testing (which can be time consuming and costly), deficits in knowledge of how they are prepared in NEPs, and uncertainties with dose metrics (Becker et al., 2011). However, there are a few studies that have characterized aerosolized nanoparticle releases and the results have indicated a need for further testing and characterization of the potential effects of released ENMs (Pal, Watson, et al., 2015; Vorbau, Hillemann, & Stintz, 2009).

2.8 Impact of Engineered Nanomaterial Exposure on Body Systems

Along with gaps in rNPs, gaps exist in knowing how ENMs affect body systems. However, there is some knowledge from physiological changes in the lungs, breasts, and brain. Adverse physiological effects in the lungs tend to be more prominent in small nanoparticles compared to their larger counterparts (Inoue et al., 2007). The lung tends to get mostly damaged by overproduction of ROS, lowering effectiveness of protective systems, and decreasing clearance by the mucociliary system (Inoue et al., 2007). ENM exposure can also disrupt cardiovascular homeostatic or increase effects of cardiovascular disease (Mann, Thompson, Shannahan, & Wingard, 2012). Identified vascular changes, such as increased vascular permeability, loss of reactivity, and increased vasoconstricted states have also been reported (Mann et al., 2012).

Epigenetic changes, genotoxic, and non-genotoxic effects have been observed in breast carcinoma tissue when exposed to quantum dots (Choi, Brown, Szyf, & Maysinger, 2008). ENMs have been observed to be possible endocrine disruptors or alter the endocrine system, which can contribute to fibrocystic disease of the breast and breast cancer (Iavicoli, Fontana, Leso, & Bergamaschi, 2013). Some nanoparticles are being used to aid in detecting breast cancer

cells, so doing further testing on the potential harms these can have on fatty tissues can aid in designing safer protocols for medical diagnoses and ambient exposure via all routes of exposure (C. S. S. R. Kumar, 2009).

ENM exposure impacts on the brain and the central nervous system (CNS) has been rarely studied thus far and, while some therapeutic and diagnostic treatments have been established, there is the potential of oxidative stress, among other components, to have adverse effects (Oberdörster, Elder, & Rinderknecht, 2009; Suh, Suslick, Stucky, & Suh, 2009). ENMs can transport through the blood brain barrier, the brain's protective shield, and settle in the CNS for an unknown amount of time and has been observed in testing dental resin, bonding systems, coatings on dentures, and other dental devices and substances composed of ENMs that are placed in close proximity to the brain (Feng et al., 2015). It has been observed that any contact with nanoparticles at higher doses, regardless of route of exposure, can result in significant uptake and exposure to fragile organs and systems, such as the CNS, and cause permanent damage (Minkel, 2007; Oberdörster et al., 2009). The brain and related organs is especially sensitive to ROS and can cause morphological and cellular changes in microglia and other biological targets, which show implications of much needed research in potential substantial neurotoxic properties of ENMs (Long, Saleh, Tilton, Lowry, & Veronesi, 2006).

2.9 Epithelial Mesenchymal Transition

Epithelial mesenchymal transition (EMT) is a process of diversifying cells of various tissues. It occurs when epithelial cells lose their polarity and migrate and become multipotent mesenchymal stem cells. The mesenchymal cells have more migratory properties, invasiveness, and a higher risk for apoptosis (Kalluri & Neilson, 2003). Molecules involved in the initiation of

EMT are transcription factors, expression of specific cell-surface and cytoskeletal proteins, production of Extracellular Matrix (EMC) degrading enzymes, and changes in the expression of specific microRNAs (Kalluri & Neilson, 2003).

There are three types of EMT that result in different severities of consequences. Type 1 does not cause fibrosis or is invasive, so it spreads easily throughout the body and can generate secondary epithelia (Kalluri & Neilson, 2003). Type 2 is associated with wound healing, tissue regeneration, and fibrosis and, unlike type 1 EMTs, they are only present with inflammation, and can lead to persistent inflammation and eventual organ damage (Kalluri & Neilson, 2003). Type 3 EMTs have undergone both epigenetic and genetic changes and favor overgrowth and creating tumors, which can lead to increased risk of developing many types of cancers (Kalluri & Neilson, 2003). EMT can cause cancer as it transforms cells, changes their morphology, increases motility and cell proliferation. Epithelial cells can also exhibit only a few characteristics of EMT, which can be considered partial EMT (Lamouille, Xu, & Derynck, 2014). There is also changes in regulation of gene expression, where some proteins may get upregulated and some downregulated. Examples of transcription factors that are activated early on with the mesenchymal cell transformation is SNAIL, TWIST, and zinc-finger-E-box-binding (ZEB) (Lamouille et al., 2014). These can lead to changes in other protein regulation levels, translational and transcriptional players, expression of non-coding RNAs, protein stability, and splicing (De Craene & Berx, 2013).

ROS also has been observed to act as a mediator to the EMT process (M. Li et al., 2016). However, many other factors can contribute to progression of EMT and can be further studied to gain more knowledge to prevent potential cancers and irreversible damage due to fibrosis or

other diseases. Currently, not too much is known about ENM exposure and its effect on EMT. However, one study showed that inhalation exposure to single-walled carbon nanotubes increase the incidence of K-ras oncogene mutations and inflammatory response, as well as increased induced micronuclei formations and nuclear protrusions (Shvedova et al., 2014). There is also evidence for ENMs developing ROS that may contribute to EMT (Tsuda & Gehr, 2014).

3. METHODS AND PROCEDURES

3.1 Pristine Nanoparticle Preparation

The pNPs used in this study were iron (III) oxide (Fe_2O_3) and titanium oxide (TiO_2) (Sigma-Aldrich, Missouri, USA). Approximately 10 mg of pNP powders were placed into 15 mL Falcon conical tubes in a disinfected fume hood using Georgia State University (GSU) approved safety measures and protocols. A 1 mg/mL suspension was prepared using a 1:1 ratio of powder to deionized H_2O (di H_2O) and vortexed until all the particles dispersed. One mL of each of these suspensions were transferred to new conical tubes and were sonicated using 75% amplitude for 4 minutes to minimize agglomerates (ThermoFisher /Branson Ultrasonics Sonifier S-250D), Massachusetts, USA). These particle suspensions were then diluted to 5, 10, 15, and 20 µg/mL concentrations using either Small Airway Basil Media (SABM, Lonza, Maryland, USA) supplemented with 3% heat inactivated fetal bovine serum (FBS) if exposing SAEC or Dulbecco's Modified Eagle's medium (DMEM, Corning Inc., New York, USA) supplemented with 3% FBS and 1% penicillin/streptomycin (P/S) if exposing 16HBE. Only 3% FBS was used in each exposure media to ensure minimal agglomerate formation. Each suspension was vortexed for 30 seconds before use to ensure complete mixing.

3.2 Released Nanoparticle Collection

3.2.1 Selection of Nano-enabled Products

The released aerosols were collected from four liquid NEPs known to contain each of the pNPs tested in this experiment in their chemical formulation in varying concentrations. These products were also chosen because of their novelty and abundance in the consumer market as cosmetics. Products for both lighter skin tones and darker skin tones were chosen to assess the

potentially differing levels of toxicity from exposure for Caucasian versus African American women. In addition, costly products that are thought to be of higher quality versus more affordable, lesser quality ones were both selected to try to establish an association between SES and levels of exposure. A basic summary of all ENMs evaluated can be observed below in Table 1.

3.2.2 Released Nanoparticle Exposure System

To collect released aerosolized particles from the NEPs in a controlled setting, an Aerosol Generation System was used, which consists of a glove box chamber, real time aerosol characterization instruments, and animal exposure chambers that are all controlled by fully automated custom software created and built by IEStechno (IES, Inc, West Virginia, USA). The instruments attached to the exposure system to measure real-time monitoring included a miniRAE 3000 (Honeywell, RAE systems) to measure VOCs, an air compressor (California Air Tools, San Diego, CA, USA), an air sampler with charcoal filter, DataRAM pDR-1500 Aerosol Monitor (ThermoFisher, Massachusetts, USA) to accurately measure active aerosol concentration, and laptop with software. An image of the Aerosol Generation System setup can be observed in Figure 1. To measure particle size and concentration, the TSI 3910 Nanoscan Nanoparticle Sizer (TSI, Inc., Minnesota, USA) was used to detect and size airborne particles between 10 – 1000 nm. A mannequin head was placed on rods inside of the chamber 10-12 inches away from the airbrush wand (per manufacturer instructions for consumer application of products) with a “breathing” hole put near the nose to simulate inhalation. The air compressor was set at 30 PSI and the computer software regulated a constant flow rate of air inside the chamber at 11 L/min. A steel enforced hose connected to the exposure chamber was attached to a vacuum output in a biosafety cabinet to create a closed system. Prior to collection, a test run

was conducted to ensure all connections were secure to each instrument and that the instruments and software displayed the correct settings and agreeable readings, as observed in Table 2.

Particles were collected on mixed cellulose ester (MCE, pore size =0.8 µm, diameter = 37 mm, SKC Inc., Pennsylvania, USA) membrane filter and support pad that were discharged of static and weighed before being placed in a cassette. The cassettes were sealed with electrical tape and attached to a hose on the outside of the exposure chamber. 8-10 drops of product were placed in the reservoir on top of the airbrush wand, as per manufacturer instructions for consumer use. The exposure was conducted for 20 minutes for each product and each filter was visibly checked for particles. Once each exposure was completed, the filter was removed and sealed while the entire chamber was thoroughly cleaned with 70% ethanol (EtOH) and allowed to dry to allow VOCs created from EtOH to dissipate. The filters were weighed after collection after discharging static which counted as a pre-extraction weight. The airbrush wand was removed, disassembled, and cleaned by pouring 70% EtOH in the reservoir and spraying it until no cosmetic residue was observed. This action was repeated with cleaning solution and di H_2O to ensure no contamination occurred when switching exposures between products. The particles collected on the filter were removed into an aqueous sonication solution by placing 5 mL of di H_2O into a sterilized plastic beaker and sonicated at 75% amplitude for 2 minutes. This solution represented a stock NEP solution that would be serially diluted into various concentrations of media upon exposure as described in the "Cell Exposure" section below. The filters were left to dry for 24 hours in a sterile fume hood and reweighed after discharging static to obtain the post-exposure weight. The pre-exposure weight was subtracted from the post-exposure weight to obtain the concentration of particles in milligrams (mg) and were converted to micrograms (µg) (Table 4).

3.3 Colloidal Characterization

Since the rNPs contain several different compounds that may exhibit various physico-chemical and toxicological properties, it is important to characterize them to determine structure activity relationships. To determine the colloidal characteristics of dispersed rNPs and pNPs, particle size distribution was conducted using dynamic light scattering (DLS). DLS was conducted using a laser to scatter photons throughout a suspension of complete media and NPs and detects the magnitude and direction the photons bounce off from each molecule in the sample (Cohen, DeLoid, Pyrgiotakis, & Demokritou, 2013). This method can calculate parameters such as volume, count rate, settling velocity, presence of agglomerates via intensity of particle sizes (size distributions), hydrodynamic diameter (average size of agglomerates in nanometers), and zeta potential (electrostatic charges) to determine particle interaction and stability.

To analyze inorganic particulate constituents of the suspensions, the scanning electron microscopy with energy dispersive X-ray spectroscopy (SEM-EDS) method was used. SEM-EDS provided data on morphological features of the NEPs, as well as an identification of metals (in percent) found in the formulation. These characterization assessments were performed at the Georgia Institute of Technology Institute of Electronics and Nanotechnology. To prepare the sample for SEM-EDS analysis, 1 mg/mL stock solutions for each released NEP was generated and 10 µL of each sample was placed on aluminum sample holder disks and dried for at least 24 hours in a dehumidifying chamber. The samples were vacuum sealed prior to analysis to ensure removal of residual hydration.

3.4 Cell Culture

SAEC were cultured using 21 mL of complete Small Airway Growth Media (SAGM, Lonza, Maryland, USA), which was prepared by adding the contents of SAGM SingleQuots™ Kit (Lonza, Catalog No. CC-4124, Maryland, USA), which contained growth factors, such as Bovine Pituitary Extract (BPE), Hydrocortisone, Triiodothyronine, human Epidermal Growth Factor (hEGF), Retinoic Acid, Epinephrine, Transferrin, Insulin, Gentamicin/Amphotericin-B, and Bovine Serum Albumin – Fatty Acid Free (BSA-FAF) into SABM and homogenizing thoroughly. 16HBE were cultured using 21 mL of complete DMEM supplemented with 10% FBS and 1% P/S. Both cell types were maintained in T-75 flasks in an incubator set at 37°C in a 5% CO_2 atmosphere. The media were changed every other day, or as it was necessary, and cells were monitored under a light microscope to visualize day-to-day morphology and confluency.

3.5 Cell Exposure to Pristine Nanoparticles and Released Nanoparticles

SAEC were subcultured from T-75 flasks into 96-well black plates (Corning Inc., New York, USA) before reaching a 100% complete cell monolayer using a saline buffer (Phosphate-buffered saline (PBS) or (4-(2-hydroxyethyl)-1-piperazineethanesulfonic acid) (HEPES), ThermoFisher, Massachusetts, USA), gentle cell dissociation reagent (GCDR, ThermoFisher, Massachusetts, USA), and trypsin neutralizing solution (TNS, Lonza, Maryland, USA). This was conducted by aspirating the existing media in the flask, adding 4 mL of HEPES to the flask, recapping and gently swirling, removing the HEPES, then placing 4 mL of GCDR into the flask. The cells were viewed under the light microscope every 2-3 minutes and gently agitated to help release the cells from the bottom of the flask into the suspension. After the cells were in suspension (taking about 10-15 minutes, depending on the age of the passage), 4 mL of TNS was

incorporated into the flask and the cell surface area was washed gently multiple times with the solution. A total of 8 mL of cell suspension was pipetted into a clean 15 mL conical tube and spun in a centrifuge at 250xg for 10 minutes. After centrifugation, the supernatant from the conical tube was discarded and the cell pellet was resuspended in 1 mL of SAGM. Cell number and viability was visualized using a hemocytometer with 10 µL of cell suspension mixed with 10 µL of 0.4% Trypan Blue Solution (ThermoFisher, Massachusetts, USA). Dilution of the cell suspension into SAGM was calculated using a guideline of a cell density of 2,200 cells/well. The 96-well plates were seeded using 100 µL of the diluted cell suspension. The media was replaced after 24 hours and cells were used for exposure after 2-3 days, or when 80-90% confluency was reached.

16HBE cells were subcultured in a similar fashion, apart from using a 1:4 ratio of complete DMEM media and recovered cells. Trypsin (0.25%, Corning, New York, USA) was utilized instead of GCDR as they are a cell line and are less sensitive to damage from trypsin. In addition, 16HBE cells are smaller and tend to proliferate more rapidly than primary SAEC, thus trypsin ensured that all the cells were collected off the flask and into suspension. When placed into 96-well plates, the cells were confluent enough for exposure within 24-48 hours.

Once the cells on the 96-well plates reached optimal confluency, the media was aspirated, and cells were washed 3x with 200 µL PBS. After ENM suspensions and dilutions were prepared for that day as per “Pristine Nanoparticle Preparation” instructions above, 50 µL of SABM + 3% FBS (or DMEM exposure media for the 16HBE cells) were added to all wells, as well as exposed to 50 µL of the designated ENM suspensions with the various concentrations listed above. The positive and negative controls were not exposed to any ENM suspension and were instead given 100 µL of exposure media. The positive controls are listed in each assays’ sections

that follow. The cells were exposed for a period of 24 hours. After the exposures concluded, various assays were conducted to measure the endpoints for this research including quantitative and qualitative analysis of oxidative stress due to reactive oxygen species (ROS) created by rNPs and pNPs, cellular viability, and epithelial mesenchymal transition (EMT) via immunohistochemistry and western blot.

3.6 Reactive Oxygen Species Generation

ENMs produce ROS that can have copious deleterious effects on normal, healthy cells. The CellRox® Oxidative Stress Orange Reagent (Invitrogen, California, USA), which localized in the cytoplasm, was utilized to detect and visualize interaction of ROS with live cells post-exposure to ENMs. The positive control for this assay was made using a stock solution of 100 µL hydrogen peroxide into 10 mL of PBS and adding 100 µL of this dilution to the positive control cells. The reagent was prepared by combining 10 µL of CellRox® Orange to 5 mL of PBS to create a 5 µM concentration and covered in tin foil until use.

This assay was conducted by removing the ENM particle suspension from the cells and cells were washed 2x with 200 µL of PBS. Fifty µL of the prepared reagent was added to the cells and incubated in the dark at 37°C for 30 minutes. After incubation, the reagent was removed, and cells were washed 3x with 200 µL of PBS. To fix cells, 50 µL 3% paraformaldehyde (Invitrogen, California, USA) was added for 15 minutes, removed, and cells were washed 2x with 200 µL of PBS before adding 100 µL of PBS to keep cells in solution. The relative fluorescence intensities were analyzed and imaged using a fluorescent microscope (EVOS FL Auto 2, ThermoFisher, Massachusetts, USA) using excitation/emission maxima of ~ 545/565 nm.

3.7 Total Glutathione Assessments

Glutathione (GSH) is an antioxidant normally found in eukaryotic cells. GSH is a three-amino acid polypeptide used as an indicator for oxidative stress. The GSH-Glo™ assay (Promega, Wisconsin, USA) was a luminescent assay used that measured total glutathione levels in cells and served as a quantitative validation for the CellRox® assay in this study. The positive control for this assay was made using a stock solution of 100 µL hydrogen peroxide into 10 mL of PBS and adding 100 µL of this dilution to the positive control cells. This assay works by transforming Luciferin-NT, catalyzed by the enzyme Glutathione S-Transferase, into Luciferin when GSH is present, producing a detectable light emission.

When the GSH-Glo™ Reagent 1X was prepared, 10 µL of Luciferin-NT and Glutathione S-Transferase were each added to every 1 mL of GSH-Glo™ Reaction Buffer that was needed and the reagent was deposited into a 15-mL conical tube and shielded from light. When the Luciferin Detection Reagent was prepared, a bottle of reconstitution buffer with esterase was combined with the bottle of Luciferin Detection Reagent and mixed by inversion until fully dissolved. This assay was conducted by removing the ENM particle suspension from the cells and washing them 2x with 200 µL of PBS. Fifty µL of GSH-Glo™ Reagent 1X was added to the wells, shaken briefly, then incubated at room temperature for 30 minutes. After incubation was complete, 50 µL of Luciferin Detection Reagent was added to the wells, shaken briefly, and incubated at room temperature for 15 minutes. Luminescence was then measured in a microplate reader (EnSpire by PerkinElmer/Cytation5 by BioTek).

3.8 Cellular Viability Evaluations

Cellular viability was assessed using the 3-(4,5-dimethylthiazol-2-yl)-2,5-

diphenyltetrazolium bromide (MTS) colorimetric assay (CellTiter 96 Aqueous One Solution, Promega, Wisconsin, USA). The MTS assay measured the cells' metabolic activity by introducing tetrazolium salt to determine the metabolic capacity of cells after exposure to rNPs and pNPs. Prior to conducting the MTS assay, 10 µL of 10X lysis solution (Promega, Wisconsin, USA) was added to positive control wells for 10-15 minutes. The MTS reagent was prepared making a 1:10 dilution of the reagent into SABM/DMEM, vortexed thoroughly, and shielded from light. This assay was conducted by first removing the particle suspension and washing cells 2x with 200 µL PBS. Next, 100 µL of the prepared MTS reagent was administered to each well and incubated at 37°C for 1 hour, while examining periodically for color change. After incubation, the absorbance of each well/plate was analyzed by a fluorescent microplate reader (EnSpire by PerkinElmer/Cytation5 by BioTek) at 490nm.

3.9 Epithelial-mesenchymal transition

EMT is a biological process that occurs when epithelial cells lose their adhesive properties during inflammation and transform into fibroblasts (Kalluri & Neilson, 2003). Once these epithelial cells display fibroblast or myofibroblast phenotype, they can translocate to the extracellular matrix, where they accumulate, and fibrosis can begin to occur (Guarino, Tosoni, & Nebuloni, 2009). This study looked at 2 proteins related to EMT: E-cadherin and vimentin. The immunocytochemistry (ICC) assay (R&D Systems, Minnesota, USA) contained 2 fluorescent antibodies to stain (pseudo-white and green fluorescent protein (GFP)) and visualize protein levels differences of E-cadherin and vimentin, respectively. A 4',6-diamidino-2-phenylindole (DAPI, Thermofisher, Massachusetts, USA) stain was utilized to visualize cell nuclei. Transforming growth factor beta (TGFβ, R & D Systems, Minnesota, USA) served as the

positive control for this assay as it has been known to trigger EMT and 1.5 µL of 2 µg/mL stock was added 24 hours before the assay was conducted (Guarino et al., 2009).

This assay was conducted by removing the ENM particle suspension from the cells and washing them 2x with 200 µL of PBS. Cells were fixed by adding 50 µL of 3% paraformaldehyde (Invitrogen, California, USA) for 15 minutes then washed off 1x with 200 µL of PBS. To block, 100 µL of 3% Bovine Serum Albumin (BSA) blocking agent (Invitrogen, California, USA) was added to the cells and incubated at 37°C for 1 hour. After incubation, 35 µL of both stains were pipetted into 245 µL of 3% BSA solution and 45 µL of this stain solution was added to wells and incubated from 1.5-3 hours at 37°C. After completion of the previous step, cells were washed 2x with 200 µL of PBS and 100 µL of PBS was added along with one drop of DAPI for 20 minutes then imaged using a fluorescent microscope (EVOS FL Auto 2, ThermoFisher, Massachusetts, USA).

3.10 Protein Expression

To determine if there were detectable differences in EMT-related protein levels between treatments and exposure time frames, western blots were conducted. To extract the protein lysates, 6 well plates were seeded at a cell density of 3,000 cells/well and grew until 80-90% confluency. Once confluent, dilutions of the rNPs and pNPs were conducted and the cells were exposed for either 24 hours, 7 days, or 21 days. Protein extraction was conducted by removing the spent exposure and adding 10 µL Halt™ Protease Inhibitor Cocktail 100X (ThermoFisher, Massachusetts, USA) to every 1 mL Mammalian Protein Extraction Reagent (M-PER™, ThermoFisher, Massachusetts, USA). This solution was applied to the cells and the wells were scraped using a cell scraper to remove all the cells adherent to the plate. These protein lysates

were collected into microcentrifuge tubes and spun at max speed (13,000 x g) for 10 minutes. The supernatant was collected into sterile microcentrifuge tubes and frozen in -80 °C until use for western blot.

Prior to conducting western blots, a Bradford protein assay (Thermofisher, Massachusetts, USA) was conducted to determine the protein concentration found in each lysate. The protein concentration determined what percent polyacrylamide gel was best to use and how much lysate to load in each well of the gel. 10 µL of a protein marker was used on each gel and gels were run at 80 V for 2 hours. When transferring the proteins to blotting paper, once the cassettes were assembled with a tight seal, they were covered in ice and the transfer was run at 0.35 A for 2 hours. After the transfer was complete, the blots were submerged in Ponceau S stain (Sigma Aldrich, Missouri, USA) for a few minutes, then rinsed with mixture of tris-buffered saline (TBS) and Tween 20 (TBST) until coloration disappeared. The blots were blocked 20-30 minutes in a 10% skim milk solution with primary antibodies (either E-cadherin, vimentin, and beta-actin or Glyceraldehyde-3-phosphate dehydrogenase (GAPDH) as the positive control), rinsed, and stored overnight at 4°C. The next day, 10 µL of secondary antibodies (either mouse or rabbit) were added to 10 mL BSA. The blots were washed 3 times for 5 minutes each with 1X TBST on a shaker. The gels were cut based on protein size and were covered in the secondary antibody solution for two hours and then developed on films or visualized electronically (Amersham™ Imager 680, GE Healthcare Life Sciences, Pennsylvania, USA).

ImageJ (NIH, Maryland, USA) was used to analyze protein intensities and changes in expression quantitatively. This was conducted by converting each image into greyscale (8-bit) and outlining each lane to obtain a profile plot for each band. The profile plots displayed peaks of intensity found within each band, along with any background noise the western blot may have

generated. Each peak was closed off and each area obtained was converted to percent value of the standard (negative control for each gel). Relative density was calculated by dividing the percent value for each sample by the percent value for the negative control. To correct for any possible unequal protein loading errors during western blots, adjusted densities were calculated by dividing the relative density from each sample from either E-cadherin or vimentin by the relative density of the same sample from Beta-actin (loading-control). This procedure was conducted for each gel and protein analyzed.

4. RESULTS

4.1 Selection of Nano-enabled Products

Cosmetics are one of the more widely used products that are known to contain ENMs, as well as metal NPs (Contado, 2015). The guiding framework that was used to select the specific NEPs included in this study was based on a panel of emerging products that are increasing in popularity amongst various consumers and products that contained a high amount of metal NPs. The following selection criteria were also used: **(1)** Two brands of cosmetics with different price points were chosen to address a possible differing level of exposure risk between higher and lower levels SES; **(2)** Light and dark shades of each brand were chosen to address any potential differences in toxicity and chemical makeup that could influence health disparities and outcomes for different races.

4.2 Detection of Metal Nanoparticles in Selected Nano-Enabled Products

To determine the metal composition and indirectly determine the amount of metal NPs of each selected NEP, we employed inductively coupled plasma mass spectrometry (ICP-MS). In Figure 2, the metal composition of each selected NEP was labeled and displayed in parts-per-million (ppm) or parts-per-billion (ppb). “Cosmetic Line 1” represents the expensive brand and “Cosmetic Line 2” was the inexpensive brand. Both AA4 and S4 were composed of aluminum (Al), magnesium (Mg), iron (Fe), and titanium (Ti), with most of the abundance belonging to the latter two metals. Although both products were darker shades, AA4 had close to 30,000 ppm of Ti and about 5,000 ppm of Fe, while S4 had almost equivalent quantities of Fe and Ti (~30,000 ppm). The other shades included in the figure have considerably less metal composition. S1 was the lightest shade available from Cosmetic Line 1 and Ti was still observed within its

composition (Figure 2). The lightest shade of Cosmetic Line 2 (AA8) was chosen to be comparable to S1. AA9 was not chosen as it was not a foundation and was meant to be applied as a shimmer over the initial layer of makeup. Given the prevalence of Fe_2O_3 and TiO_2 within the products, they were selected as the most relevant pNPs of interest.

4.3 Monitoring of Aerosolized Nano-enabled Products

To monitor the concentration of released rNPs during normal consumer usage of about 20 minutes, proprietary software provided by IES Tech was used. The Aerosol Generation System was set to regulate the total concentration level of 10 mg/m^3 in the chamber and each exposure reached that threshold limit, as observed in Figure 3, before decreasing until a safe level (<1 mg/m^3) was reached. The average concentration over the total duration was recorded with the highest average concentrations observed in both darker shades and the lowest average concentration observed in AA8. AA4 also had the most gradual and consistent increase in concentration, as compared to the other rNPs (Figure 3).

4.3.1 Aerodynamic diameter of Nano-enabled Products

In addition to recording the concentrations over the duration of exposure, we employed scanning mobility particle sizer analysis (SMPS) for S4 to assess the aerodynamic diameter during consumer usage. In Figure 4, the SMPS data for S4 was observed during the same exposure as S4 in Figure 3. In Figure 4, the mean particle diameter size aerosolized from S4 ranged from 0 to ~180 nm, with both particle concentration (>6,000 particles/cm^3) and average particles count (~500) peaking at ~125 nm. The highest particle concentration was observed at or below this threshold, which indicates that, when aerosolized, S4 produces many small particles that agglomerate in elevated concentrations. Subsequently, we observed the smallest

particle concentration and average particle count with the largest particles (~180 nm), indicating there were less of these larger particles present during exposure to S4. There was a large decrease observed as the exposure finished and the concentration of particles decreased to a safe level. The data indicated that there was a substantial amount of ultrafine (nano) particles present in S4 in high concentrations, which warranted the need for toxicological investigation for inhalation exposure.

4.4 Offline Physico-chemical Characterization of Released Nanoparticles

4.4.1 Scanning Electron Microscopy with Energy Dispersive Spectroscopy

To understand the physical topography and elemental composition of the sampled/ collected rNPs, Scanning Electron Microscopy with Energy Dispersive Spectroscopy (SEM-EDS) was utilized and the results can be observed in Figure 5 and Table 3. Figure 4 displays the morphology of each rNP observed using SEM that was taken from a 1 mg/mL sonicated stock suspension of each rNP. There were observed agglomerations in all images but AA4 had the most complex looking structure, as it was observed to be layered with a more uneven textured appearance than the three other rNPs. AA8 was observed to have the smallest particle sizes and numerous agglomerates of differing sizes scattered around the field of view. S1 and S4 appeared nearly identical, save the additional agglomeration and particles found in S4. Visualizing the sizes of these particles may provide evidence that can be complimentary with the toxicological assessment results to understand how agglomeration and particle size may affect the toxicological outcomes of cells.

In Table 3, a comprehensive elemental assessment was provided for each of the rNPs to provide more information of chemical formulation differences between the shades and brands.

Each rNP had a differing number of elements, as each of the detected "spectra" labeled on Figure 4 emitted X-rays for specific elements contained within their agglomerates as "peaks" based on the abundance of each element. Information displayed on the table included sample name, the elements examined in each product, line type (electron shell that was filled by an electron when vacant), apparent concentration, k ratio, percent weight of each element (Wt%), percent weight σ (error, Wt% Sigma), and standard label. The two pNPs tested in this study were bolded with red text for each sample and all percent weights were sorted in descending order. Three out of the four rNPs had titanium (Ti) within their composition with the largest percent weight in AA8 at 52.19%, followed by S1 with 38.79%. This outcome was expected as AA8 and S1 were the lighter shades of product and Ti powder is white and commonly used to lighten the pigments in various NEPs. However, AA8 was the only rNP that does not have aluminum (Al) or oxygen (O) within its composition but instead had bromine as its only other element reported (47.81%), which might contribute to the smaller particle size observed in Figure 5. Iron (Fe) made up over 65% of AA4's composition, which would explain why it was such a dark shade and could have impacts on toxicity. S4 was the only product that had both Ti and Fe within its composition, which together made up over 50% of its overall composition. S4 also had a total of 4 reported elements as its composition, which was the most out of all rNPs tested. Since S4 was darker and part of the more expensive cosmetic line, it could explain the slightly more complex elemental composition compared to AA4 and AA8.

4.5 Extraction of Sampled Aerosolized Nano-enabled Products from Collection Media

4.5.1 Filter Weights and Calculations

Aerosolized NEPs were sampled and the resulting rNPs were collected onto mixed cellulose ester filters (MCE). The rNPs were then extracted using aqueous sonication method (see extraction protocol in Methods and Protocols section). In Table 4, the pre- and post-extraction filter weights were measured on a balance and milligrams (mg) of mass collected were calculated by subtracting those values. To convert from mg to micrograms (µg), the mass collected was multiplied by 1,000 and divided by the amount of deionized water (di H_2O) used to sonicate the particles off the filter into a stock suspension (5 mL). This provided the percent of total mass collected off filter. The darker shades (AA4 and S4) accumulated the greatest amounts of particles on the filter during real time exposure.

4.6 Colloidal Characterization

4.6.1 Colloidal Properties of Raw Products, Released Nanoparticles, and Pristine Nanoparticles

The colloidal properties of the raw or whole product, rNP and pNPs were tested to determine how factors such as size distribution and zeta potential might affect toxicity and cellular responses. In Table 5, dynamic light scattering (DLS) values for raw products, rNPs, and pNPs colloidal properties were listed, with pNPs serving as the reference controls. These values were conducted in triplicate with means and standard deviations reported on the table. Values that were unable to be collected were listed as "N/A". Only raw product data was collected for the darker shaded cosmetics, as those were hypothesized to be the most toxic. Each sample was diluted in either di H_2O or exposure media used for SAEC and 16HBE (SABM and DMEM, respectively) that contained 3% FBS. Column 3 displays the hydrodynamic diameter with S1 and S4 (in both raw and released) had a more noticeably larger hydrodynamic diameter in all types of media, compared to the other raw and released products. The raw products had the largest

diameters in SABM, while, except for Fe_2O_3, all other samples had the smallest diameter when diluted in the same media. Out of all the rNPs, AA4, AA8, and S1 had the largest hydrodynamic diameter when dispersed in di H_2O, while S4 had a slightly larger hydrodynamic diameter in DMEM. Light shades AA8 and S1 varied considerably in size, as AA8 had the smallest hydrodynamic diameters in every media compared to all the samples and S1 had the largest for rNPs, especially in di H_2O. Fe_2O_3 had almost doubled in size when comparing dispersion in di H_2O to SABM. The opposite trend was apparent in TiO_2.

Polydispersity Index (PdI) was used to determine the uniformity of the colloidal suspensions. According to column 4 on Table 5, TiO_2 had the lowest PdI out of all samples in both exposure media, therefore had the most uniformity. AA8 was the only rNP that had the most similar uniformity as the raw products, followed by AA4. Both S1 and S4 had much higher PdI values in all types of dispersion media, suggesting that there could be particles of contrasting sizes present, which could affect exposure and toxicity outcomes.

The zeta potential of samples determined how positive or negative the pNPs and rNPs were, thus influencing their surface chemistry. The most notable zeta potential values on Table 5 belonged to both darker shades of cosmetics AA4 and S4 and were extremely negative in both exposure media compared to the other samples. The only positive values for zeta potential were for the raw product AA4 dispersed in di H_2O, S4 in SABM, and pNP Fe_2O_3 in di H_2O. Pristine Fe_2O_3 was also observed as moderately negative when dispersed in SABM but still less negative than AA4 and S4.

Conductance measured the amount of current that was permitted to pass through the substance. In Table 5, both the darker shades AA4 and S4 were highly conductive in both the cell media but had little-to-no conductivity in di H_2O. Fe_2O_3 also had a high conductivity when

dispersed in SABM and was only slightly higher than AA4 and S4. All samples have a conductance value of <2.2 when dispersed in di H_2O.

4.7 Comparative Toxicological Assessments of Pristine and Released Nanoparticles

4.7.1 Rationale

SAEC and 16HBE cells were chosen for this study because they each represent an important cell type found in the lungs that were potential targets of NEP exposures during consumer usage. 16HBE are smaller and reside in the upper airways while SAEC are larger and reside in the distal regions of the lung. Since ultrafine particles tend to agglomerate and penetrate deeper into the lungs, it was expected that SAEC might experience greater effects when exposed. Since human bronchial cells are exposed at a higher frequency to xenobiotic insults, they may be inherently more tolerant and resilient to airborne insults in comparison to SAEC. Furthermore, we chose to compare human, primary SAEC and an immortalized cell line 16HBE to understand the difference in sensitivity, susceptibility, and toxicity on using these two types of cells with acute exposure to pNPs and rNPs. Thus, these cell types were chosen to mimic and model inhalation exposures of NEPs. There is an increasing trend in the cosmetic industry to aerosolize products that have never been tested before with regard to pulmonary exposures. A product may be deemed “safe” but, unless studied intensely and tested thoroughly before release into the market, it may become more toxic when introduced to other exposure routes. Importantly, the assessed NEPs or cosmetics were determined “safe” for dermal exposure and application only using irritation and sensitization assessments. Companies that are choosing to use ENMs in their products may be seeking better visibility using these materials as a marketing strategy, which may overshadow safety considerations. The hypotheses that were analyzed during this study

were as follows: **(1)** The rNPs may be more toxic than pNPs due to enhanced toxicological effects mediated by their complex composition. **(2)** The darker shades of cosmetics (AA4 and S4) may exhibit the most toxic effects because of higher levels of constituent metal NP, thereby posing more risk for medium and darker skinned individuals. **(3)** The inexpensive brand of cosmetics (AA, cosmetic line 2 in Figure 2) may exert more toxic effects and pose more risk for individuals with lower SES because of detected contaminants such as arsenic and lead that may be the result of manufacturing or the use of poorer quality materials.

4.7.2 Reactive Oxygen Species Generation Assessment

ROS generation and resulting oxidative stress can affect cellular functioning, signaling, and viability that may eventually lead to inflammation, cardiovascular disease, and other adverse health outcomes. First, preliminary data was gathered to assess if raw product AA4 would produce ROS. Figure 6 demonstrated a serial dilution of AA4 in SABM with SAEC with an addition of DAPI stain to visualize the nuclei. Through this serial dilution, it was observed that the oxidative stress peaked at 1-400 dilution (Panel C) and decreased with increased dilutions (Panels D and E). This image confirmed that there was ROS generated after 24-hour exposure to AA4. This information helped detect the dose-response relationship for AA4 and SAEC, which can be applied to other products.

Figures 7-12 presented detection of ROS using a fluorescent permeating dye that had an excitation/emission maxima of ~ 545/565 nm. Fe_2O_3, TiO_2 and the rNPs were exposed for 24 hours according to the “Cell Exposure” section of Methods and Protocols above using 5, 10, 15, and 20 µg concentrations. These concentrations were compared to a negative control consisting of cells being only exposed to exposure media during the 24-hour period. SAEC had increased ROS levels occur with every treatment compared to 16HBE, indicating that SAEC were more

sensitive to generation of ROS upon exposure even only after 24 hours. Comparing the pNPs (Figures 7 and 8), TiO_2 produced significant amounts ROS with the 10 µg dose and became less noticeable at 15 µg. Fe_2O_3 induced a small but visible increase in ROS as concentration increases, which was also observed in 16HBE. Regarding the rNPs (Figures 9-12), ROS were generated by each treatment in SAEC. AA4, like Fe_2O_3, elicited higher levels of ROS due to the 10 µg dose and less at 15 µg. AA8 had an ample but consistent amount of ROS production at all doses, like the other light shade S1. S4 exposure induced increased ROS in both 10 and 15 µg doses for SAEC. For 16HBE, the only prominent increases in ROS were for AA4 and S4 exposures at 15 µg.

4.7.3 Total Glutathione - GSH

To determine oxidative stress quantitatively, the total GSH assay was conducted with an additional dose of 20 µg (Figures 13 and 14). Data was normalized and analyzed for significance using ordinary one-way ANOVA testing followed by Dunnett's test with alpha = 0.05. SAEC GSH were affected with each treatment and several values were deemed to be significant. For the highest dose of Fe_2O_3 (Figure 13, panel A), total GSH production was reduced by 50% compared to the negative control ($p < 0.0001$). TiO_2 displayed a steady decline in panel B with the highest dose having slightly increased luminescence than 20 µg Fe_2O_3. On Figure 14, AA4 (panel A) and S1 (panel C) induced more than a 50% decrease in luminescence for SAEC but AA4 was found to be significant in 3 out of the 4 doses administered, with the lowest dose (5 µg) mean being 71.6874. S4 exposures (panel D) caused a significant decrease in GSH for 3 of the 4 doses but lesser than AA4. The lighter shades AA8 (panel B) and S1 (panel C) appeared to display similar shapes in their graphs, with 20 µg S1 being the exception, which indicates that there was less oxidative stress compared to the darker shades of rNPs. In comparison to SAEC, 16HBE was not

significantly affected by any doses or treatments and, in fact, continued to proliferate more than the negative control in most cases. The only significant values were determined in Figure 14 at the 5 µg dose for S1 and S4 (panels G and H, respectively) for increased proliferation compared to the negative control ($p = 0.0182$ and $p=0.0357$, respectively).

4.7.4 Cellular Viability – MTS

To determine the effects of pNPs and rNPs exposures on cellular viability, the MTS assay was conducted for 5, 10, 15 and 20 µg doses (Figures 15 and 16). Data was calculated as described above in the "Total Glutathione - GSH" section. The viability of SAEC was affected by all treatments significantly with at least one dose. Both pNPs displayed a decreasing linear trend with 15 and 20 µg doses of TiO_2 having $p < 0.0001$ (Figure 15, panel B). For the rNPs (Figure 15), AA4 had the most uniform decreasing linear trend with the highest concentration reducing SAEC viability by about 40% (panel A). S4 significantly reduced viability with each dose but, apart from the 15 µg dose, the mean of each hovered around 75-77%, or a 23-25% reduction in cell viability (panel D). S1 had a reduction in viability except for 20 µg, which increased possibly due to human error (panel C). AA8 was the only released treatment that had only one significant value, which was 20 µg, and had a less linear shape and more cosine-like, with wider standard deviations compared to the other treatments (panel B). 16HBE did not have any significant decrease in cellular viability as compared to SAEC but the largest decrease was observed for 20 µg S1 and S4 by about 15% (Figure 16, panels G and H).

4.7.5 Epithelial Mesenchymal Transition - Immunocytochemistry

After determining that SAEC were more sensitive to exposure to ENMs acutely at the previously described concentrations, the immunocytochemistry (ICC) fluorochrome assay was conducted to see if any phenotypic changes occurred after exposure to 5, 10, and 20 µg

concentrations of either pristine Fe_2O_3 or released AA4. Due to financial and time constraints, AA4 was the only rNP that the ICC assay was conducted on and was chosen based on its heightened toxicity compared to the other rNPs. The results of 24-hour exposure can be observed in Figure 17. For this assay, the proteins E-cadherin and vimentin were visualized, using pseudo-white and green fluorophores, respectively. The nuclei were also stained blue with DAPI in the AA4 treatment. According to the EMT pathway, a decrease in E-cadherin expression can lead to increased vimentin expression. Since E-cadherin is involved with adherence, this decrease can be associated with morphologic change. In the negative control, all the proteins were readily observed but, with the 5 µg Fe_2O_3 concentration, a decrease in E-cadherin was observed with primarily vimentin. At the 10 µg concentration, vimentin was observed to be less prominent and at 20 µg, vimentin was the only protein visualized. For the AA4 exposures, it was difficult to visualize the stains based on poor washing or human error in techniques, however the cells were not as tightly formed together as they were with Fe_2O_3, suggesting loss of tight cell junctions and viability. In Figure 18, the ICC assay was conducted after a 7 day-long exposure to Fe_2O_3. The results were more dramatic as compared to the 24-hour exposure. Compared to the negative control and 24-hour treatments (Figure 17), all 3 doses of Fe_2O_3 produced notably increased vimentin and were observed as decreasing incrementally with increasing doses. This could be due to an increased loss of E-cadherin expression, therefore a less “white” or bright image. The cell morphology was also altered from a spherical shape to an elongated shape indicating EMT commonly found in airway epithelium undergoing fibrotic changes.

4.7.6 Western Blot

Although EMT was found in ICC assessments, western blot analysis of SAEC protein aliquots obtained after 3-week exposures were not as conclusive. Three-week exposures were

conducted to observe how sub-chronic exposures might affect the SAEC EMT protein levels but, as they are sensitive, reduced concentrations of 2 µg and 5 µg were used to ensure adequate protein collection. The western blot data was conducted in Figure 19 for pNPs (Fe_2O_3 and TiO_2 abbreviated as "Fe" and "Ti", respectively) and rNPs. Beta-actin was used as a loading control, which was observed in all samples but did not display uniform intensities. This could have been attributed to uneven transfer. In both gels, there was little visual difference in E-cadherin intensities between the negative controls and positive controls (TGFβ), save NC2 on gel 1. Regarding the pNPs and rNPs, E-cadherin intensities in gel 1 were relatively similar but the vimentin intensity for 2 µg AA4 was highest, which could indicate there was increase in vimentin. In gel 2, higher intensities of E-cadherin were observed in the higher (5 µg) doses of AA8, S1, and S4 and there were little visible bands for vimentin for the same gel. To provide a more comprehensive comparison of band intensities, graphs were created using the relative intensities adjusted for a negative control on each gel (Figure 19). This was conducted in ImageJ by calculating percent peak area and relative density by dividing by the area of the negative controls then adjusting to include differences in beta-actin for each treatment (see Methods and Protocols section labeled "Protein Expression" for further details). Comparing the treatments in the graph to the negative controls, there was a decrease in E-cadherin only for the positive control on gel 1 but a decrease for all treatments on gel 2. For vimentin, there was an increase in all treatments on gel 1 compared to the negative control and a slight elevation in 2 µg AA8 and 5 µg S4. When comparing treatments across both proteins, one positive control on gel 1 displayed a decrease in E-cadherin and increase in vimentin. On gel 2, all treatments had a decrease in E-cadherin and an increase in vimentin, except for 5 µg AA4 and the positive control on gel 2, which increased but to a lesser extent than the negative control. This suggested that EMT might

have occurred with most of the rNPs and these western blot results warrant subsequent trials to obtain more reliable data for sub-chronic exposure effects on EMT.

5. DISCUSSION AND CONCLUSION

Innovation in nanotechnology has led to rapid and increased development of NEPs that has warranted the need for safety investigations due to the incorporation of metal ENMs. Previous studies have shown that exposure to ENMs elicit toxic effects through complex mechanisms, which can lead to adverse health outcomes, such as fibrosis and reduced pulmonary function (Gatoo et al., 2014; Maynard et al., 2006; Meng et al., 2007; Nel, Xia, Mädler, & Li, 2006; N. Singh et al., 2009). Yet, over 70% of NEPs do not have enough information to support the claim that ENMs are used, which indicates lack of safety or ethical considerations (Vance et al., 2015). This lack of knowledge has piqued interest in the scientific community as the applications and uses for ENMs have increased to encompass a variety of products, thereby widening the potentially exposed population (Ray, Yu, & Fu, 2009). Since ENMs are being developed continually and are used to make products more durable, it raises concerns for the possible adverse effects that might result from this enhancement. Specifically, in cosmetics, almost all major brands are utilizing nanotechnology in their products to make them longer-lasting, penetrate skin deeper, and improve color and chemical reactivity (Raj, Jose, Sumod, & Sabitha, 2012). TiO_2 is commonly used as a protectant from UV rays and iron oxides are used as pigments to produce various shades of cosmetics, such as red and orange (Borowska & Brzóska, 2015). Specifically, Fe_2O_3 is one of the most universal and widely-used iron oxides in cosmetics (Wawrzynczak & Nowak, 2011). With these differences in various levels of metal-containing ENMs, such as Fe_2O_3, used to manufacture darker and lighter shades of NEPs, it may cause dissimilar effects in darker-skinned individuals versus lighter-skinned individuals. Since some of these NEPs now have a more widespread application technique via airbrush, inhalation exposure has become a more prominent exposure pathway as popularity of this use has increased. This has

led to the characterization of aerosolized nanoparticle releases from NEPs (Nazarenko et al., 2011, 2012; Pal, Watson, et al., 2015; D. Singh et al., 2017). In an effort to build on this research, this study was conducted to examine the potential toxicological effects and differences regarding inhalation exposure to pNPs and rNPs and determine if there is any increased risk for susceptible populations.

This study compared the physico-chemical characteristics and toxicological profiles of pNPs and rNPs using SAEC and 16HBE cell types to determine ROS generation, cellular viability, EMT, and up- or downregulation of EMT proteins using western blots. The darker shades of NEPs AA4 and S4 had the highest Fe concentrations when examined through ICP-MS and EDS, compared to the lighter shades AA8 and S1 containing more Ti. This chemical compositional difference alone can affect how particles interact with their environment and influence toxicological endpoints, such as cellular viability (Gatoo et al., 2014; Maurer-Jones, Gunsolus, Murphy, & Haynes, 2013; Pal, Watson, et al., 2015). In addition, the zeta potential values for AA4 and S4 obtained when dispersed in either exposure media was approximately between 8 and 25-fold more negative than AA8 and S1. The changes in zeta potential can be affected by factors such as change in pH and this changed zeta potential can influence cellular viability, as supported by Berg *et al.* (2009). The negative zeta potential values are also reflected in the high conductance both darker shades of rNPs exhibited in exposure media. Fe_2O_3 was also found to have an extremely negative zeta potential in exposure media, which was in abundance in the darker shades and explain partially why there was a huge zeta potential difference between dark and light shades of NEPs. However, since the negative zeta potential was greater in rNPs, they may exhibit greater effects, such as influenced toxicity, based on their surface properties

compared to pNPs, as described in multiple studies (Berg et al., 2009; Lundqvist et al., 2008; Nan, Bai, Son, Lee, & Ghandehari, 2008; Xia et al., 2006).

The differences in composition between the expensive and inexpensive cosmetic lines (cosmetic lines 1 and 2, respectively) are also apparent when the hydrodynamic diameter was observed, with cosmetic line 2 rNPs having a smaller diameter compared to cosmetic line 1 rNPs. This was observed in the SEM images, save for AA4, which had a more textured, rough structure with large agglomerations present, which could be expected with the higher percentage of Fe present. The differing sizes in pNPs observed when dispersed in exposure media versus di H_2O has been observed in other studies and has played a role in changes in toxicity (Colvin, 2003; Hou, Westerhoff, & Posner, 2012; Jiang, Malavia, Suresh, & George, 2009; Sager et al., 2007). When comparing uniformity of particle suspensions (PdI), cosmetic line 2 rNPs had the most uniformity while cosmetic line 1 rNPs had much lower uniformity compared to cosmetic line 2 rNPs and raw products. This could be indicative of the more complex chemical formulations found in the more expensive products. These complex physico-chemical properties, such as shape, aggregation, and surface area, has been thought to play a major part in toxicity and has been confirmed in a few studies to increase cytotoxicity with pNPs (Gatoo et al., 2014; Hu, Xie, Tong, & Wang, 2007; Yin, Too, & Chow, 2005).

Increased generation of ROS and oxidative stress were observed in SAEC upon 24-hour exposure to all treatments. Qualitatively, it was observed that AA4 exhibited the highest generation of ROS at 10 µg compared to the highest generation of ROS at 10 and 15 µg for S4. For 16HBE, the only prominent increase in ROS generation for rNPs occurred at the highest concentrations of AA4 and S4, which could indicate a higher generation of ROS exhibited by the darker shades. When comparing this data to the qualitative total glutathione (GSH) levels, AA4

exhibited much lower total GSH levels for SAEC than any other treatment, especially at the highest concentration, which could indicate that this cheaper, darker product generates more ROS. Oxidative stress due to exposure to pNPs (particularly metal oxides) has been documented to be a mechanism responsible for genotoxicity *in vitro*, which could provide evidence towards enhanced risk of oxidative stress and inflammation in African Americans, who might already have a higher rate of inflammation compared to Caucasians (Carroll et al., 2009; Charles et al., 2018; Feairheller et al., 2011; Sharma et al., 2014; N. Singh, Jenkins, Asadi, & Doak, 2010; Xia et al., 2006; Zhang et al., 2012). Use of these products may have a more pronounced effect on African Americans' health, in combination with SES differences, such as location, medical care, and accessibility of resources and stress (Williams, 2002; Williams, Priest, & Anderson, 2016). The effect from resulting oxidative stress caused by increased ROS in AA4 can be seen in the decreased cellular viability of SAEC of about 40% at the highest concentration, which is lower than the lighter shades. Oxidative stress effects were also observed from SAEC exposure to S4 but had a 23-25% viability reduction in all but one treatment. However, S1 and S4 seemed to decrease viability in 16HBE at 20 µg, though not significantly, which could demonstrate that the expensive products may have had a different effect on the 16HBE cells. When comparing the pNPs to the rNPs, Fe_2O_3 and TiO_2 both generated ROS, reduced total glutathione levels, and reduced cellular viability with increasing doses but not as much as the AA4 or some of the other doses of rNPs did, which indicates that rNPs may exert more toxic effects than pNPs based on the evidence of oxidative stress being associated with particle mediated toxicity observed in other studies (N. Li, Xia, & Nel, 2008; Manke, Wang, & Rojanasakul, 2013; A. Nel et al., 2006).

EMT and western blot data was used to determine the loss of adherence and phenotypic changes in SAEC due to exposure to pNPs and rNPs. From these results, it was determined that

there was indication of EMT after exposure to Fe_2O_3 for 24 hours and 7 days, with more prominence in the latter exposure. This could suggest that more sub-chronic exposure to the pristine ENM powder could induce EMT, cellular response, and fibrotic changes, which may lead to adverse outcomes such as respiratory inflammation and asthma (Ijaz et al., 2014; Lambrecht & Hammad, 2012). Differences between EMT in AA4 and Fe_2O_3 could not be comparable, though the EMT data on Fe_2O_3 may be useful to occupational workers exposed to these pNP powders more frequently and in larger doses. To examine effects on EMT in the sensitive SAEC, western blot analysis was conducted on 3-week exposures and indicated that the AA8, S1, and S4 may induce EMT but further study is warranted to ensure results, possibly with introduction of other EMT-related proteins in airways, such as CD44 (Hackett et al., 2009).

While this study may have provided some evidence towards differences in toxicity from rNPs and pNPs and how they can affect the susceptible populations, there are some limitations. One notable limitation was that static 2-D cell cultures were used, as opposed to *in vivo* methods. As a result, the data cannot be directly extrapolated to human risk but can provide a foundation in which to develop an *in vivo* experiment upon to get closer to identifying a realistic human risk when exposed to pNPs and rNPs in the air. Another limitation is that the dosimetry was not determined for each rNP. This is important as each rNP may not be delivering the same dose based on differences in dispersion and other characteristics unique to each rNP (Cohen et al., 2013; Pal et al., 2014; Pal, Watson, et al., 2015; Pal, Bello, Cohen, & Demokritou, 2015). To ensure more accurate results, a dose-response relationship could be determined for each rNP incorporating in vitro dosimetry, especially when using cell types with different media. Another limitation is that only one-time point was used for cellular viability and oxidative stress assays, so by adding in more acute or sub-chronic time points, it may provide a broader picture to the

effects of these NEPs on pulmonary function. Finally, since 16HBE were not as much affected as the primary SAEC were, the doses administered to 16HBE could be increased until there is an effect observed.

In summation, the desire to make cheaper and better products quicker will always be present in the minds of manufacturers and thus the use of ENMs will inevitably increase as nanotechnological techniques improve and chemical formulations are tweaked. As a result, this increased insertion of ENMs in products will likely rapidly increase the number of NEPs released into the marketplace globally as well as human and environmental exposure to these products. Thus, the importance of determining the toxicological effects of these products on human health is paramount in closing the gap in lack of knowledge and safely protecting present and future generations from adverse effects due to NEP exposure, especially since knowledge is limited on rNPs as compared to ambient or pNPs. This investigation provides evidence to conduct further studies regarding NEP exposure via more refined *in vitro* or *in vivo* methodologies.

REFERENCES

Adeleye, A. S., Conway, J. R., Garner, K., Huang, Y., Su, Y., & Keller, A. A. (2016). Engineered nanomaterials for water treatment and remediation: Costs, benefits, and applicability. *Chemical Engineering Journal*, *286*, 640–662. https://doi.org/10.1016/j.cej.2015.10.105

Ames, B. N., Durston, W. E., Yamasaki, E., & Lee, F. D. (1973). Carcinogens are Mutagens: A Simple Test System Combining Liver Homogenates for Activation and Bacteria for Detection. *Proceedings of the National Academy of Sciences of the United States of America*, *70*(8), 2281–2285. Retrieved from http://www.ncbi.nlm.nih.gov/pmc/articles/PMC433718/

Anderson, W., Kozak, D., Coleman, V. A., Jämting, Å. K., & Trau, M. (2013). A comparative study of submicron particle sizing platforms: Accuracy, precision and resolution analysis of polydisperse particle size distributions. *Journal of Colloid and Interface Science*, *405*, 322–330. https://doi.org/10.1016/j.jcis.2013.02.030

Armstead, A. L., & Li, B. (2016). Nanotoxicity: emerging concerns regarding nanomaterial safety and occupational hard metal (WC-Co) nanoparticle exposure. *International Journal of Nanomedicine*, *11*, 6421–6433. https://doi.org/10.2147/IJN.S121238

Barnes, C. A., Elsaesser, A., Arkusz, J., Smok, A., Palus, J., Leśniak, A., … Howard, C. V. (2008). Reproducible comet assay of amorphous silica nanoparticles detects no genotoxicity. *Nano Letters*, *8*(9), 3069–3074. https://doi.org/10.1021/nl801661w

Becker, H., Herzberg, F., Schulte, A., & Kolossa-Gehring, M. (2011). The carcinogenic potential of nanomaterials, their release from products and options for regulating them. *International Journal of Hygiene and Environmental Health*, *214*(3), 231–238. https://doi.org/10.1016/j.ijheh.2010.11.004

Berg, J. M., Romoser, A., Banerjee, N., Zebda, R., & Sayes, C. M. (2009). The relationship between pH and zeta potential of ∼ 30 nm metal oxide nanoparticle suspensions relevant to in vitro

toxicological evaluations. *Nanotoxicology*, *3*(4), 276–283. https://doi.org/10.3109/17435390903276941

Bergeson, Campbell, Avenue, P. C. 2200 P., Suite 100W, N. W., Washington, D.C, & Phone: 202-557-3800, 20037-1701. (2010, September 17). EPA Issues Final SNURs for Carbon Nanotubes. Retrieved from http://nanotech.lawbc.com/2010/09/epa-issues-final-snurs-for-carbon-nanotubes/

Binh, C. T. T., Peterson, C. G., Tong, T., Gray, K. A., Gaillard, J.-F., & Kelly, J. J. (2015). Comparing Acute Effects of a Nano-TiO2 Pigment on Cosmopolitan Freshwater Phototrophic Microbes Using High-Throughput Screening. *PLoS ONE*, *10*(4). https://doi.org/10.1371/journal.pone.0125613

Borowska, S., & Brzóska, M. M. (2015). Metals in cosmetics: implications for human health. *Journal of Applied Toxicology*, *35*(6), 551–572. https://doi.org/10.1002/jat.3129

Bouwmeester, H., van der Zande, M., & Jepson, M. A. (2017). Effects of food-borne nanomaterials on gastrointestinal tissues and microbiota. *Wiley Interdisciplinary Reviews. Nanomedicine and Nanobiotechnology*. https://doi.org/10.1002/wnan.1481

Boxall, A., Tiede, K., Chaudhry, Q., Aitken, R., Jones, A., Jefferson, B., & Lewis, J. (2007). Current and Future Predicted Exposure to Engineered Nanoparticles.

Brouwer, D. H., Spaan, S., Roff, M., Sleeuwenhoek, A., Tuinman, I., Goede, H., … Cherrie, J. W. (2016). Occupational dermal exposure to nanoparticles and nano-enabled products: Part 2, exploration of exposure processes and methods of assessment. *International Journal of Hygiene and Environmental Health*, *219*(6), 503–512. https://doi.org/10.1016/j.ijheh.2016.05.003

Brown, C., Lacharme-Lora, L., Mukonoweshuro, B., Sood, A., Newson, R. B., Fisher, J., … Ingham, E. (2013). Consequences of exposure to peri-articular injections of micro- and nano-particulate cobalt–chromium alloy. *Biomaterials*, *34*(34), 8564–8580. https://doi.org/10.1016/j.biomaterials.2013.07.073

Bunderson-Schelvan, M., Holian, A., & Hamilton, R. F. (2017). Engineered nanomaterial-induced lysosomal membrane permeabilization and anti-cathepsin agents. *Journal of Toxicology and*

Environmental Health. Part B, Critical Reviews, *20*(4), 230–248. https://doi.org/10.1080/10937404.2017.1305924

Cabello, N., Mishra, V., Sinha, U., DiAngelo, S. L., Chroneos, Z. C., Ekpa, N. A., … Silveyra, P. (2015). Sex differences in the expression of lung inflammatory mediators in response to ozone. *American Journal of Physiology - Lung Cellular and Molecular Physiology*, *309*(10), L1150–L1163. https://doi.org/10.1152/ajplung.00018.2015

Cao, M., Li, J., Tang, J., Chen, C., & Zhao, Y. (2016). Gold Nanomaterials in Consumer Cosmetics Nanoproducts: Analyses, Characterization, and Dermal Safety Assessment. *Small*, *12*(39), 5488–5496. https://doi.org/10.1002/smll.201601574

Carroll, J. F., Fulda, K. G., Chiapa, A. L., Rodriquez, M., Phelps, D. R., Cardarelli, K. M., … Cardarelli, R. (2009). Impact of race/ethnicity on the relationship between visceral fat and inflammatory biomarkers. *Obesity (Silver Spring, Md.)*, *17*(7), 1420–1427. https://doi.org/10.1038/oby.2008.657

Charles, S., Jomini, S., Fessard, V., Bigorgne-Vizade, E., Rousselle, C., & Michel, C. (2018). Assessment of the in vitro genotoxicity of TiO2 nanoparticles in a regulatory context. *Nanotoxicology*, *0*(0), 1–18. https://doi.org/10.1080/17435390.2018.1451567

Chen, T., Yan, J., & Li, Y. (2014). Genotoxicity of titanium dioxide nanoparticles. *Journal of Food and Drug Analysis*, *22*(1), 95–104. https://doi.org/10.1016/j.jfda.2014.01.008

Cho, Y. S., & Moon, H.-B. (2010). The Role of Oxidative Stress in the Pathogenesis of Asthma. *Allergy, Asthma & Immunology Research*, *2*(3), 183–187. https://doi.org/10.4168/aair.2010.2.3.183

Choi, A. O., Brown, S. E., Szyf, M., & Maysinger, D. (2008). Quantum dot-induced epigenetic and genotoxic changes in human breast cancer cells. *Journal of Molecular Medicine (Berlin, Germany)*, *86*(3), 291–302. https://doi.org/10.1007/s00109-007-0274-2

Cohen, J., DeLoid, G., Pyrgiotakis, G., & Demokritou, P. (2013). Interactions of Engineered Nanomaterials in Physiological Media and Implications for In Vitro Dosimetry. *Nanotoxicology*, *7*(4), 417–431. https://doi.org/10.3109/17435390.2012.666576

Colvin, V. L. (2003). The potential environmental impact of engineered nanomaterials. *Nature Biotechnology*, *21*(10), 1166–1170. https://doi.org/10.1038/nbt875

Contado, C. (2015). Nanomaterials in consumer products: a challenging analytical problem. *Frontiers in Chemistry*, *3*. https://doi.org/10.3389/fchem.2015.00048

Cozens, A. L., Yezzi, M. J., Kunzelmann, K., Ohrui, T., Chin, L., Eng, K., … Gruenert, D. C. (1994). CFTR expression and chloride secretion in polarized immortal human bronchial epithelial cells. *American Journal of Respiratory Cell and Molecular Biology*, *10*(1), 38–47. https://doi.org/10.1165/ajrcmb.10.1.7507342

Crystal, R. G., Randell, S. H., Engelhardt, J. F., Voynow, J., & Sunday, M. E. (2008). Airway Epithelial Cells. *Proceedings of the American Thoracic Society*, *5*(7), 772–777. https://doi.org/10.1513/pats.200805-041HR

De Craene, B., & Berx, G. (2013). Regulatory networks defining EMT during cancer initiation and progression. *Nature Reviews. Cancer*, *13*(2), 97–110. https://doi.org/10.1038/nrc3447

De Silva, M. (2007). Nanotechnology and nanomedicine: a new horizon for medical diagnostics and treatment. *Arch Soc Esp Oftalmol*, *82*, 331–334. Retrieved from http://www.oftalmo.com/seo/archivos/maquetas/9/0EA69CF8-C284-74E9-4ACD-000074354D49/articulo.pdf

Donaldson, K., Tran, L., Jimenez, L. A., Duffin, R., Newby, D. E., Mills, N., … Stone, V. (2005). Combustion-derived nanoparticles: a review of their toxicology following inhalation exposure. *Particle and Fibre Toxicology*, *2*, 10. https://doi.org/10.1186/1743-8977-2-10

Eom, Y., Song, J. S., Lee, H. K., Kang, B., Kim, H. C., Lee, H. K., & Kim, H. M. (2016). The Effect of Ambient Titanium Dioxide Microparticle Exposure to the Ocular Surface on the Expression of Inflammatory Cytokines in the Eye and Cervical Lymph NodesInflammatory Cytokines Following TiO2 Exposure. *Investigative Ophthalmology & Visual Science*, *57*(15), 6580–6590. https://doi.org/10.1167/iovs.16-19944

Feairheller, D. L., Park, J., Sturgeon, K. M., Williamson, S. T., Diaz, K. M., Veerabhadrappa, P., & Brown, M. D. (2011). Racial Differences in Oxidative Stress and Inflammation: In Vitro and In Vivo. *Clinical and Translational Science*, *4*(1), 32–37. https://doi.org/10.1111/j.1752-8062.2011.00264.x

Feng, X., Chen, A., Zhang, Y., Wang, J., Shao, L., & Wei, L. (2015). Application of dental nanomaterials: potential toxicity to the central nervous system. *International Journal of Nanomedicine*, *10*, 3547–3565. https://doi.org/10.2147/IJN.S79892

Fröhlich, E. (2016). Cellular elimination of nanoparticles. *Environmental Toxicology and Pharmacology*, *46*, 90–94. https://doi.org/10.1016/j.etap.2016.07.003

Fung, H., Kow, Y. W., Van Houten, B., & Mossman, B. T. (1997). Patterns of 8-hydroxydeoxyguanosine formation in DNA and indications of oxidative stress in rat and human pleural mesothelial cells after exposure to crocidolite asbestos. *Carcinogenesis*, *18*(4), 825–832.

Gaiser, B. K., Biswas, A., Rosenkranz, P., Jepson, M. A., Lead, J. R., Stone, V., … Fernandes, T. F. (2011). Effects of silver and cerium dioxide micro- and nano-sized particles on Daphnia magna. *Journal of Environmental Monitoring: JEM*, *13*(5), 1227–1235. https://doi.org/10.1039/c1em10060b

Gaiser, B. K., Fernandes, T. F., Jepson, M., Lead, J. R., Tyler, C. R., & Stone, V. (2009). Assessing exposure, uptake and toxicity of silver and cerium dioxide nanoparticles from contaminated environments. *Environmental Health*, *8*(Suppl 1), S2. https://doi.org/10.1186/1476-069X-8-S1-S2

Gatoo, M. A., Naseem, S., Arfat, M. Y., Mahmood Dar, A., Qasim, K., & Zubair, S. (2014). Physicochemical Properties of Nanomaterials: Implication in Associated Toxic Manifestations. *BioMed Research International*, *2014*. https://doi.org/10.1155/2014/498420

Geiser, M., & Kreyling, W. G. (2010). Deposition and biokinetics of inhaled nanoparticles. *Particle and Fibre Toxicology*, *7*, 2. https://doi.org/10.1186/1743-8977-7-2

Gopee, N. V., Roberts, D. W., Webb, P., Cozart, C. R., Siitonen, P. H., Warbritton, A. R., … Howard, P. C. (2007). Migration of intradermally injected quantum dots to sentinel organs in mice. *Toxicological Sciences: An Official Journal of the Society of Toxicology*, *98*(1), 249–257. https://doi.org/10.1093/toxsci/kfm074

Gref, R., Minamitake, Y., Peracchia, M. T., Trubetskoy, V., Torchilin, V., & Langer, R. (1994). Biodegradable long-circulating polymeric nanospheres. *Science (New York, N.Y.)*, *263*(5153), 1600–1603.

Guarino, M., Tosoni, A., & Nebuloni, M. (2009). Direct contribution of epithelium to organ fibrosis: epithelial-mesenchymal transition. *Human Pathology*, *40*(10), 1365–1376. https://doi.org/10.1016/j.humpath.2009.02.020

Hackett, T.-L., Warner, S. M., Stefanowicz, D., Shaheen, F., Pechkovsky, D. V., Murray, L. A., … Knight, D. A. (2009). Induction of Epithelial–Mesenchymal Transition in Primary Airway Epithelial Cells from Patients with Asthma by Transforming Growth Factor-β1. *American Journal of Respiratory and Critical Care Medicine*, *180*(2), 122–133. https://doi.org/10.1164/rccm.200811-1730OC

Handy, R. D., Owen, R., & Valsami-Jones, E. (2008). The ecotoxicology of nanoparticles and nanomaterials: current status, knowledge gaps, challenges, and future needs. *Ecotoxicology*, *17*(5), 315–325. https://doi.org/10.1007/s10646-008-0206-0

Harik-Khan, R. I., Muller, D. C., & Wise, R. A. (2004). Racial difference in lung function in African-American and White children: effect of anthropometric, socioeconomic, nutritional, and environmental factors. *American Journal of Epidemiology*, *160*(9), 893–900. https://doi.org/10.1093/aje/kwh297

Hendley, J. O., Wenzel, R. P., & Gwaltney, J. M. J. (1973). Transmission of Rhinovirus Colds by Self-Inoculation. *New England Journal of Medicine*, *288*(26), 1361–1364. https://doi.org/10.1056/NEJM197306282882601

Herzog, E., Casey, A., Lyng, F. M., Chambers, G., Byrne, H. J., & Davoren, M. (2007). A new approach to the toxicity testing of carbon-based nanomaterials—The clonogenic assay. *Toxicology Letters*, *174*(1), 49–60. https://doi.org/10.1016/j.toxlet.2007.08.009

Heylings, J. R., Clowes, H. M., Cumberbatch, M., Dearman, R. J., Fielding, I., Hilton, J., & Kimber, I. (1996). Sensitization to 2,4-dinitrochlorobenzene: influence of vehicle on absorption and lymph node activation. *Toxicology*, *109*(1), 57–65.

Hillegass, J. M., Shukla, A., Lathrop, S. A., MacPherson, M. B., Fukagawa, N. K., & Mossman, B. T. (2010). Assessing nanotoxicity in cells in vitro. *Wiley Interdisciplinary Reviews. Nanomedicine and Nanobiotechnology*, *2*(3), 219–231. https://doi.org/10.1002/wnan.54

Hirn, S., Semmler-Behnke, M., Schleh, C., Wenk, A., Lipka, J., Schäffler, M., … Kreyling, W. G. (2011). Particle size-dependent and surface charge-dependent biodistribution of gold nanoparticles after intravenous administration. *European Journal of Pharmaceutics and Biopharmaceutics: Official Journal of Arbeitsgemeinschaft Fur Pharmazeutische Verfahrenstechnik e.V*, *77*(3), 407–416. https://doi.org/10.1016/j.ejpb.2010.12.029

Hodgson, E. (2010). *A Textbook of Modern Toxicology* (Fourth). Hoboken NJ.: John Wiley & Sons, Inc.

Hood, E. (2004). Nanotechnology: looking as we leap. *Environmental Health Perspectives*, *112*(13), A740–A749. Retrieved from http://ezproxy.gsu.edu/login?url=http://search.ebscohost.com/login.aspx?direct=true&db=mnh&AN=15345364&site=eds-live

Hou, W.-C., Westerhoff, P., & Posner, J. D. (2012). Biological accumulation of engineered nanomaterials: a review of current knowledge. *Environmental Science: Processes & Impacts*, *15*(1), 103–122. https://doi.org/10.1039/C2EM30686G

Howard, A. G. (2010). On the challenge of quantifying man-made nanoparticles in the aquatic environment. *Journal of Environmental Monitoring: JEM*, *12*(1), 135–142. https://doi.org/10.1039/b913681a

Hu, Y., Xie, J., Tong, Y. W., & Wang, C.-H. (2007). Effect of PEG conformation and particle size on the cellular uptake efficiency of nanoparticles with the HepG2 cells. *Journal of Controlled Release*, *118*(1), 7–17. https://doi.org/10.1016/j.jconrel.2006.11.028

Huang, C., Sun, M., Yang, Y., Wang, F., Ma, X., Li, J., … Wang, H. (2017). Titanium dioxide nanoparticles prime a specific activation state of macrophages. *Nanotoxicology*, 1–14. https://doi.org/10.1080/17435390.2017.1349202

Husain, M., Wu, D., Saber, A. T., Decan, N., Jacobsen, N. R., Williams, A., … Halappanavar, S. (2015). Intratracheally instilled titanium dioxide nanoparticles translocate to heart and liver and activate complement cascade in the heart of C57BL/6 mice. *Nanotoxicology*, *9*(8), 1013–1022. https://doi.org/10.3109/17435390.2014.996192

Iavicoli, I., Fontana, L., Leso, V., & Bergamaschi, A. (2013). The Effects of Nanomaterials as Endocrine Disruptors. *International Journal of Molecular Sciences*, *14*(8), 16732–16801. https://doi.org/10.3390/ijms140816732

Ihrie, M. D., & Bonner, J. C. (2018). The Toxicology of Engineered Nanomaterials in Asthma. *Current Environmental Health Reports*. https://doi.org/10.1007/s40572-018-0181-4

Ijaz, T., Pazdrak, K., Kalita, M., Konig, R., Choudhary, S., Tian, B., … Brasier, A. R. (2014). Systems biology approaches to understanding Epithelial Mesenchymal Transition (EMT) in mucosal remodeling and signaling in asthma. *The World Allergy Organization Journal*, *7*(1), 13. https://doi.org/10.1186/1939-4551-7-13

Inoue, K., Takano, H., Yanagisawa, R., Sakurai, M., Abe, S., Yoshino, S., … Yoshikawa, T. (2007). Effects of nanoparticles on lung physiology in the presence or absence of antigen. *International Journal of Immunopathology and Pharmacology*, *20*(4), 737–744. Retrieved from http://journals.sagepub.com/doi/abs/10.1177/039463200702000409

Jahromi, M. A. M., Zangabad, P. S., Basri, S. M. M., Zangabad, K. S., Ghamarypour, A., Aref, A. R., … Hamblin, M. R. (2017). Nanomedicine and advanced technologies for burns: Preventing infection

and facilitating wound healing. *Advanced Drug Delivery Reviews*. https://doi.org/10.1016/j.addr.2017.08.001

Jiang, J., Malavia, N., Suresh, V., & George, S. C. (2009). Nitric oxide gas phase release in human small airway epithelial cells. *Respiratory Research*, *10*(1), 3. https://doi.org/10.1186/1465-9921-10-3

Johnson, M. M., Mendoza, R., Raghavendra, A. J., Podila, R., & Brown, J. M. (2017). Contribution of engineered nanomaterials physicochemical properties to mast cell degranulation. *Scientific Reports*, *7*, 43570. https://doi.org/10.1038/srep43570

Johnston, M. V., Klems, J. P., Zordan, C. A., Pennington, M. R., Smith, J. N., & HEI Health Review Committee. (2013). Selective detection and characterization of nanoparticles from motor vehicles. *Research Report (Health Effects Institute)*, (173), 3–45.

Kalluri, R., & Neilson, E. G. (2003). Epithelial-mesenchymal transition and its implications for fibrosis. *Journal of Clinical Investigation*, *112*(12), 1776–1784. https://doi.org/10.1172/JCI200320530

Kelly, F. J., & Zhu, T. (2016). Transport solutions for cleaner air. *Science (New York, N.Y.)*, *352*(6288), 934–936. https://doi.org/10.1126/science.aaf3420

Kessler, R. (2011). Engineered Nanoparticles in Consumer Products: Understanding a New Ingredient. *Environmental Health Perspectives*, *119*(3), A120–A125. Retrieved from http://www.ncbi.nlm.nih.gov/pmc/articles/PMC3060016/

Kisin, E. R., Murray, A. R., Keane, M. J., Shi, X.-C., Schwegler-Berry, D., Gorelik, O., … Shvedova, A. A. (2007). Single-walled Carbon Nanotubes: Geno- and Cytotoxic Effects in Lung Fibroblast V79 Cells. *Journal of Toxicology and Environmental Health, Part A*, *70*(24), 2071–2079. https://doi.org/10.1080/15287390701601251

Klaine, S. J., Koelmans, A. A., Horne, N., Carley, S., Handy, R. D., Kapustka, L., … von der Kammer, F. (2012). Paradigms to assess the environmental impact of manufactured nanomaterials. *Environmental Toxicology and Chemistry*, *31*(1), 3–14. https://doi.org/10.1002/etc.733

Kozak, D., Anderson, W., Grevett, M., & Trau, M. (2012). Modeling Elastic Pore Sensors for Quantitative Single Particle Sizing. *The Journal of Physical Chemistry. C, Nanomaterials and Interfaces*, *116*(15), 8554–8561. https://doi.org/10.1021/jp211845t

Kozak, D., Anderson, W., Vogel, R., Chen, S., Antaw, F., & Trau, M. (2012). Simultaneous Size and ζ-Potential Measurements of Individual Nanoparticles in Dispersion Using Size-Tunable Pore Sensors. *ACS Nano*, *6*(8), 6990–6997. https://doi.org/10.1021/nn3020322

Kreyling, W., & Scheuch, G. (2000). Clearance of particles deposited in the lungs. *Particle–lung Interactions*, 323–376.

Kumar, A., & Dhawan, A. (2013). Genotoxic and carcinogenic potential of engineered nanoparticles: an update. *Archives of Toxicology*, *87*(11), 1883–1900. https://doi.org/10.1007/s00204-013-1128-z

Kumar, C. S. S. R. (2009). *Mixed Metal Nanomaterials*. John Wiley & Sons.

Lademann, J., Richter, H., Meinke, M. C., Lange-Asschenfeldt, B., Antoniou, C., Mak, W. C., … Patzelt, A. (2013). Drug Delivery with Topically Applied Nanoparticles: Science Fiction or Reality. *Skin Pharmacology and Physiology*, *26*(4–6), 227–233. https://doi.org/10.1159/000351940

Lambrecht, B. N., & Hammad, H. (2012). The airway epithelium in asthma. *Nature Medicine*, *18*(5), 684–692. https://doi.org/10.1038/nm.2737

Lamouille, S., Xu, J., & Derynck, R. (2014). Molecular mechanisms of epithelial–mesenchymal transition. *Nature Reviews. Molecular Cell Biology*, *15*(3), 178–196. https://doi.org/10.1038/nrm3758

Li, M., Luan, F., Zhao, Y., Hao, H., Zhou, Y., Han, W., & Fu, X. (2016). Epithelial-mesenchymal transition: An emerging target in tissue fibrosis. *Experimental Biology and Medicine*, *241*(1), 1–13. https://doi.org/10.1177/1535370215597194

Li, N., Xia, T., & Nel, A. E. (2008). The role of oxidative stress in ambient particulate matter-induced lung diseases and its implications in the toxicity of engineered nanoparticles. *Free Radical Biology & Medicine*, *44*(9), 1689–1699. https://doi.org/10.1016/j.freeradbiomed.2008.01.028

Lim, J. P., Baeg, G. H., Srinivasan, D. K., Dheen, S. T., & Bay, B. H. (2017). Potential adverse effects of engineered nanomaterials commonly used in food on the miRNome. *Food and Chemical Toxicology*. https://doi.org/10.1016/j.fct.2017.07.030

Long, T. C., Saleh, N., Tilton, R. D., Lowry, G. V., & Veronesi, B. (2006). Titanium dioxide (P25) produces reactive oxygen species in immortalized brain microglia (BV2): implications for nanoparticle neurotoxicity. *Environmental Science & Technology*, *40*(14), 4346–4352.

Lundqvist, M., Stigler, J., Elia, G., Lynch, I., Cedervall, T., & Dawson, K. A. (2008). Nanoparticle size and surface properties determine the protein corona with possible implications for biological impacts. *Proceedings of the National Academy of Sciences of the United States of America*, *105*(38), 14265–14270. https://doi.org/10.1073/pnas.0805135105

Luo, H., Jiang, B., Li, B., Li, Z., Jiang, B.-H., & Chen, Y. C. (2012). Kaempferol nanoparticles achieve strong and selective inhibition of ovarian cancer cell viability. *International Journal of Nanomedicine*, *7*, 3951–3959. https://doi.org/10.2147/IJN.S33670

Lux Research. (2014, February 17). Nanotechnology Update: Corporations Up Their Spending as Revenues for Nano-enabled Products Increase. Retrieved February 19, 2018, from https://members.luxresearchinc.com/research/report/13748

Manke, A., Wang, L., & Rojanasakul, Y. (2013). Mechanisms of Nanoparticle-Induced Oxidative Stress and Toxicity [Research article]. https://doi.org/10.1155/2013/942916

Mann, E. E., Thompson, L. C., Shannahan, J. H., & Wingard, C. J. (2012). Changes in Cardiopulmonary Function Induced by Nanoparticles. *Wiley Interdisciplinary Reviews. Nanomedicine and Nanobiotechnology*, *4*(6), 691–702. https://doi.org/10.1002/wnan.1194

Martirosyan, A., & Schneider, Y.-J. (2014). Engineered Nanomaterials in Food: Implications for Food Safety and Consumer Health. *International Journal of Environmental Research and Public Health*, *11*(6), 5720–5750. https://doi.org/10.3390/ijerph110605720

Maurer-Jones, M. A., Gunsolus, I. L., Murphy, C. J., & Haynes, C. L. (2013). Toxicity of Engineered Nanoparticles in the Environment. *Analytical Chemistry*, *85*(6), 3036–3049. https://doi.org/10.1021/ac303636s

Maynard, A. D., Aitken, R. J., Butz, T., Colvin, V., Donaldson, K., Oberdörster, G., … Warheit, D. B. (2006, November 15). Safe handling of nanotechnology [Comments and Opinion]. https://doi.org/10.1038/444267a

Mehra, N. K., Cai, D., Kuo, L., Hein, T., & Palakurthi, S. (2016). Safety and toxicity of nanomaterials for ocular drug delivery applications. *Nanotoxicology*, *10*(7), 836–860. https://doi.org/10.3109/17435390.2016.1153165

Meng, H., Chen, Z., Xing, G., Yuan, H., Chen, C., Zhao, F., … Zhao, Y. (2007). Ultrahigh reactivity provokes nanotoxicity: Explanation of oral toxicity of nano-copper particles. *Toxicology Letters*, *175*(1), 102–110. https://doi.org/10.1016/j.toxlet.2007.09.015

Miller, M. R., Raftis, J. B., Langrish, J. P., McLean, S. G., Samutrtai, P., Connell, S. P., … Mills, N. L. (2017). Inhaled Nanoparticles Accumulate at Sites of Vascular Disease. *ACS Nano*, *11*(5), 4542–4552. https://doi.org/10.1021/acsnano.6b08551

Miller, M. R., Shaw, C. A., & Langrish, J. P. (2012). From particles to patients: oxidative stress and the cardiovascular effects of air pollution. *Future Cardiology*, *8*(4), 577–602. https://doi.org/10.2217/fca.12.43

Mills, N. L., Donaldson, K., Hadoke, P. W., Boon, N. A., MacNee, W., Cassee, F. R., … Newby, D. E. (2009). Adverse cardiovascular effects of air pollution. *Nature Clinical Practice. Cardiovascular Medicine*, *6*(1), 36–44. https://doi.org/10.1038/ncpcardio1399

Minkel, J. (2007). The truth about nanopollution. *Popular Science*, *270*(1), 62.

Mitrano, D. M., Motellier, S., Clavaguera, S., & Nowack, B. (2015). Review of nanomaterial aging and transformations through the life cycle of nano-enhanced products. *Environment International*, *77*, 132–147. https://doi.org/10.1016/j.envint.2015.01.013

Miura, N., & Shinohara, Y. (2009). Cytotoxic effect and apoptosis induction by silver nanoparticles in HeLa cells. *Biochemical and Biophysical Research Communications*, *390*(3), 733–737. https://doi.org/10.1016/j.bbrc.2009.10.039

Mori, T., Takada, H., Ito, S., Matsubayashi, K., Miwa, N., & Sawaguchi, T. (2006). Preclinical studies on safety of fullerene upon acute oral administration and evaluation for no mutagenesis. *Toxicology*, *225*(1), 48–54. https://doi.org/10.1016/j.tox.2006.05.001

Morris, A. A., Zhao, L., Patel, R. S., Jones, D. P., Ahmed, Y., Stoyanova, N., … Quyyumi, A. A. (2012). Differences in Systemic Oxidative Stress Based on Race and the Metabolic Syndrome: The Morehouse and Emory Team up to Eliminate Health Disparities (META-Health) Study. *Metabolic Syndrome and Related Disorders*, *10*(4), 252–259. https://doi.org/10.1089/met.2011.0117

Musee, N., Thwala, M., & Nota, N. (2011). The antibacterial effects of engineered nanomaterials: implications for wastewater treatment plants. *Journal of Environmental Monitoring*, *13*(5), 1164. https://doi.org/10.1039/c1em10023h

Nan, A., Bai, X., Son, S. J., Lee, S. B., & Ghandehari, H. (2008). Cellular uptake and cytotoxicity of silica nanotubes. *Nano Letters*, *8*(8), 2150–2154. https://doi.org/10.1021/nl0802741

Nazarenko, Y., Han, T. W., Lioy, P. J., & Mainelis, G. (2011). Potential for exposure to engineered nanoparticles from nanotechnology-based consumer spray products. *Journal of Exposure Science and Environmental Epidemiology*, *21*(5), 515–528. https://doi.org/10.1038/jes.2011.10

Nazarenko, Y., Zhen, H., Han, T., Lioy, P. J., & Mainelis, G. (2012). Nanomaterial inhalation exposure from nanotechnology-based cosmetic powders: a quantitative assessment. *Journal of Nanoparticle Research : An Interdisciplinary Forum for Nanoscale Science and Technology*, *14*(11). https://doi.org/10.1007/s11051-012-1229-2

Nel, A. E., Mädler, L., Velegol, D., Xia, T., Hoek, E. M. V., Somasundaran, P., … Thompson, M. (2009). Understanding biophysicochemical interactions at the nano–bio interface. *Nature Materials*, *8*(7), 543–557. https://doi.org/10.1038/nmat2442

Nel, A., Xia, T., Mädler, L., & Li, N. (2006). Toxic Potential of Materials at the Nanolevel. *Science*, *311*(5761), 622–627. https://doi.org/10.1126/science.1114397

Nikota, J., Williams, A., Yauk, C. L., Wallin, H., Vogel, U., & Halappanavar, S. (2016). Meta-analysis of transcriptomic responses as a means to identify pulmonary disease outcomes for engineered nanomaterials. *Particle and Fibre Toxicology*, *13*. https://doi.org/10.1186/s12989-016-0137-5

Noonan, G. O., Whelton, A. J., Carlander, D., & Duncan, T. V. (2014). Measurement Methods to Evaluate Engineered Nanomaterial Release from Food Contact Materials. *Comprehensive Reviews in Food Science and Food Safety*, *13*(4), 679–692. https://doi.org/10.1111/1541-4337.12079

Nowack, B., & Bucheli, T. D. (2007). Occurrence, behavior and effects of nanoparticles in the environment. *Environmental Pollution*, *150*(1), 5–22. https://doi.org/10.1016/j.envpol.2007.06.006

NSF. (2014). Market report on emerging nanotechnology now available | NSF - National Science Foundation. Retrieved August 13, 2017, from https://www.nsf.gov/news/news_summ.jsp?cntn_id=130586

Nurkiewicz, T. R., Porter, D. W., Hubbs, A. F., Stone, S., Moseley, A. M., Cumpston, J. L., … HEI Health Review Committee. (2011). Pulmonary particulate matter and systemic microvascular dysfunction. *Research Report (Health Effects Institute)*, (164), 3–48.

Oberdörster, G., Elder, A., & Rinderknecht, A. (2009). Nanoparticles and the brain: cause for concern? *Journal of Nanoscience and Nanotechnology*, *9*(8), 4996–5007.

Oberdörster, G., Sharp, Z., Atudorei, V., Elder, A., Gelein, R., Lunts, A., … Cox, C. (2002). Extrapulmonary translocation of ultrafine carbon particles following whole-body inhalation exposure of rats. *Journal of Toxicology and Environmental Health. Part A*, *65*(20), 1531–1543. https://doi.org/10.1080/00984100290071658

Ostiguy, C., & IRSST (Québec). (2010). *Engineered nanoparticles: current knowledge about OHS risks and prevention measures*. Montréal, Qué.: Institut de recherche Robert-Sauvé en santé et en sécurité du travail. Retrieved from http://www.deslibris.ca/ID/224691

Pal, A. K., Aalaei, I., Gadde, S., Gaines, P., Schmidt, D., Demokritou, P., & Bello, D. (2014). High Resolution Characterization of Engineered Nanomaterial Dispersions in Complex Media Using Tunable Resistive Pulse Sensing Technology. *ACS Nano*, *8*(9), 9003–9015. https://doi.org/10.1021/nn502219q

Pal, A. K., Bello, D., Budhlall, B., Rogers, E., & Milton, D. K. (2011). Screening for Oxidative Stress Elicited by Engineered Nanomaterials: Evaluation of Acellular DCFH Assay. *Dose-Response*, *10*(3), 308–330. https://doi.org/10.2203/dose-response.10-036.Pal

Pal, A. K., Bello, D., Cohen, J., & Demokritou, P. (2015). Implications of in-vitro dosimetry on toxicological ranking of low aspect ratio engineered nanomaterials. *Nanotoxicology*, *9*(7), 871–885. https://doi.org/10.3109/17435390.2014.986670

Pal, A. K., Watson, C. Y., Pirela, S. V., Singh, D., Chalbot, M.-C. G., Kavouras, I., & Demokritou, P. (2015). Linking Exposures of Particles Released From Nano-Enabled Products to Toxicology: An Integrated Methodology for Particle Sampling, Extraction, Dispersion, and Dosing. *Toxicological Sciences*, *146*(2), 321–333. https://doi.org/10.1093/toxsci/kfv095

Park, J., Ham, S., Jang, M., Lee, J., Kim, S., Kim, S., … Yoon, C. (2017). Spatial–Temporal Dispersion of Aerosolized Nanoparticles During the Use of Consumer Spray Products and Estimates of Inhalation Exposure. *Environmental Science & Technology*, *51*(13), 7624–7638. https://doi.org/10.1021/acs.est.7b00211

Peer, D., Karp, J. M., Hong, S., Farokhzad, O. C., Margalit, R., & Langer, R. (2007). Nanocarriers as an emerging platform for cancer therapy. *Nature Nanotechnology*, *2*(12), 751–760. https://doi.org/10.1038/nnano.2007.387

Peruzynska, M., Cendrowski, K., Barylak, M., Tkacz, M., Piotrowska, K., Kurzawski, M., … Drozdzik, M. (2017). Comparative in vitro study of single and four layer graphene oxide nanoflakes —

Cytotoxicity and cellular uptake. *Toxicology in Vitro*, *41*, 205–213. https://doi.org/10.1016/j.tiv.2017.03.005

Pombo García, K., Zarschler, K., Barbaro, L., Barreto, J. A., O'Malley, W., Spiccia, L., … Graham, B. (2014). Zwitterionic-coated "stealth" nanoparticles for biomedical applications: recent advances in countering biomolecular corona formation and uptake by the mononuclear phagocyte system. *Small (Weinheim an Der Bergstrasse, Germany)*, *10*(13), 2516–2529. https://doi.org/10.1002/smll.201303540

Poulsen, S. S., Saber, A. T., Williams, A., Andersen, O., Købler, C., Atluri, R., … Vogel, U. (2015). MWCNTs of different physicochemical properties cause similar inflammatory responses, but differences in transcriptional and histological markers of fibrosis in mouse lungs. *Toxicology and Applied Pharmacology*, *284*(1), 16–32. https://doi.org/10.1016/j.taap.2014.12.011

Puzyn, T., Leszczynska, D., & Leszczynski, J. (2009). Toward the development of "nano-QSARs": advances and challenges. *Small (Weinheim an Der Bergstrasse, Germany)*, *5*(22), 2494–2509. https://doi.org/10.1002/smll.200900179

Raj, S., Jose, S., Sumod, U. S., & Sabitha, M. (2012). Nanotechnology in cosmetics: Opportunities and challenges. *Journal of Pharmacy & Bioallied Sciences*, *4*(3), 186–193. https://doi.org/10.4103/0975-7406.99016

Ray, P. C., Yu, H., & Fu, P. P. (2009). Toxicity and Environmental Risks of Nanomaterials: Challenges and Future Needs. *Journal of Environmental Science and Health. Part C, Environmental Carcinogenesis & Ecotoxicology Reviews*, *27*(1), 1–35. https://doi.org/10.1080/10590500802708267

Rice University. (2007, April 4). The future of nanotechnology: A Rice Q&A with the NSF's Mike Roco. Retrieved February 19, 2018, from http://news.rice.edu/2007/04/04/the-future-of-nanotechnology-a-rice-qa-with-the-nsfs-mike-roco/

Ryman-Rasmussen, J. P., Tewksbury, E. W., Moss, O. R., Cesta, M. F., Wong, B. A., & Bonner, J. C. (2009). Inhaled Multiwalled Carbon Nanotubes Potentiate Airway Fibrosis in Murine Allergic

Asthma. *American Journal of Respiratory Cell and Molecular Biology*, *40*(3), 349–358. https://doi.org/10.1165/rcmb.2008-0276OC

Sager, T. M., Porter, D. W., Robinson, V. A., Lindsley, W. G., Schwegler-Berry, D. E., & Castranova, V. (2007). Improved method to disperse nanoparticles for in vitro and in vivo investigation of toxicity. *Nanotoxicology*, *1*(2), 118–129. https://doi.org/10.1080/17435390701381596

Sahiner, U. M., Birben, E., Erzurum, S., Sackesen, C., & Kalayci, O. (2011). Oxidative Stress in Asthma. *The World Allergy Organization Journal*, *4*(10), 151–158. https://doi.org/10.1097/WOX.0b013e318232389e

Schmidt, K. (2007). NanoFrontiers: Visions for the Future of Nanotechnology. *Woodrow Wilson International Center for Scholars*.

Schrand, A. M., Dai, L., Schlager, J. J., & Hussain, S. M. (2012). Toxicity Testing of Nanomaterials. In *New Technologies for Toxicity Testing* (pp. 58–75). Springer, New York, NY. https://doi.org/10.1007/978-1-4614-3055-1_5

Schulz, A. J., Mentz, G. B., Sampson, N. R., Dvonch, J. T., Reyes, A. G., & Izumi, B. (2015). Effects of Particulate Matter and Antioxidant Dietary Intake on Blood Pressure. *American Journal of Public Health*, *105*(6), 1254–1261. https://doi.org/10.2105/AJPH.2014.302176

Sharma, G., Kodali, V., Gaffrey, M., Wang, W., Minard, K. R., Karin, N. J., … Thrall, B. D. (2014). Iron oxide nanoparticle agglomeration influences dose rates and modulates oxidative stress-mediated dose–response profiles in vitro. *Nanotoxicology*, *8*(6), 663–675. https://doi.org/10.3109/17435390.2013.822115

Shi, H., Magaye, R., Castranova, V., & Zhao, J. (2013). Titanium dioxide nanoparticles: a review of current toxicological data. *Particle and Fibre Toxicology*, *10*, 15. https://doi.org/10.1186/1743-8977-10-15

Shvedova, A. A., Kisin, E. R., Yanamala, N., Farcas, M. T., Menas, A. L., Williams, A., … Kagan, V. E. (2016). Gender differences in murine pulmonary responses elicited by cellulose nanocrystals. *Particle and Fibre Toxicology*, *13*(1), 28. https://doi.org/10.1186/s12989-016-0140-x

Shvedova, A. A., Yanamala, N., Kisin, E. R., Tkach, A. V., Murray, A. R., Hubbs, A., … Castranova, V. (2014). Long-term effects of carbon containing engineered nanomaterials and asbestos in the lung: one year postexposure comparisons. *American Journal of Physiology - Lung Cellular and Molecular Physiology*, *306*(2), L170–L182. https://doi.org/10.1152/ajplung.00167.2013

Singh, D., Schifman, L. A., Watson-Wright, C., Sotiriou, G. A., Oyanedel-Craver, V., Wohlleben, W., & Demokritou, P. (2017). Nanofiller Presence Enhances Polycyclic Aromatic Hydrocarbon (PAH) Profile on Nanoparticles Released during Thermal Decomposition of Nano-enabled Thermoplastics: Potential Environmental Health Implications. *Environmental Science & Technology*, *51*(9), 5222–5232. https://doi.org/10.1021/acs.est.6b06448

Singh, G., Stephan, C., Westerhoff, P., Carlander, D., & Duncan, T. V. (2014). Measurement Methods to Detect, Characterize, and Quantify Engineered Nanomaterials in Foods. *Comprehensive Reviews in Food Science and Food Safety*, *13*(4), 693–704. https://doi.org/10.1111/1541-4337.12078

Singh, N., Jenkins, G. J. S., Asadi, R., & Doak, S. H. (2010). Potential toxicity of superparamagnetic iron oxide nanoparticles (SPION). *Nano Reviews*, *1*. https://doi.org/10.3402/nano.v1i0.5358

Singh, N., Manshian, B., Jenkins, G. J. S., Griffiths, S. M., Williams, P. M., Maffeis, T. G. G., … Doak, S. H. (2009). NanoGenotoxicology: The DNA damaging potential of engineered nanomaterials. *Biomaterials*, *30*(23), 3891–3914. https://doi.org/10.1016/j.biomaterials.2009.04.009

Smulders, S., Golanski, L., Smolders, E., Vanoirbeek, J., & Hoet, P. h. m. (2015). Nano-TiO2 modulates the dermal sensitization potency of dinitrochlorobenzene after topical exposure. *British Journal of Dermatology*, *172*(2), 392–399. https://doi.org/10.1111/bjd.13295

Smulders, Stijn, Ketkar-Atre, A., Luyts, K., Vriens, H., Nobre, S. D. S., Rivard, C., … Hoet, P. H. (2016). Body distribution of SiO_2-Fe_3O_4 core-shell nanoparticles after intravenous injection and intratracheal instillation. *Nanotoxicology*, *10*(5), 567–574. https://doi.org/10.3109/17435390.2015.1100761

Sonane, M., Moin, N., & Satish, A. (2017). The role of antioxidants in attenuation of Caenorhabditis elegans lethality on exposure to TiO2 and ZnO nanoparticles. *Chemosphere*, *187*, 240–247. https://doi.org/10.1016/j.chemosphere.2017.08.080

Song, Y., Li, X., Wang, L., Rojanasakul, Y., Castranova, V., Li, H., & Ma, J. (2011). Nanomaterials in Humans: Identification, Characteristics, and Potential Damage. *Toxicologic Pathology*, *39*(5), 841–849. https://doi.org/10.1177/0192623311413787

Sotiriou, G. A., Watson, C., Murdaugh, K. M., Darrah, T. H., Pyrgiotakis, G., Elder, A., … Demokritou, P. (2014). Engineering safer-by-design, transparent, silica-coated ZnO nanorods with reduced DNA damage potential. *Environmental Science. Nano*, *1*(2), 144–153. https://doi.org/10.1039/C3EN00062A

Stoccoro, A., Di Bucchianico, S., Coppedè, F., Ponti, J., Uboldi, C., Blosi, M., … Migliore, L. (2017). Multiple endpoints to evaluate pristine and remediated titanium dioxide nanoparticles genotoxicity in lung epithelial A549 cells. *Toxicology Letters*, *276*, 48–61. https://doi.org/10.1016/j.toxlet.2017.05.016

Stone, V., Johnston, H., & Schins, R. P. F. (2009). Development of in vitro systems for nanotoxicology: methodological considerations. *Critical Reviews in Toxicology*, *39*(7), 613–626. https://doi.org/10.1080/10408440903120975

Suh, W. H., Suslick, K. S., Stucky, G. D., & Suh, Y.-H. (2009). Nanotechnology, nanotoxicology, and neuroscience. *Progress in Neurobiology*, *87*(3), 133–170. https://doi.org/10.1016/j.pneurobio.2008.09.009

Sun, R. W.-Y., Chen, R., Chung, N. P.-Y., Ho, C.-M., Lin, C.-L. S., & Che, C.-M. (2005). Silver nanoparticles fabricated in Hepes buffer exhibit cytoprotective activities toward HIV-1 infected cells. *Chemical Communications*, (40), 5059. https://doi.org/10.1039/b510984a

Szakal, C., Roberts, S. M., Westerhoff, P., Bartholomaeus, A., Buck, N., Illuminato, I., … Rogers, M. (2014). Measurement of Nanomaterials in Foods: Integrative Consideration of Challenges and Future Prospects. *ACS Nano*, *8*(4), 3128–3135. https://doi.org/10.1021/nn501108g

Tolaymat, T., El Badawy, A., Sequeira, R., & Genaidy, A. (2015). An integrated science-based methodology to assess potential risks and implications of engineered nanomaterials. *Journal of Hazardous Materials*, *298*, 270–281. https://doi.org/10.1016/j.jhazmat.2015.04.019

Tsuda, A., & Gehr, P. (2014). *Nanoparticles in the Lung: Environmental Exposure and Drug Delivery*. CRC Press.

Tsugita, M., Morimoto, N., & Nakayama, M. (2017). SiO2 and TiO2 nanoparticles synergistically trigger macrophage inflammatory responses. *Particle and Fibre Toxicology*, *14*. https://doi.org/10.1186/s12989-017-0192-6

Tungittiplakorn, W., Lion, L. W., Cohen, C., & Kim, J.-Y. (2004). Engineered Polymeric Nanoparticles for Soil Remediation. *Environmental Science & Technology*, *38*(5), 1605–1610. https://doi.org/10.1021/es0348997

United States National Nanotechnology Initiative. (2014). Nanotechnology Timeline | Nano. Retrieved February 19, 2018, from https://www.nano.gov/timeline

United States National Nanotechnology Initiative. (n.d.). Benefits and Applications | Nano. Retrieved February 19, 2018, from https://www.nano.gov/you/nanotechnology-benefits

Ursini, C. L., Cavallo, D., Fresegna, A. M., Ciervo, A., Maiello, R., Tassone, P., … Iavicoli, S. (2014). Evaluation of cytotoxic, genotoxic and inflammatory response in human alveolar and bronchial epithelial cells exposed to titanium dioxide nanoparticles. *Journal of Applied Toxicology*, *34*(11), 1209–1219. https://doi.org/10.1002/jat.3038

US Department of Commerce, B. E. A. (2018). Bureau of Economic Analysis. Retrieved February 19, 2018, from https://www.bea.gov/iTable/index_nipa.cfm

US EPA, O. (2015a, March 27). Control of Nanoscale Materials under the Toxic Substances Control Act [Collections and Lists]. Retrieved February 19, 2018, from https://www.epa.gov/reviewing-new-chemicals-under-toxic-substances-control-act-tsca/control-nanoscale-materials-under

US EPA, O. (2015b, September 2). Fact Sheet: Nanoscale Materials [Overviews and Factsheets]. Retrieved from https://www.epa.gov/reviewing-new-chemicals-under-toxic-substances-control-act-tsca/fact-sheet-nanoscale-materials

Valavanidis, A., & Vlachogianni, T. (2016). Engineered Nanomaterials for Pharmaceutical and Biomedical Products New Trends, Benefits and Opportunities. *Journal of Pharmacological Reports*, *1*(1). Retrieved from https://www.omicsonline.org/open-access/engineered-nanomaterials-for-pharmaceutical-and-biomedical-productsnew-trends-benefits-and-opportunities-jpr-1000105.php?aid=69521

van den Brule, S., Ambroise, J., Lecloux, H., Levard, C., Soulas, R., De Temmerman, P.-J., … Lison, D. (2016). Dietary silver nanoparticles can disturb the gut microbiota in mice. *Particle and Fibre Toxicology*, *13*(1), 38. https://doi.org/10.1186/s12989-016-0149-1

Vance, M. E., Kuiken, T., Vejerano, E. P., McGinnis, S. P., Hochella, M. F., Rejeski, D., & Hull, M. S. (2015). Nanotechnology in the real world: Redeveloping the nanomaterial consumer products inventory. *Beilstein Journal of Nanotechnology*, *6*, 1769–1780. https://doi.org/10.3762/bjnano.6.181

Vorbau, M., Hillemann, L., & Stintz, M. (2009). Method for the characterization of the abrasion induced nanoparticle release into air from surface coatings. *Journal of Aerosol Science*, *40*(3), 209–217. https://doi.org/10.1016/j.jaerosci.2008.10.006

Wang, Z., Chen, Z., Zuo, Q., Song, F., Wu, D., Cheng, W., & Fan, W. (2013). Reproductive toxicity in adult male rats following intra-articular injection of cobalt-chromium nanoparticles. *Journal of Orthopaedic Science: Official Journal of the Japanese Orthopaedic Association*, *18*(6), 1020–1026. https://doi.org/10.1007/s00776-013-0458-2

Watson, C., Ge, J., Cohen, J., Pyrgiotakis, G., Engelward, B. P., & Demokritou, P. (2014). High-Throughput Screening Platform for Engineered Nanoparticle-Mediated Genotoxicity Using CometChip Technology. *ACS Nano*, *8*(3), 2118–2133. https://doi.org/10.1021/nn404871p

Watson, C. Y., DeLoid, G., Pal, A., & Demokritou, P. (2016). Buoyant Nanoparticles: Implications for Nano-biointeractions in Cellular Studies. *Small (Weinheim an Der Bergstrasse, Germany)*, *12*(23), 3172–3180. https://doi.org/10.1002/smll.201600314

Watson, C. Y., Molina, R. M., Louzada, A., Murdaugh, K. M., Donaghey, T. C., & Brain, J. D. (2015). Effects of zinc oxide nanoparticles on Kupffer cell phagosomal motility, bacterial clearance, and liver function. *International Journal of Nanomedicine*, *10*, 4173–4184. https://doi.org/10.2147/IJN.S82807

Watson-Wright, C., Singh, D., & Demokritou, P. (2017). Toxicological Implications of Released Particulate Matter during Thermal Decomposition of Nano-Enabled Thermoplastics. *NanoImpact*, *5*, 29–40. https://doi.org/10.1016/j.impact.2016.12.003

Wawrzynczak, A., & Nowak, I. (2011). Synthesis and characterization of metallic oxides with potential use in cosmetic products. *Chemtik*, *65*(2), 82–87.

Weir, A., Westerhoff, P., Fabricius, L., Hristovski, K., & von Goetz, N. (2012). Titanium dioxide nanoparticles in food and personal care products. *Environmental Science & Technology*, *46*(4), 2242–2250. https://doi.org/10.1021/es204168d

Williams, D. R. (2002). Racial/Ethnic Variations in Women's Health: The Social Embeddedness of Health. *American Journal of Public Health*, *92*(4), 588–597. Retrieved from https://www.ncbi.nlm.nih.gov/pmc/articles/PMC1447123/

Williams, D. R., Priest, N., & Anderson, N. (2016). Understanding Associations between Race, Socioeconomic Status and Health: Patterns and Prospects. *Health Psychology : Official Journal of the Division of Health Psychology, American Psychological Association*, *35*(4), 407–411. https://doi.org/10.1037/hea0000242

Wu, W., Yan, L., Wu, Q., Li, Y., Li, Q., Chen, S., … Yin, Z. Q. (2016). Evaluation of the toxicity of graphene oxide exposure to the eye. *Nanotoxicology*, *10*(9), 1329–1340. https://doi.org/10.1080/17435390.2016.1210692

Xia, T., Kovochich, M., Brant, J., Hotze, M., Sempf, J., Oberley, T., … Nel, A. E. (2006). Comparison of the abilities of ambient and manufactured nanoparticles to induce cellular toxicity according to an oxidative stress paradigm. *Nano Letters*, *6*(8), 1794–1807. https://doi.org/10.1021/nl061025k

Yin, H., Too, H. P., & Chow, G. M. (2005). The effects of particle size and surface coating on the cytotoxicity of nickel ferrite. *Biomaterials*, *26*(29), 5818–5826. https://doi.org/10.1016/j.biomaterials.2005.02.036

Yokel, R. A., & MacPhail, R. C. (2011). Engineered nanomaterials: exposures, hazards, and risk prevention. *Journal of Occupational Medicine and Toxicology (London, England)*, *6*, 7. https://doi.org/10.1186/1745-6673-6-7

Zhang, H., Ji, Z., Xia, T., Meng, H., Low-Kam, C., Liu, R., … Nel, A. E. (2012). Use of metal oxide nanoparticle band gap to develop a predictive paradigm for oxidative stress and acute pulmonary inflammation. *ACS Nano*, *6*(5), 4349–4368. https://doi.org/10.1021/nn3010087

Zhao, J., & Castranova, V. (2011). Toxicology of nanomaterials used in nanomedicine. *Journal of Toxicology and Environmental Health. Part B, Critical Reviews*, *14*(8), 593–632. https://doi.org/10.1080/10937404.2011.615113

TABLES

Table 1. Summary of Engineered Nanomaterials and Nano-Enabled Products Utilized in Study

ENM/NEP Name	Pristine (pNP)	Released (rNP)	Light Shade	Dark Shade	Expensive	Inexpensive
Fe_2O_3	✓		N/A	N/A	N/A	N/A
TiO_2	✓		N/A	N/A	N/A	N/A
AA4		✓		✓		✓
AA8		✓	✓			✓
S1		✓	✓		✓	
S4		✓		✓	✓	

Table 2. Aerosol Generation System Settings Specifics		
Condition	**Set Points**	**Units**
Calibrated Particle Concentration	10.00	mg/m^3
RAE VOC Reading	0.00	ppm*
Sprayer Air Flow	3.50	lpm**
Glove Box Air Flow	11.00	lpm**
Exposure Chamber Pressure and Glove Box Pressure	0.00 Minimum: -2.00 Maximum: 2.00	Inch H_2O
Exposure Chamber Temperature	Minimum: 55.0 (12.8) Maximum: 78.0 (25.6)	°F (°C)
Exposure Chamber Relative Humidity	Minimum: 1.00 Maximum: 70.0	%
Spray Duration	0.60	sec
Rotation Speed	2.0	rpm***
Exhaust Flow	12.01 Minimum: 0.00 Maximum: 40.00	lpm**
Safe Level to End Exposure	1.00	mg/m^3
Gain	0.100	N/A
Glove Box Pressure Zero and Exposure Chamber Pressure Zero	2.50	V
DataRAM Calibration Factor	Default is 1.00, adjusted for each product	N/A
Abbreviations: *** parts per million** **** liters per minute** ***** rotations per minute**		

Table 3. Energy Dispersive Spectroscopy Elemental Analysis of Released Nanoparticles							
Sample Name	*Element*	*Line Type*	*Apparent Concentration*	*k Ratio*	*Wt%*	*Wt% Sigma*	*Standard Label*
AA4	**Fe**	**K series**	**0.7**	**0.00703**	**65.22**	**4.25**	**Fe**
	O	K series	0.81	0.00273	27.45	3.48	SiO2
	Al	K series	0.09	0.00061	7.33	1.37	Al2O3
	Total:				100		
AA8	**Ti**	**K series**	**0.4**	**0.00403**	**52.19**	**5.22**	**Ti**
	Br	L series	0.34	0.00301	47.81	5.22	KBr
	Total:				100		
S1	O	K series	0.36	0.0012	41.21	4.16	SiO2
	Ti	**K series**	**0.3**	**0.00303**	**38.79**	**4.07**	**Ti**
	Al	K series	0.2	0.00145	20	2.26	Al2O3
	Total:				100		
S4	**Ti**	**K series**	**0.31**	**0.00307**	**34.77**	**2.63**	**Ti**
	O	K series	0.34	0.00115	32.99	2.45	SiO2
	Fe	**K series**	**0.14**	**0.00139**	**16.51**	**3.81**	**Fe**
	Al	K series	0.17	0.00121	15.72	1.25	Al2O3
	Total:				100		

Table 4. Filter Weights and Calculations of Released Nanoparticle Mass				
Sample Name	**Filter Weight Pre-Extraction (mg)**	**Dry Filter Weight Post-Extraction (mg)**	**Mass Collected (mg)**	**Stock Concentration (ug/mL)**
AA4	52.57	49.67	2.90	580
AA8	51.73	49.60	2.13	426
S1	51.46	49.37	2.09	418
S4	52.19	49.36	2.83	566

Table 5. Colloidal Characterization of Raw Products, Released Nanoparticles, and Pristine Nanoparticles Using Dynamic Light Scattering

Raw Nano-enabled Products					
Sample	**Media**	**$d_{(h, z\text{-}ave)}$ (nm)**	**PdI**	**Zeta Potential ζ (mV)**	**Conductance σ (mS/cm)**
AA4	di H2O	936.4±13.7	0.294± 0.03	0.4±0.06	0.07±0.002
	SABM	984.4±38.5	0.25± 0.04	-1.4±1.6	10.6±0.6
S4	di H2O	511.±2.4	0.26± 0.01	-0.8±0.09	0.04±0.001
	SABM	1782±186	0.28± 0.05	2.6±0.4	11.1±0.4
Released Nano-enabled Products					
Sample	**Media**	**$d_{(h, z\text{-}ave)}$ (nm)**	**PdI**	**Zeta Potential ζ (mV)**	**Conductance σ (mS/cm)**
AA4	di H2O	401.67±19.94	0.39±0.02	-0.14±0.12	2.17±0.92
	SABM	349.07±18.25	0.43±0.03	-258±39.89	920.33±123.86
	DMEM	354.27±62.03	0.40±0.07	-260±49.27	1091±191.16
AA8	di H2O	345.53±6.17	0.33±0.01	-31.1±1.4	0.01±0.0005
	SABM	280.73±14.41	0.3±0.03	-31.1±1.4	0.01±0.0005
	DMEM	260.4±3.50	0.23±0.02	-12.13±0.06	13.2±0.26
S1	di H2O	1.02E+04±13625.78	0.88±0.2	-26.93±1.07	0.01±0.0004
	SABM	1098±183.34	0.98±0.02	-16.23±1.11	10.7±0.1
	DMEM	N/A	N/A	-11.7±0.87	13.93±0.55
S4	di H2O	719.07±60.25	0.62±0.05	-0.18±0.53	1.80±0.82
	SABM	584.67±251.73	0.63±0.22	-255.33±35.85	944.67±129.68
	DMEM	778.63±288.99	0.79±0.25	-276.67±29.26	1173.67±175.59
Pristine Nanoparticles					
Sample	**Media**	**$d_{(h, z\text{-}ave)}$ (nm)**	**PdI**	**Zeta Potential ζ (mV)**	**Conductance σ (mS/cm)**
Fe2O3	di H2O	681.2±24.32	0.58±0.04	0.34±0.89	1.65±0.67
	SABM	1227.67±140.36	0.27±0.04	-208.67±29.57	964.67±156.54
	DMEM	N/A	N/A	N/A	N/A
TiO2	di H2O	1820.33±123.87	0.58±0.11	-24.93±5.76	0.02±0.0005
	SABM	268.87±4.3	0.18±0.05	-11.67±0.75	11.4±0.36
	DMEM	307.17±4.1	0.17±0.05	-11.87±0.40	12.67±0.06

FIGURES

Figure 1. Image of Aerosol Generation System Used to Collect Released Aerosolized Engineered Nanoparticles

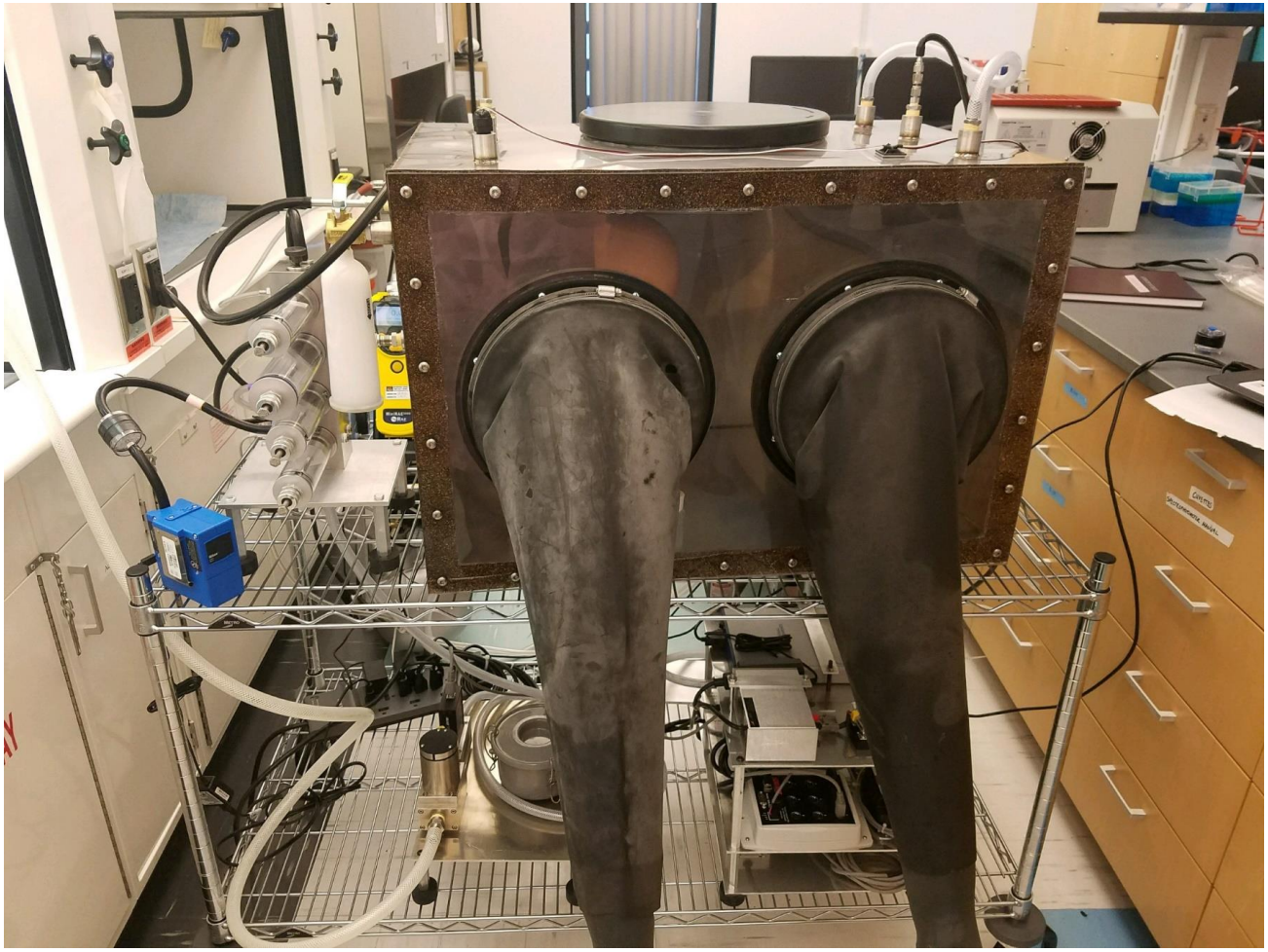

Figure 2. Composition of Metals Present in Both Expensive and Inexpensive Cosmetic Lines Determined by Inductively Coupled Plasma Mass Spectrometry

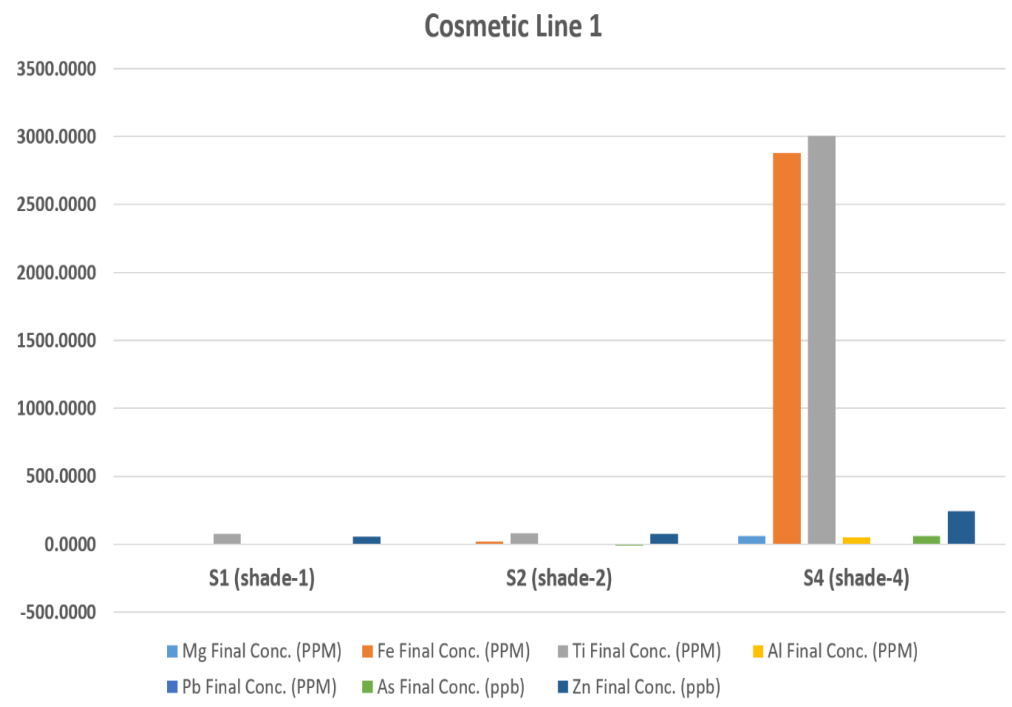

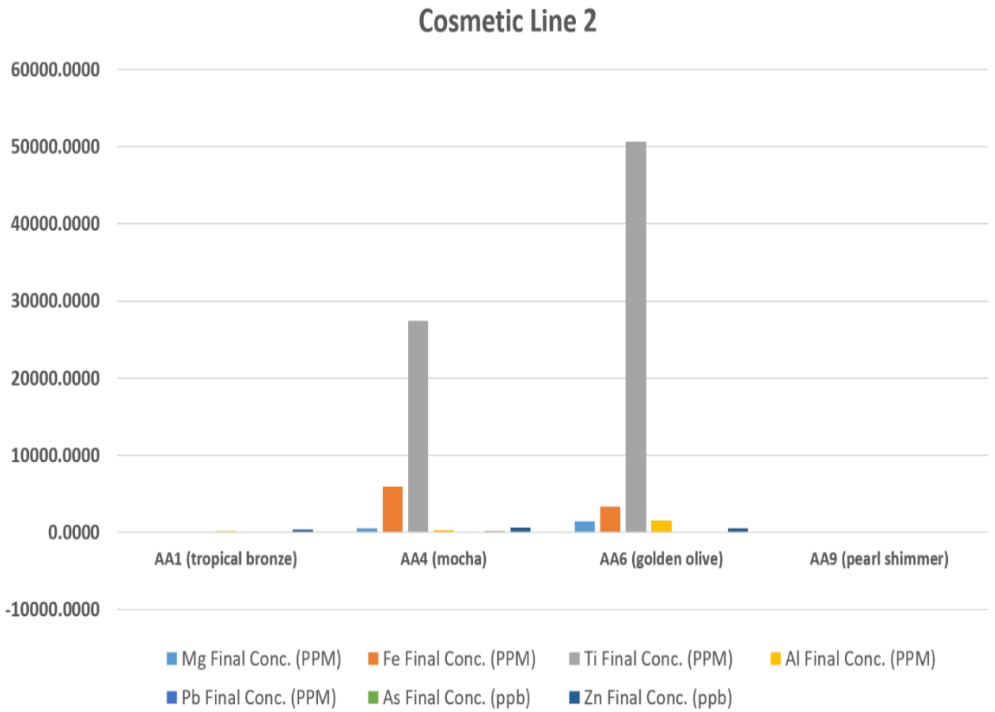

Figure 3. Aerosol Generation System Real Time Exposure Measurements for Released Nanoparticles

AA4 – Average Concentration = 7.77 mg/m3

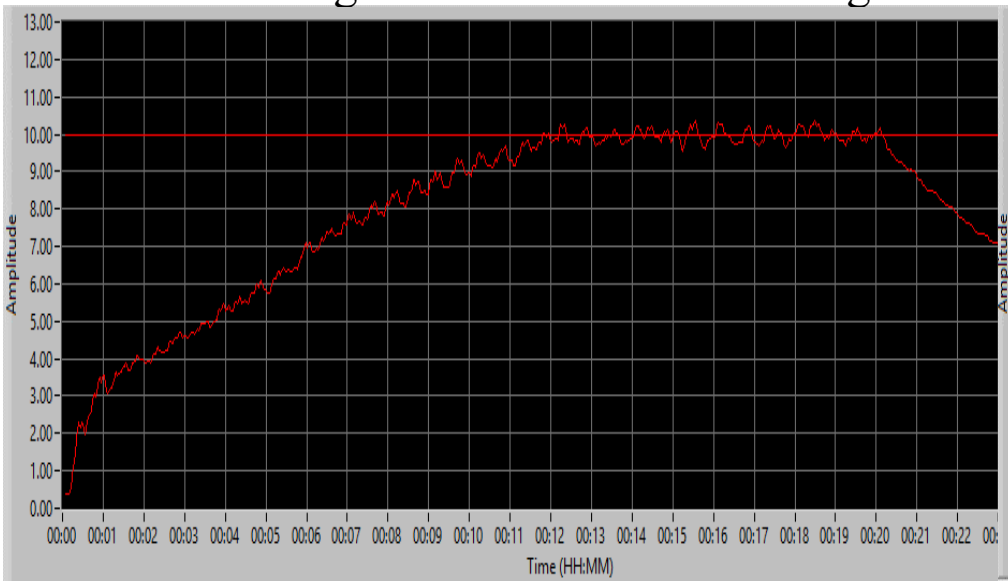

AA8 – Average Concentration = 6.40 mg/m3

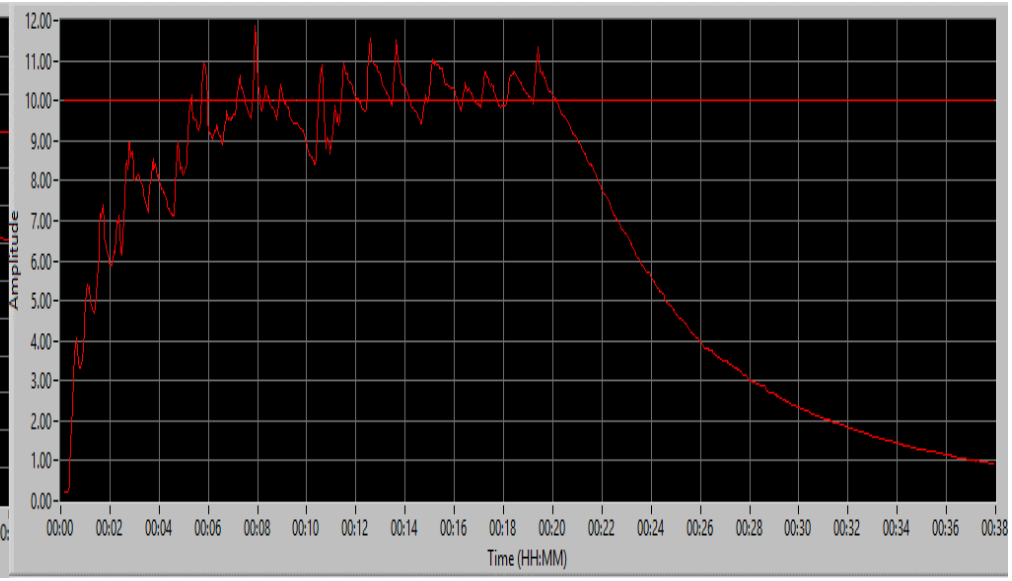

S1 – Average Concentration = 7.17 mg/m3

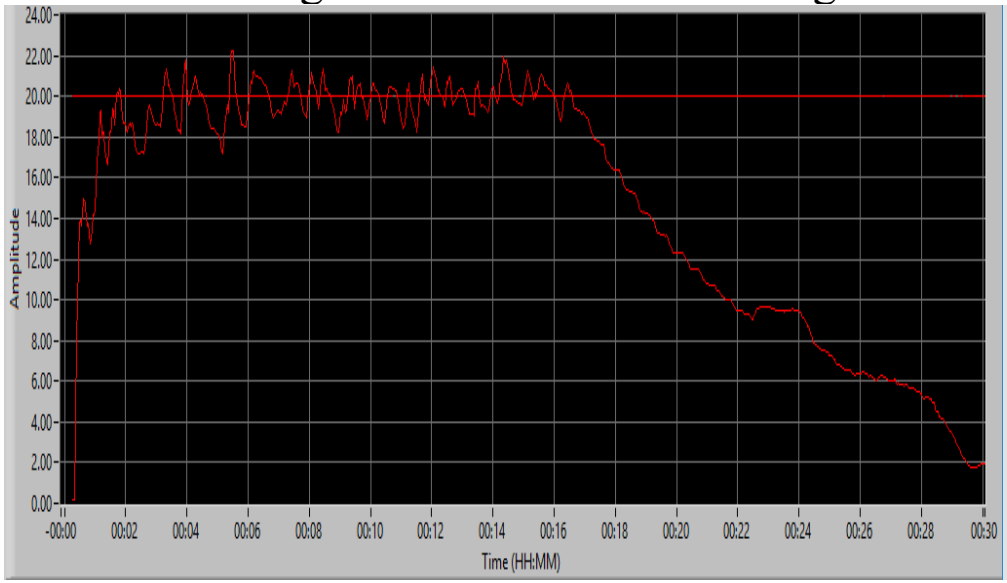

S4 – Average Concentration = 7.64 mg/m3

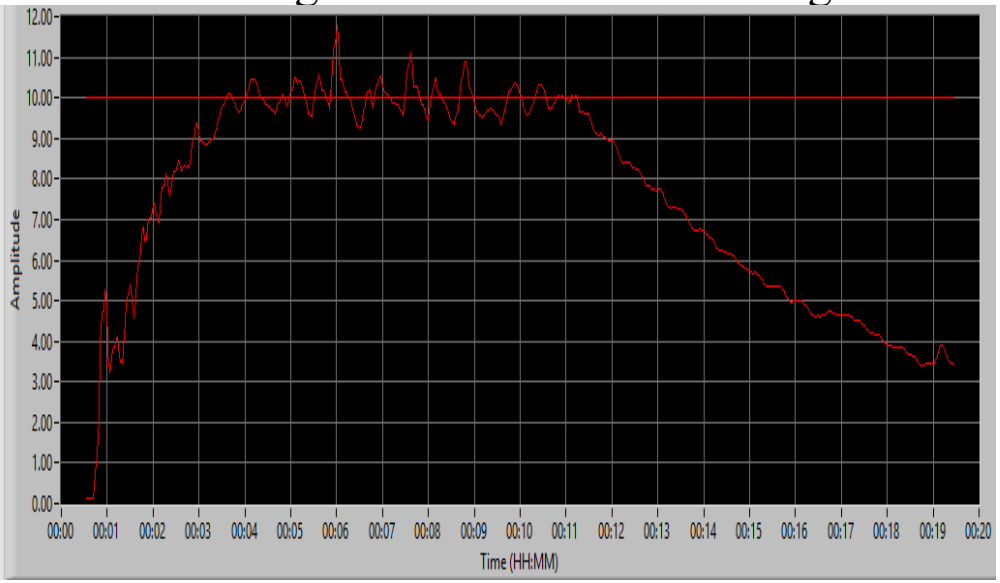

Figure 4. Scanning Mobility Particle Sizer Data for S4

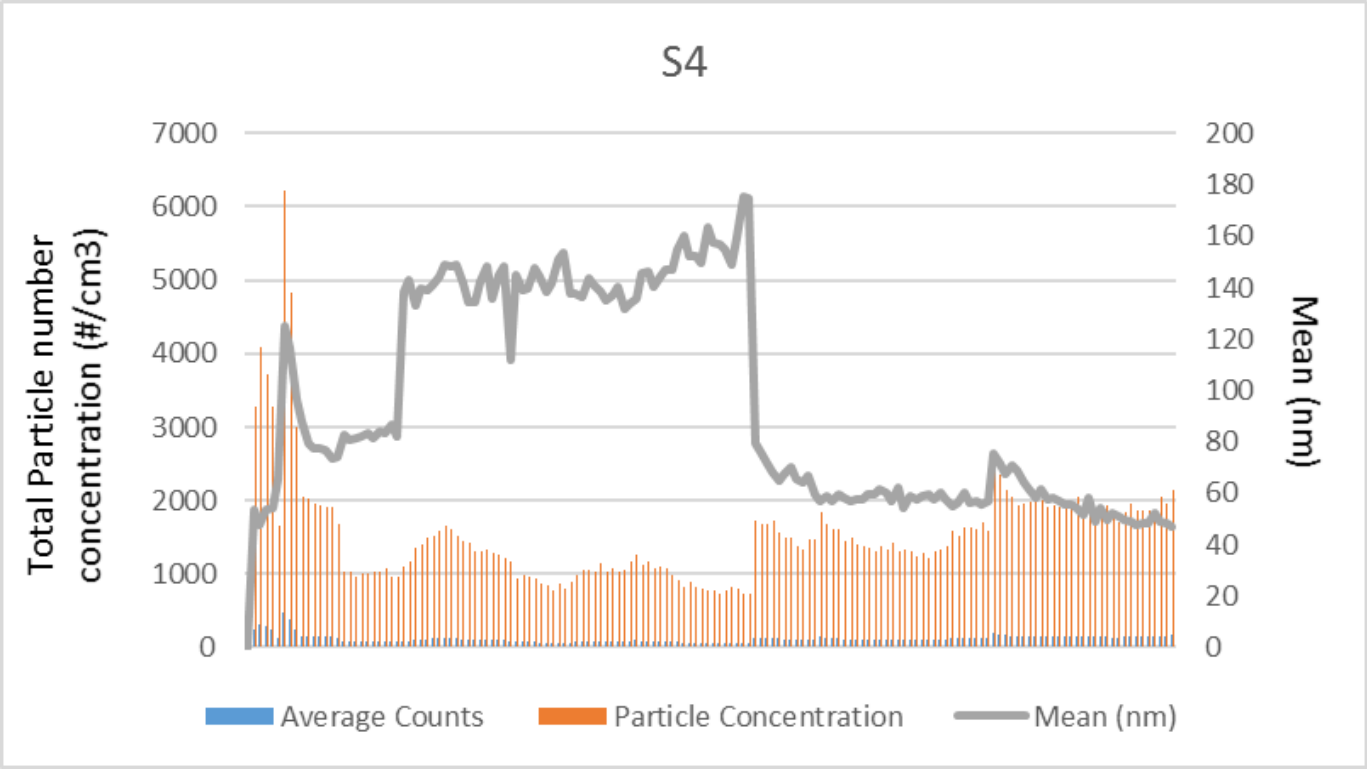

Figure 5. Scanning Electron Microscope Images of Released Nanoparticles

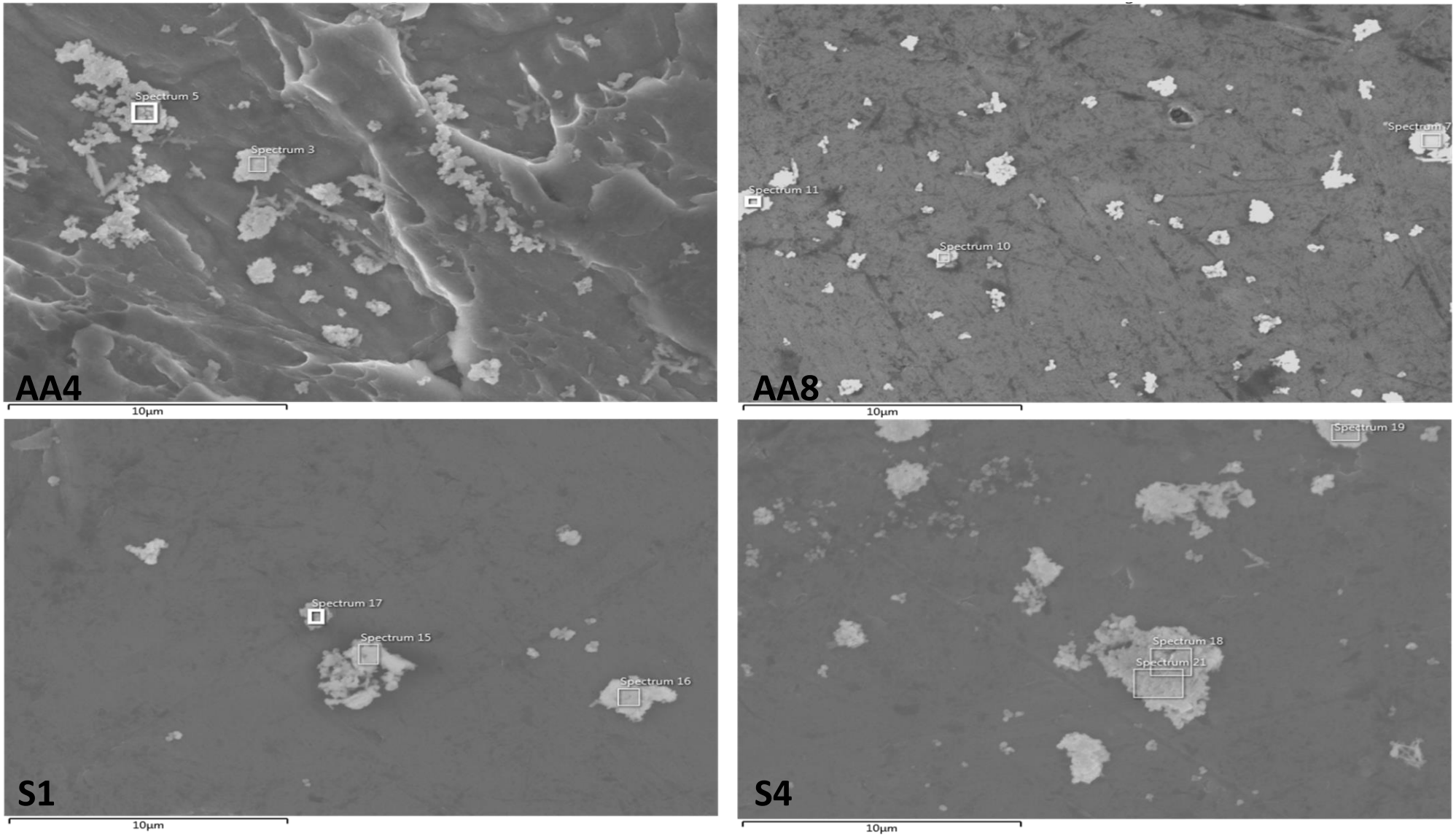

Figure 6. Preliminary Fluorescent Detection of Reactive Oxygen Species for SAEC Exposed to Serial Dilutions of Released AA4 Product for 24 Hours

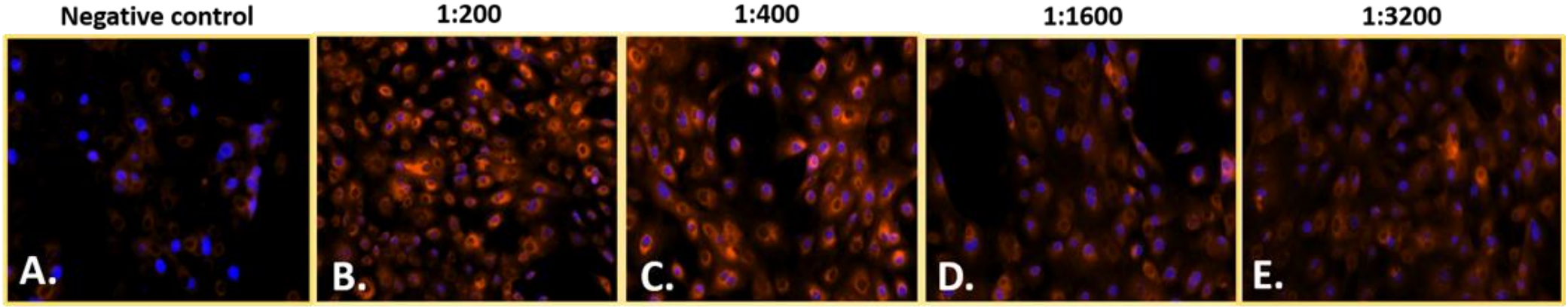

Figure 7. Fluorescent Detection of Reactive Oxygen Species for SAEC and 16HBE Cell Types Exposed to Pristine Fe2O3 Nanoparticles for 24 Hours

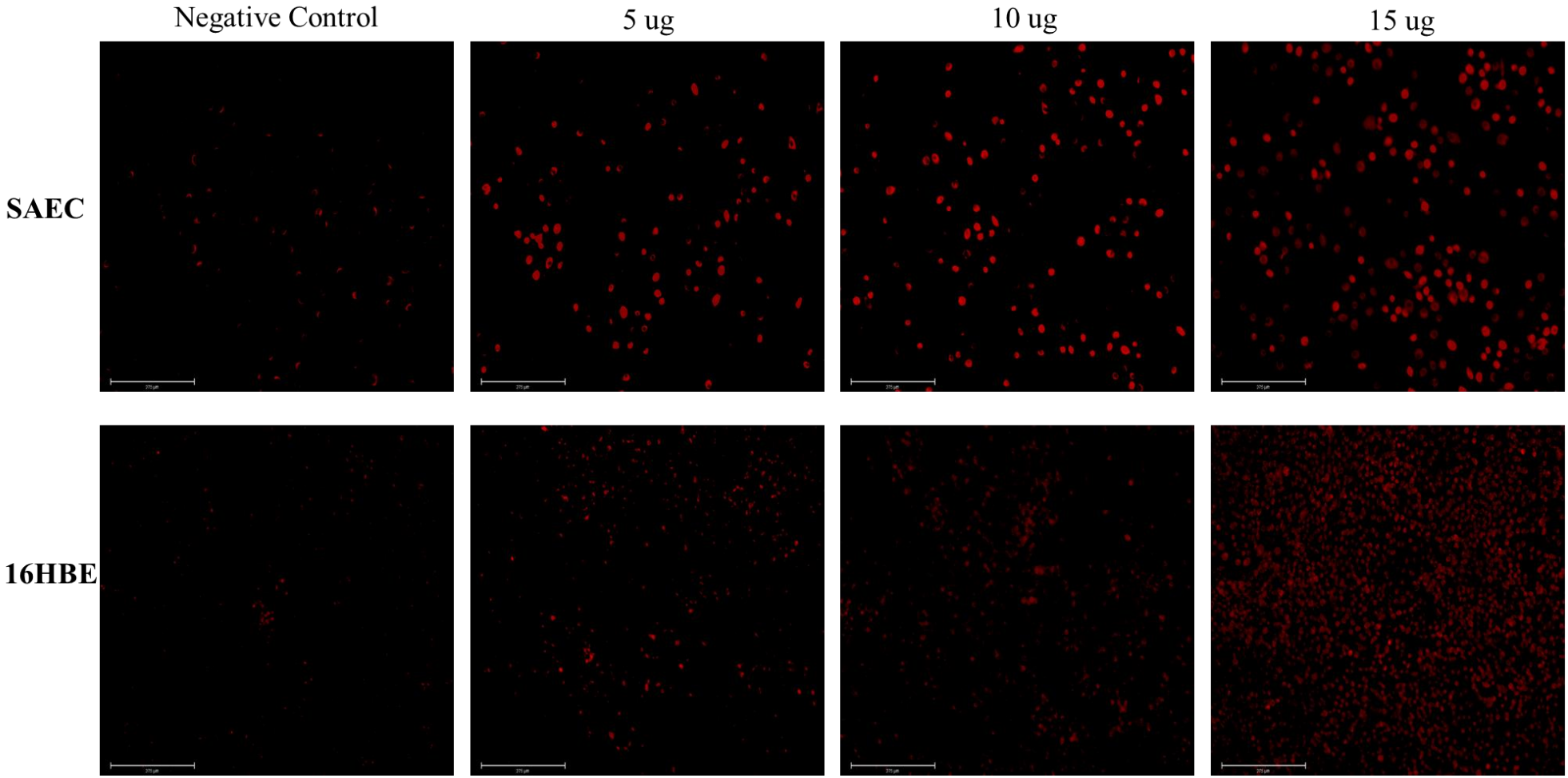

Figure 8. Fluorescent Detection of Reactive Oxygen Species for SAEC and 16HBE Cell Types Exposed to Pristine TiO2 Nanoparticles for 24 Hours

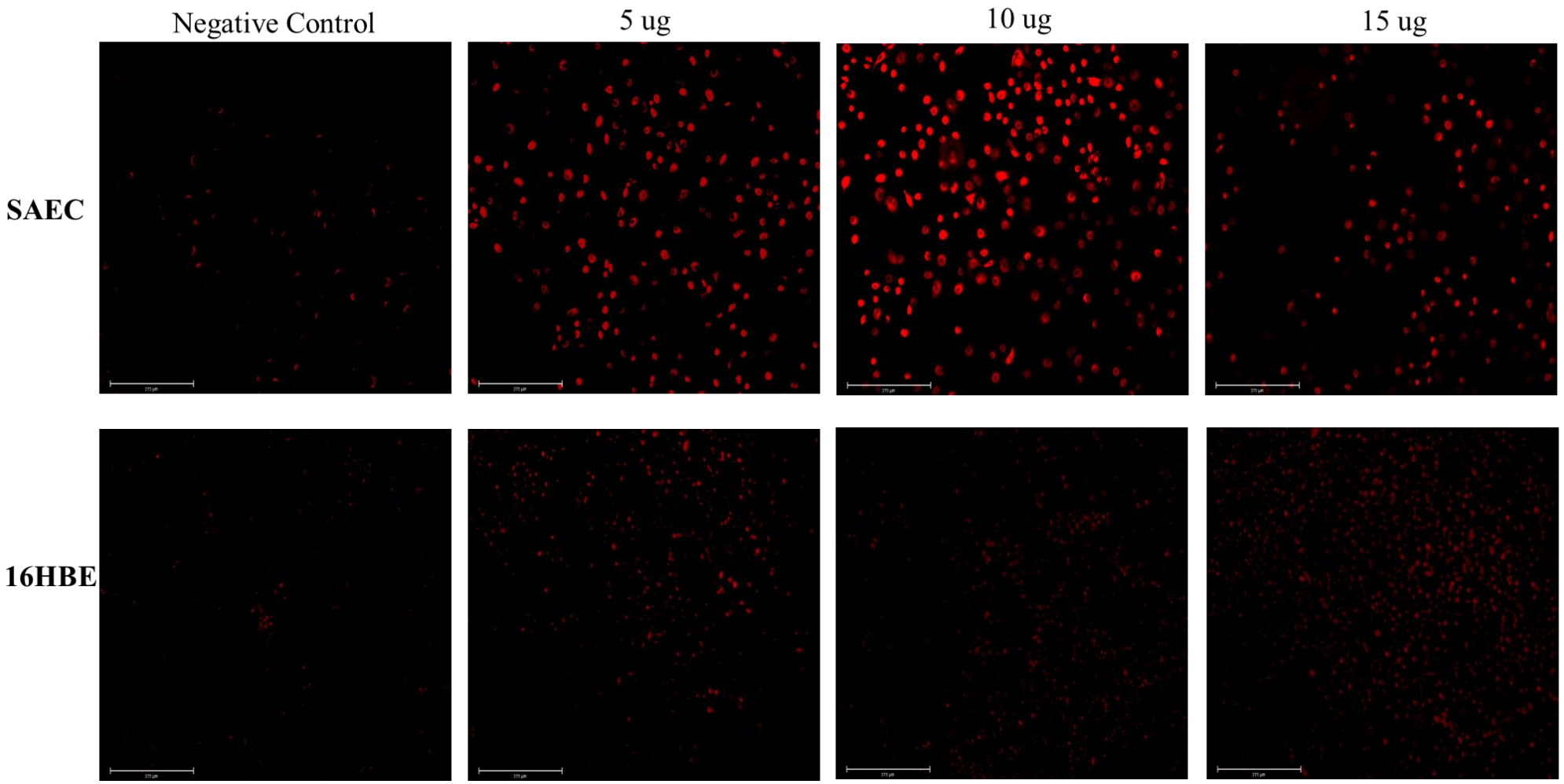

Figure 9. Fluorescent Detection of Reactive Oxygen Species for SAEC and 16HBE Cell Types Exposed to Released AA4 Nanoparticles for 24 Hours

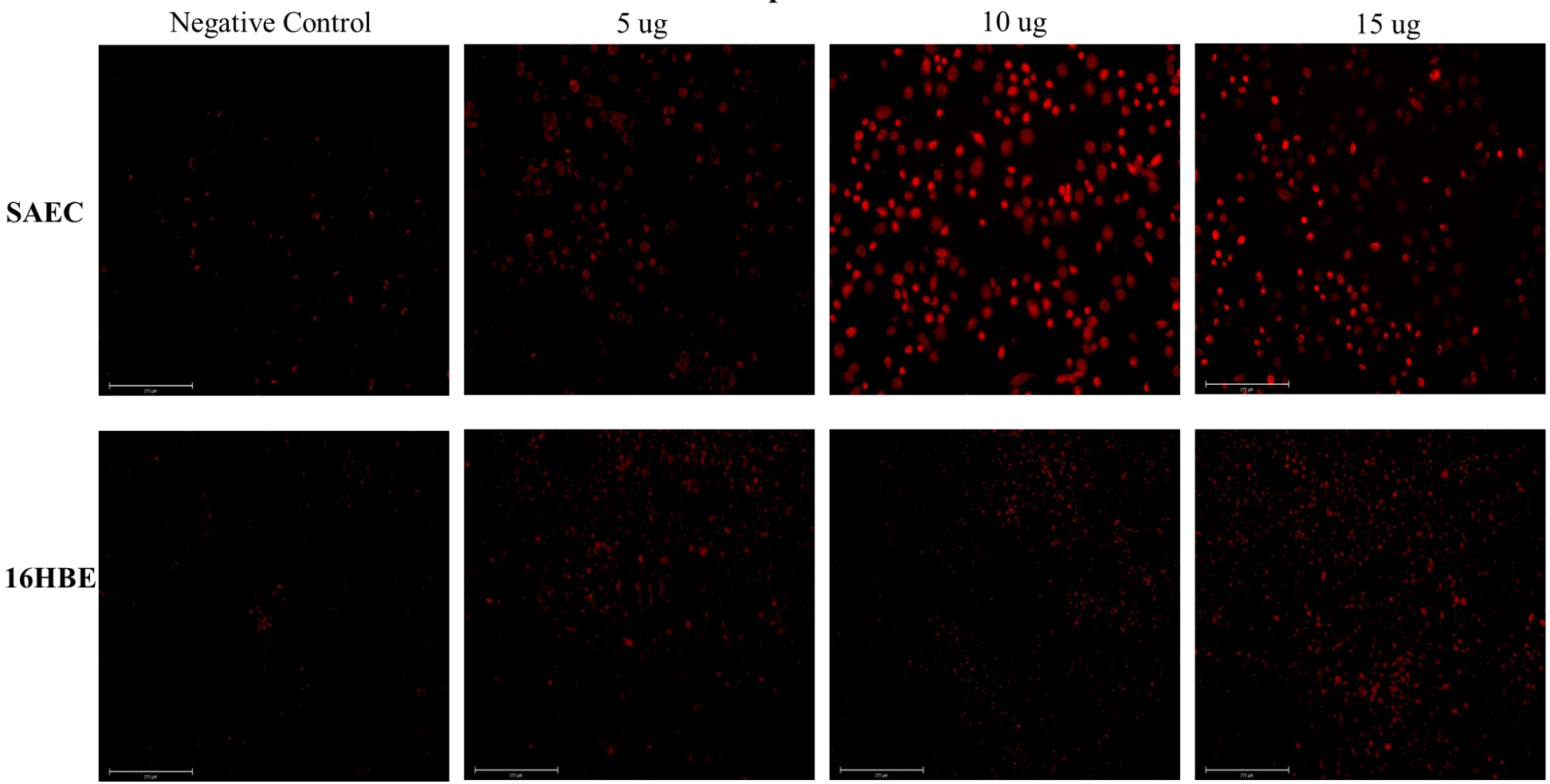

Figure 10. Fluorescent Detection of Reactive Oxygen Species for SAEC and 16HBE Cell Types Exposed to Released AA8 Nanoparticles for 24 Hours

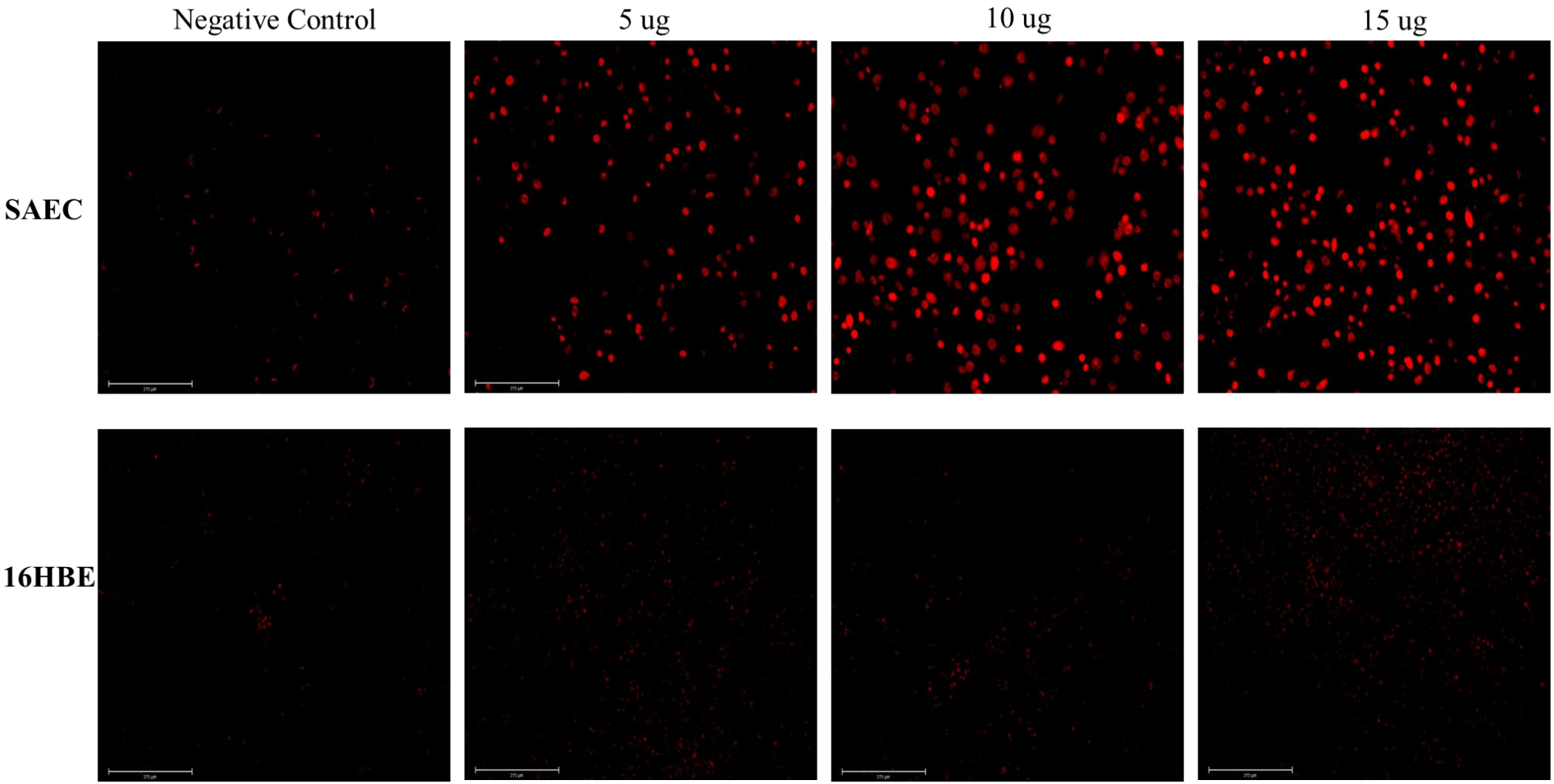

Figure 11. Fluorescent Detection of Reactive Oxygen Species for SAEC and 16HBE Cell Types Exposed to Released S1 Nanoparticles for 24 Hours

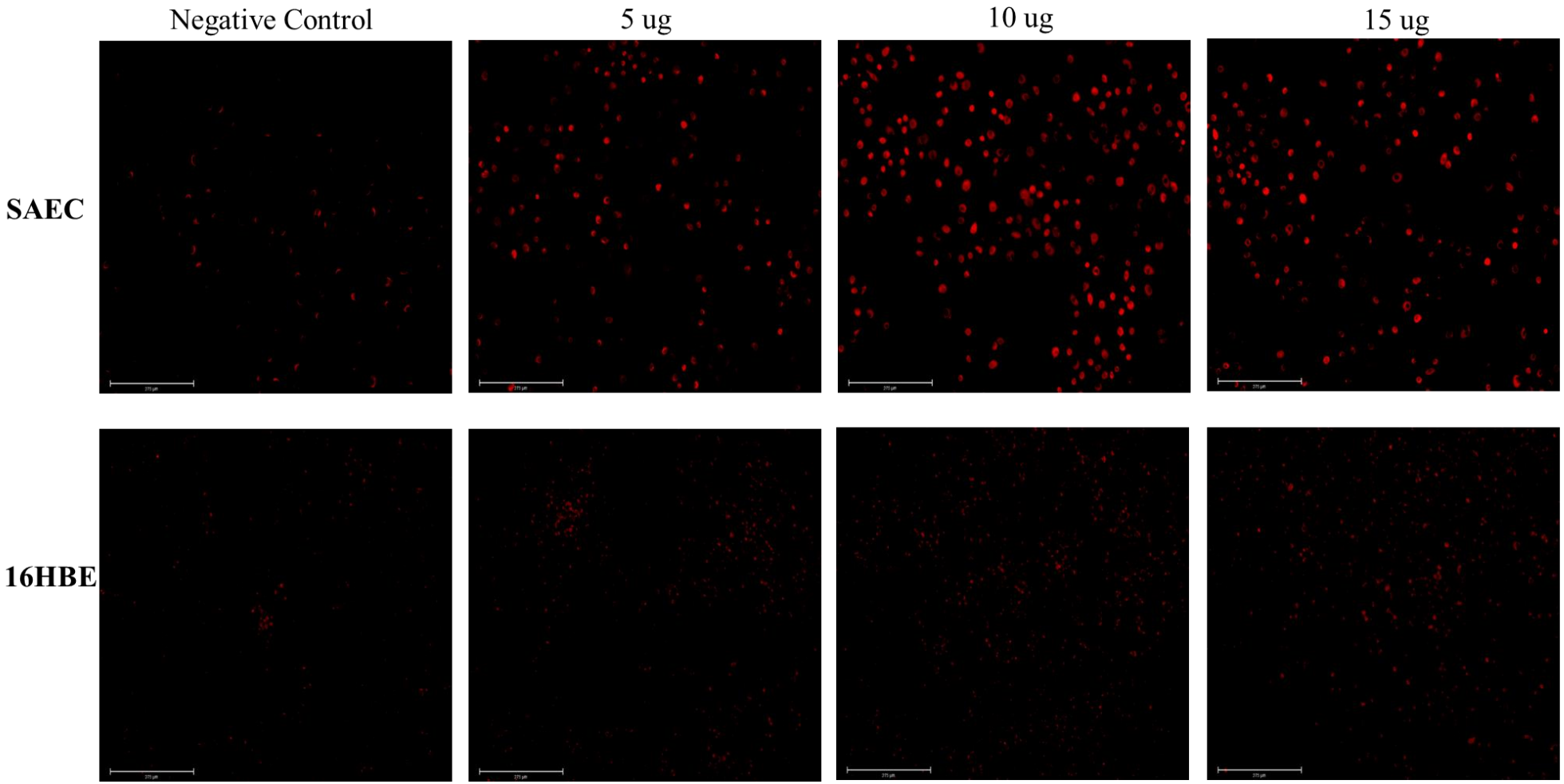

Figure 12. Fluorescent Detection of Reactive Oxygen Species for SAEC and 16HBE Cell Types Exposed to Released S4 Nanoparticles for 24 Hours

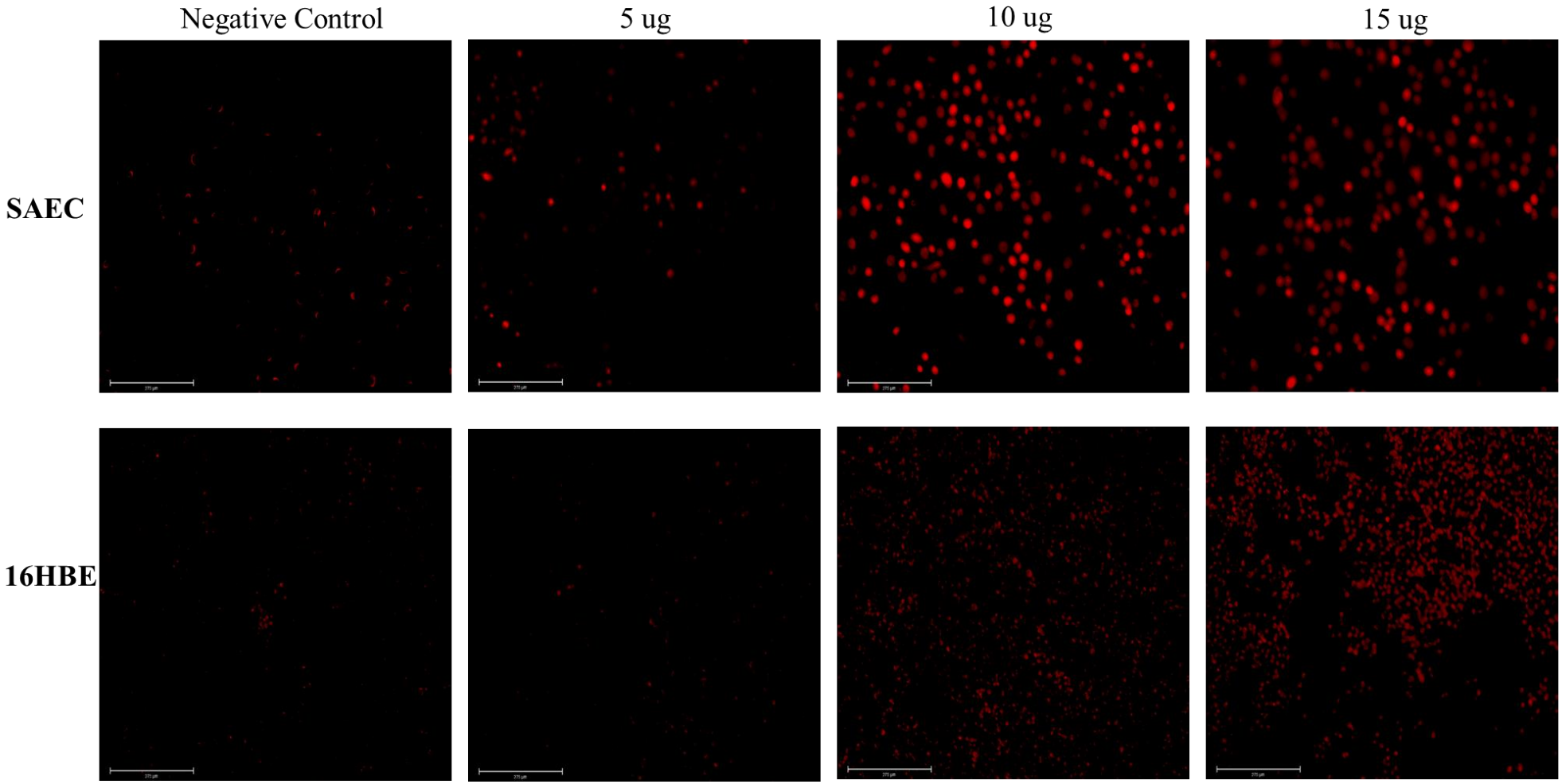

Figure 13. Total Glutathione Determined from GSH Assay After Exposure to Pristine Nanoparticles for 24 Hours

SAEC

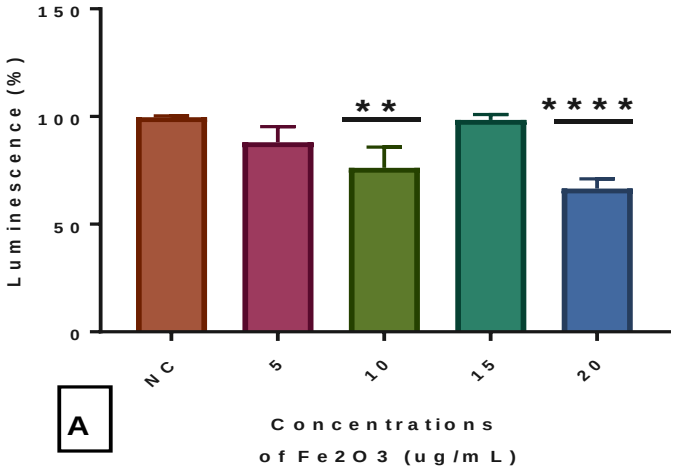

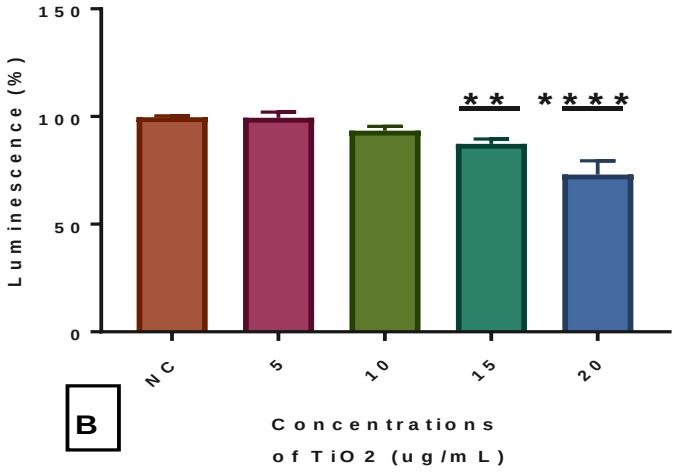

16HBE

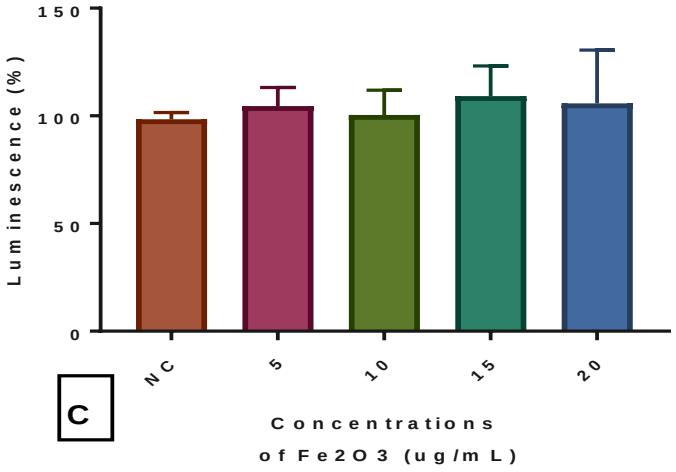

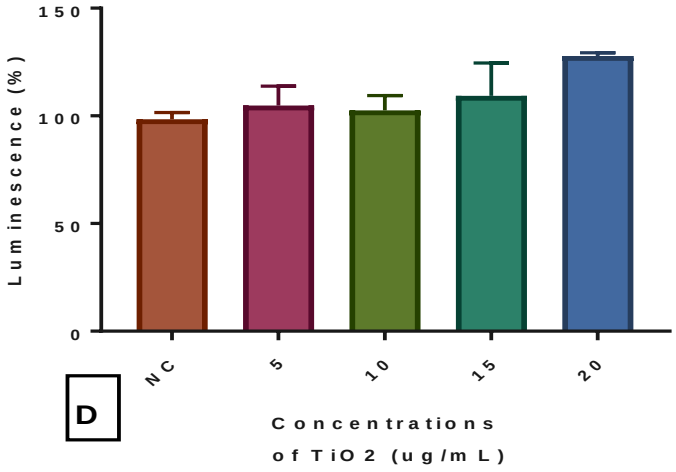

Figure 14. Total Glutathione Determined from GSH Assay After Exposure to Released Nanoparticles for 24 Hours

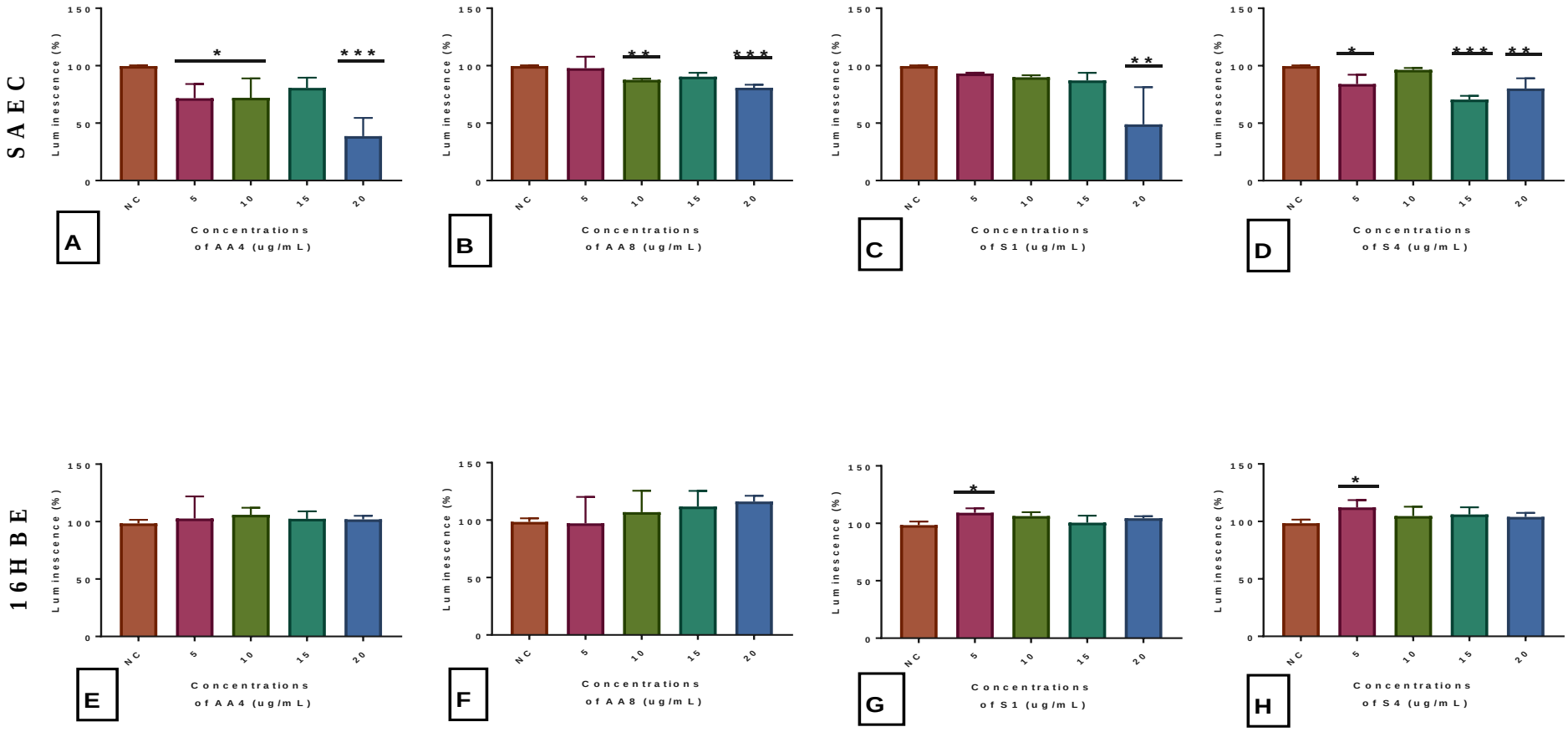

Figure 15. Cellular Viability Determined from MTS Assay After Exposure to Pristine Nanoparticles for 24 Hours

SAEC

16HBE

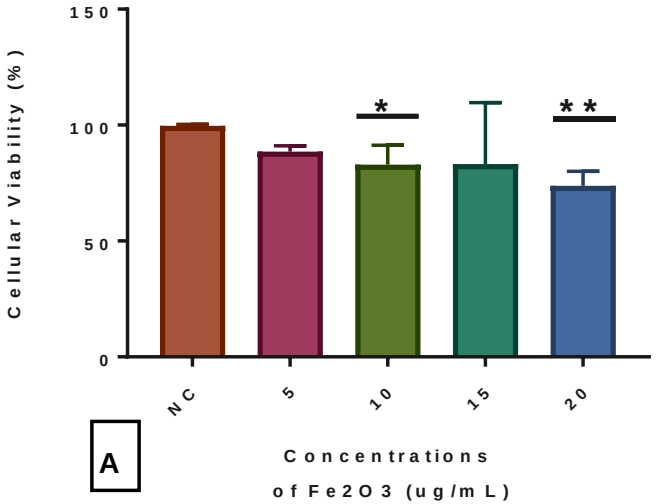

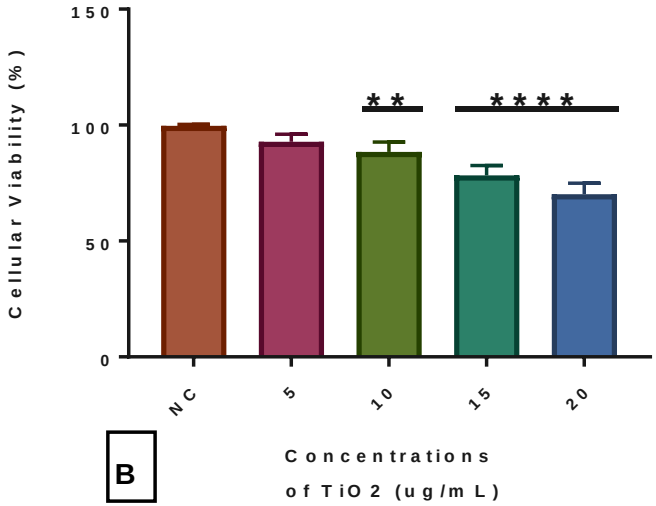

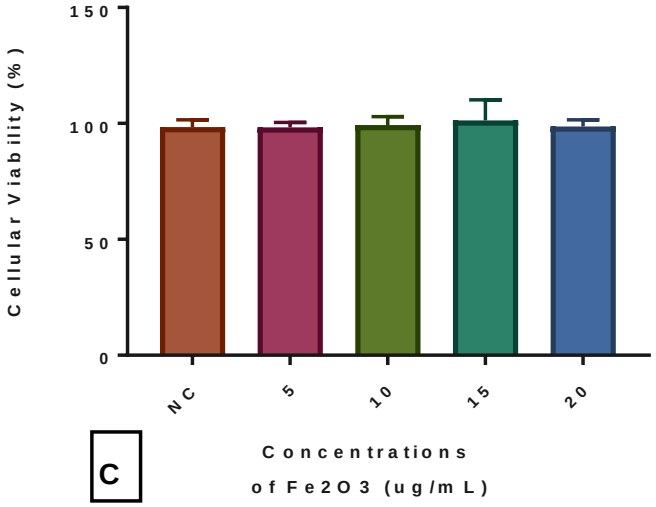

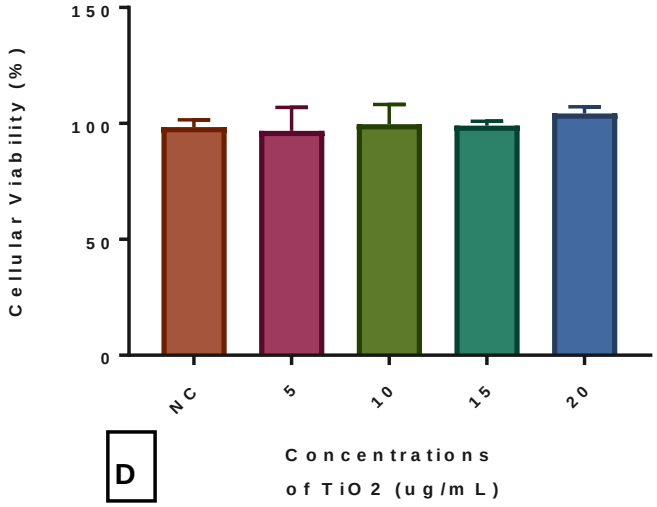

Figure 16. Cellular Viability Determined from MTS Assay After Exposure to Released Nanoparticles for 24 Hours

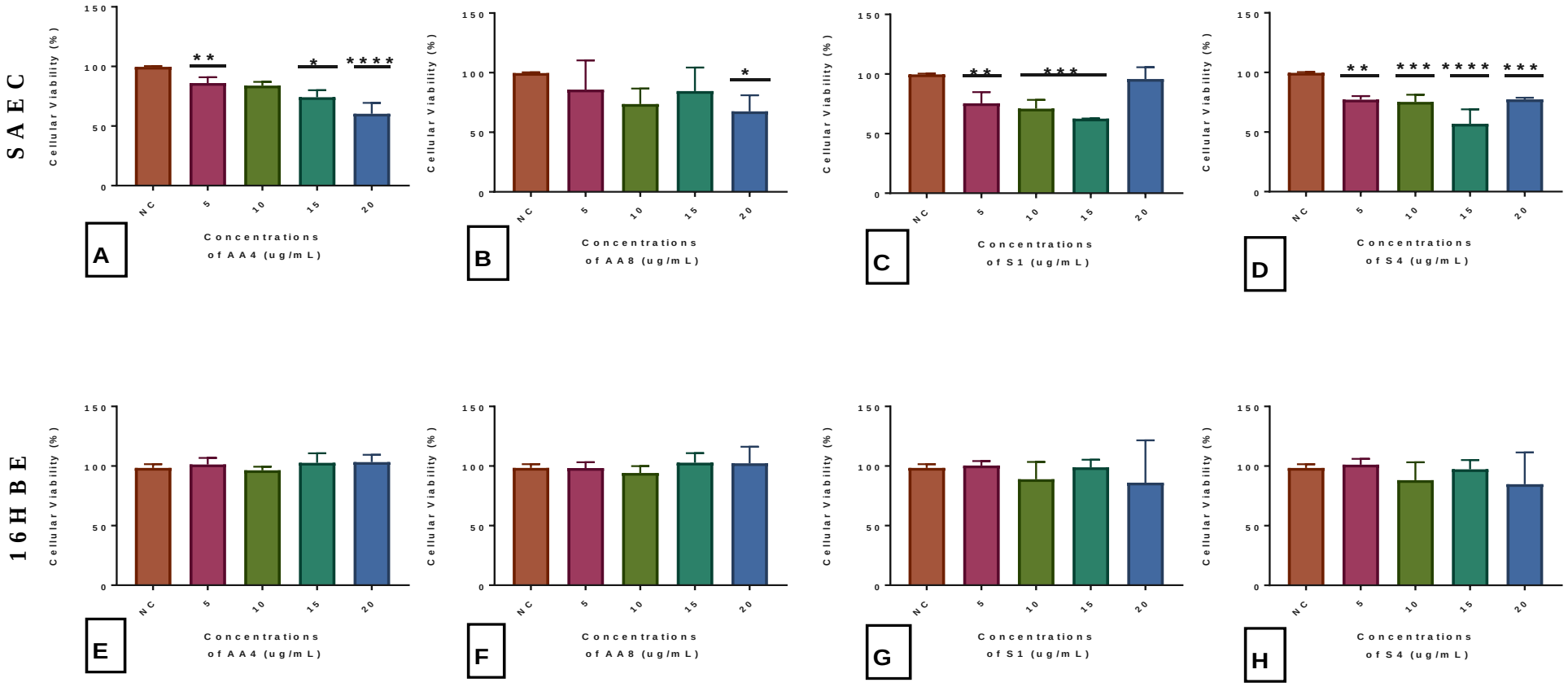

Figure 17. SAEC Epithelial Mesenchymal Transition Comparison between Fe2O3 and AA4 After Exposure for 24 Hours

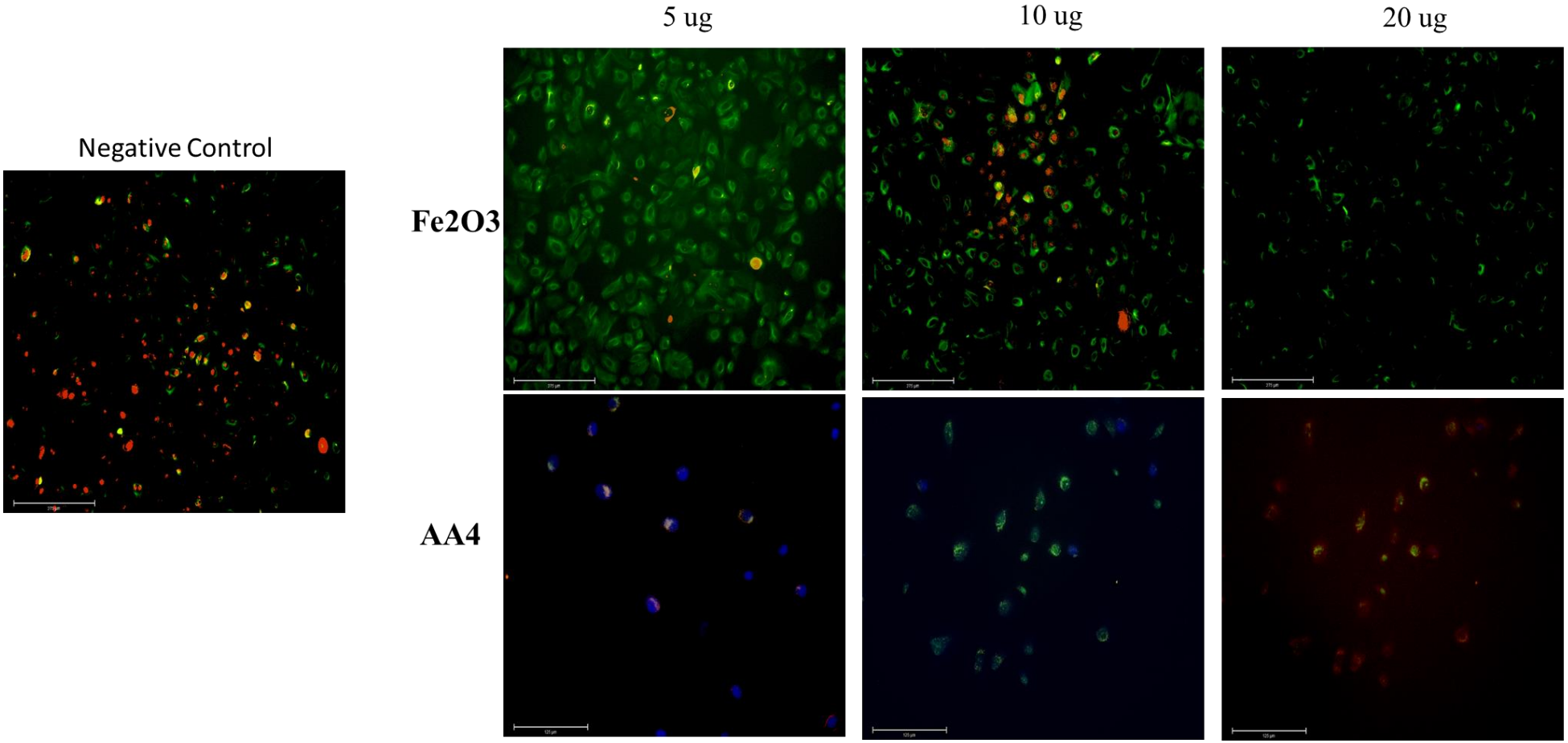

Figure 18. SAEC Epithelial Mesenchymal Transition After Exposure for 7 Days to Fe2O3

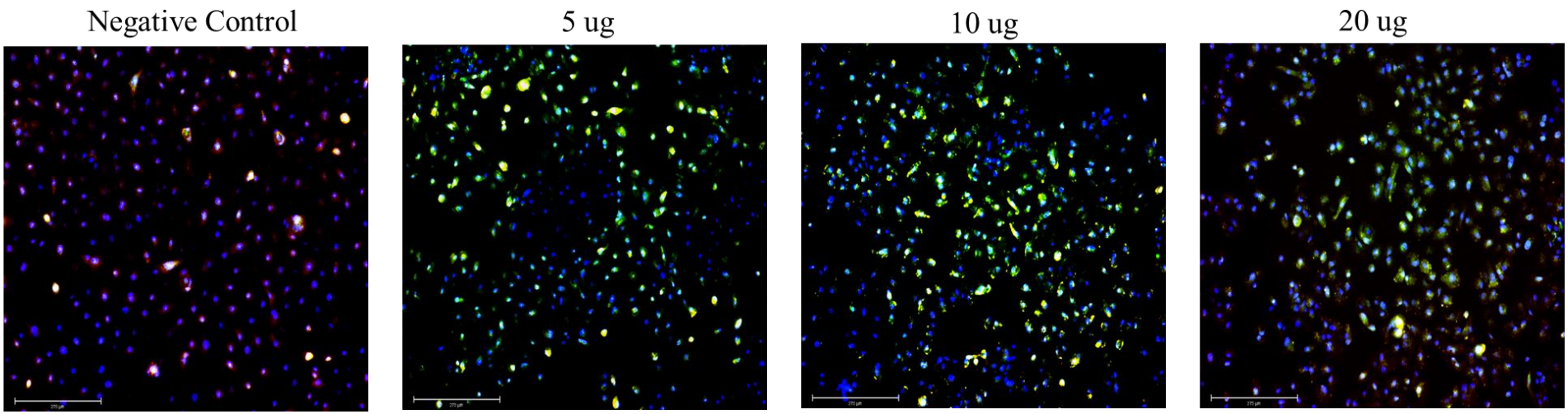

Figure 19. Western Blot Analysis for SAEC 3-Week Exposure to Pristine and Released Nanoparticles